EVALUATION OF NOVEL ENOATE REDUCTASES AS POTENTIAL BIOCATALYST FOR ENANTIOMERICALLY PURE COMPOUND SYNTHESIS

A Dissertation
Presented to
The Academic Faculty

by

Yanto Yanto

In Partial Fulfillment
of the Requirements for the Degree
Doctor of Philosophy in the
School of Chemical & Biomolecular Engineering

Georgia Institute of Technology
May 2011

EVALUATION OF NOVEL ENOATE REDUCTASES AS POTENTIAL BIOCATALYST FOR ENANTIOMERICALLY PURE COMPOUND SYNTHESIS

Approved by:

Dr. Andreas S. Bommarius, Advisor
School of Chemical & Biomolecular Engineering
Georgia Institute of Technology

Dr. Mark R. Prausnitz
School of Chemical & Biomolecular Engineering
Georgia Institute of Technology

Dr. Dale E. Edmondson
School of Chemistry & Biochemistry
Emory University

Dr. Jim C. Spain
Civil & Environmental Enginnering
Georgia Institute of Technology

Dr. Christopher W. Jones
School of Chemical & Biomolecular Engineering
Georgia Institute of Technology

Date Approved: March 17, 2011

To 父母 and 妹妹

“面對它, 接受它, 處理它, 放下它”

父親的 12 字箴言

February 18, 2009

ACKNOWLEDGEMENTS

This dissertation would not be possible without the endless support of my parents, family, and friends. First of foremost, I would like to thank my dad for all the inspirations and wisdoms in my education and career goal setting; my mom for her patience in listening to my stories and guidance in finding the balance in life; and my little sister for all the joys and laughter she shared that makes me easy even during the busiest days at work. This work will not be possible without the unconditional love and support from them, and hope the accomplishments during my journey in both UC Davis and Georgia Tech can make them proud.

This work would also not be possible without the guidance of my advisor, Prof. Andreas S. Bommarius. I thank him for all the positive feedbacks, encouragements, and trust in letting me direct as an independent researcher in this project. Andy has been an excellent mentor and irreplaceable source of scientific guidance. All the frank and honest discussions we had always provided me with new ideas and challenges to be creative in my thesis. I am glad to work with him for the past five years and proud to be one of the branches in his "academic family tree". I would like to thank all my committee members, Dr. Dale E. Edmondson, Dr. Christopher W. Jones, Dr. Mark R. Prausnitz, and Dr. Jim C. Spain for all the assistance and encouragements in my project. Particular thanks to Dr. Kurt Faber for hosting me in University of Graz, Austria, to learn and work on Old Yellow Enzyme family characterization project. The collaboration truly exposed me to the combined power of biocatalyst and organic chemistry, and inspired new ideas in my own thesis work. I like to thank all the Faber's lab members, particularly Clemens Stueckler, Christoph Winkler, and Katharina Durchschein; for experimental assistance

and showing me all the beautiful cities in Austria. Special thanks to Shirley F. Nishino from Spain's lab for help on nitroreductase project.

I extend thanks to all current members and alumni of Bommarius group for being extraordinary colleagues and friends: Dr. Thomas A. Rogers and Dr. Eduardo Vazquez-Figueroa for initial equipment trainings; Janna K. Blum and Dr. Bernard Loo for helps in molecular biology works; Dr. Mélanie Hall for bringing energy and improvements in the lab and my project; Prabuddha Bansal for collaboration on computational protein engineering project; Cherry Yu, Dorothy Copeland, and Stephanie J. Lohr for being superb undergrads and excellent contributions in research works, I hope this undergraduate research experience will be beneficial for your future endeavors both in graduate / medical school or industry; Michael J. Abrahamson, Andria L. Deaguero, Jonathan T. Park, Jonathan Rubin, Russell B. Vegh, and Yuzhi Kang, for being helpful co-workers and good friends. Thanks to all of you, and many other group members and alumni in the lab, for making IBB wing 3D a fun and productive place.

Finally, I thank my friends in Georgia Tech: Chu Hua-wei and family, Koh Pei Yoong, Dhaval Bhandari, Prashant Kumar, Dr. Yuan Yanhui and family, and many others for all the precious memories in Tech.

TABLE OF CONTENTS

LIST OF TABLES

LIST OF FIGURES

SUMMARY

Asymmetric synthesis with biocatalyst has become an increasingly interesting and cost effective manufacturing process in fine chemicals, pharmaceuticals, and agrochemical intermediates. Enoate reductases from the Old Yellow Enzyme family offer high substrate efficiency, region, stereo-, and enantioselectivity in the catalyzed biotransformations. Asymmetric reduction of activated C=C bond is one of the most widely applied synthetic tools for the potential to generate up to two stereogenic centers in one step reaction. Current existing synthetic methods of asymmetric hydrogenation involve the use of precious metals in conjunction with chiral phosphines as well as organocatalytic hydrogenation of cyclic enones to allow a wider choice of substrates and products. However, the addition of biocatalytic hydrogenation of activated alkenes proved to be highly effective to produce enantiomerically pure compounds and become a precious addition tools for both the established synthetic pathways and novel methods.

The thesis contributed to the development and characterization of the Old Yellow Enzyme family with regards to addition of new chemistry such as exploitation of nitroreductase activity with NRSal from *Salmonella typhimurium*, where we investigated the reduction of α,β-unsaturated carbonyl compounds, nitroalkenes, and nitroaromatics substrates, and also reported the first single-isolated enzyme-catalyzed reduction of nitrobenzene to aniline through the formation of nitrosobenzene and phenylhydroxylamine as intermediates. The development and characterization of novel enzymes YersER from *Yersinia bercoviei* and KYE1 from *Kluyveromyces lactis* showed both enzymes have broad enoate reductase specificity and able to operate under broad temperature and pH optima but different specificity patterns. Both substrate- and enzyme-based stereocontrol were also observed for both YersER and KYE1 to furnish opposite stereoisomeric products. Further improvement and characterization on XenA from

Pseudomonas putida showed broad catalytic activity and reduces various α,β-unsaturated and nitro compounds with moderate to excellent stereoselectivity. Mutations of XenA C25G and C25V are able to reduce nitrobenzene, a non-active substrate for the wild type, to produce aniline. The combination of computational protein engineering in form of the Principal Component Analysis method together with structure-guided consensus enabled the improvement of YersER, where significant improvements of specific activity were detected. Lastly, the work also contributed towards larger-scale system preparation by looking into enzyme stability and organic solvent behavior. We studied the total turnover number (TTN) as an indicator of lifetime biocatalyst productivity for YersER, KYE1, and XenA. The TTN of XenA proved to be dominated by chemical rather than thermal instability. Also, the effects of organic solvents on enzyme activity and stereoselectivity were tested with YersER and KYE1 to show the sustainable bioreduction efficiency even at high organic solvent content. Future work will focus to enable sustainable and stable scale-up system to demonstrate the possible applications of these enzymes.

In summary, the increasing knowledge about this Old Yellow Enzyme family together with recent advances in biotechnology renders the enoate reductases a tool of choice for industrial applications. Detailed understanding of the knowledge of Old Yellow Enzyme substrate specificity and stereoselectivity, combined with structural and computational modeling techniques enable the future development and improvement of novel enoate reductase using enzyme engineering approach.

CHAPTER 1

INTRODUCTION

Enzymes are a class of macromolecules with the ability to bind small molecules and to affect the rate of reaction. Like all other catalystsle, enzymes lower the activation energy and dramatically increase the rate of a reaction. In an enzyme reaction, initial free enzyme (E) and free substrate (S) combine reversibly to form an enzyme-substrate (ES) complex. The ES complex passes through another transition state to form enzyme-product (EP) complex, which then dissociate into free enzyme and free product (P) (Fig 1.1). Based on the proposed model, Leonor Michaelis and Maud Menten derived the first rate law for enzyme catalysis in 1913, which was later named Michaelis-Menten-Henri kinetics.[1-3]

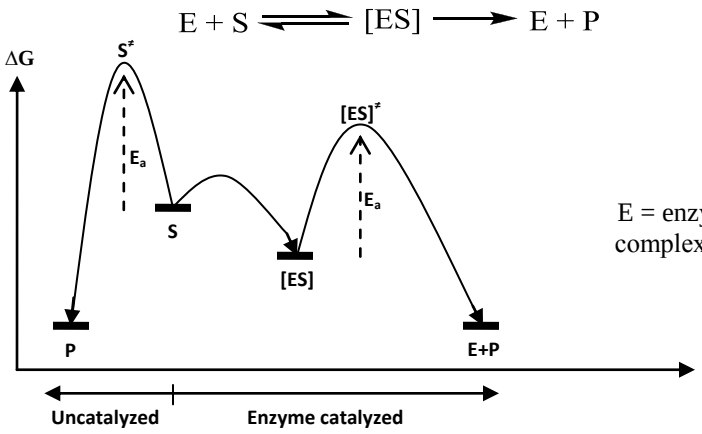

E = enzyme, S = substrate, [ES] = enzyme-substrate complex, P = product, ≠ = transition state, ΔG = free enthalpy. E_a = activation energy

Figure 1.1. Uncatalyzed reaction versus enzyme-catalyzed reaction.

Over the past 20 years, biocatalysis emerged as key toolbox in the industrial synthesis of bulk chemicals, agrochemical intermediates, pharmaceuticals intermediates, active pharmaceuticals, and food ingredients. Advancements in novel enzyme discovery with recombinant DNA technology allowed for the development of more efficient and robust enzyme systems and improved the productivity and simplicity of biocatalytic process design. Several advantages of using biocatalysis include: (i) Enzymes are very

efficient catalysts and often accelerate the rate of reaction by factor of 10^8 - 10^{10} compare to noncatalyzed reactions. (ii) Biocatalysis are environmental benign reagents that enable the sustainable development of green chemistry processes in industry. Environmental benign manufacturing processes help to prevent the depletion of non-renewable resources and reduce the production of hazardous substances. Also, since biocatalysis operates under mild reaction condition in the range around pH 5 - 10 and temperature of 20 – 50 ^{o}C, it also minimizes undesired side reactions (decomposition, isomerization, racemization, and rearrangements) that often occur in traditional chemical processes. (iii) High selectivity of enzymes often increases the chemo-, regio-, and enantio- selectivity of a reaction. This is especially important for synthesis of bioactive enantiomers such as pharmaceuticals or agrochemicals, which often required high enantiopurity to avoid unwanted side effects by the opposite enantiomer product.[1, 2]

Today, the biggest role for biocatalysis applications lies in the pharmaceutical sectors due to its exquisite region- and stereo- selectivities. Chiral pharmaceutical reagents have continuously received particular attention due to the human body functions using chiral catalysis. Survey showed that in 2000, 35% of the pharmaceutical intermediates were chiral and this number is expected to increase to 70% by 2010. The increasing complexity of the molecules that require multiple chiral centers further favor the development of biocatalytic steps in replacement of difficult chemical synthesis. Although the majority of pharmaceutical processes feature relatively small production volumes (10 – 10000 tons per annum) compared to chemical processes, there are few constraints for biocatalytic process to be economically viable. Process intensity for a biocatalytic process needs to be comparable to chemical processes with product concentration of at least 50 - 100 g/l and sufficient yield in gram product per gram catalyst used. Efficient process development will require integration of various disciplines including chemistry, enzymology, engineering, molecular biology, and microbiology. New techniques such as process miniaturization and mathematical

modeling are often exercised during the scale-up period for rapid process testing. All these advancements continuously improve the capability of biocatalysis to reach its full potential in pharmaceutical synthesis and become a promising area of research for both academia and the industrial community.[4-6]

1.1 "Old Yellow Enzyme" Family and Enoate Reductases

Flavoenzymes are a group of oxidoreductases enzymes that catalyzes a wide range of biochemical reactions ranging from dehydrogenation of metabolites, one- and two-electron transfer redox reactions, oxygen activation during oxidation and hydroxylation reactions, and light emission in bioluminescent bacteria. Flavin was first discovered around 1890s by Wynter Blyth, an English chemist, as a bright yellow pigment isolated from cow's milk. The isolated molecule was later known as riboflavin, or also known as vitamin B_2.[7-9] The flavoenzyme family consists of flavin adenine dinucleotide (FAD)-dependent and flavin mononucleotide (FMN)-dependent proteins, which both contain a unique tricyclic heteronuclear isoalloxazine ring system as coenzyme and frequently possess $(\alpha\beta)_8$ TIM barrel folding structure (Fig 1.2). The reactive site of flavin lies in the tricyclic isoalloxazine ring system. The N1-C2=O2 locus was reported to have close contact (< 3.5 Å) with positively charged side chains such as Lys or Arg. The positive charges at this position will stabilize anionic form of reduced flavin and favor protein binding by increasing the cofactor's redox potential. The N5 locus was reported to responsible for substrate binding. In most flavoproteins, N5 is within hydrogen-bond distance (~ 3 Å) from a hydrogen donor, which allows the substrate to bind on either the *si* or *re* face of flavin.[8]

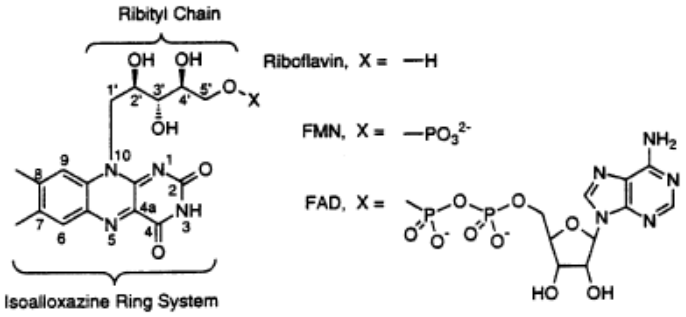

Figure 1.2. Structure of riboflavin, FMN, and FAD.

Old yellow enzyme (OYE) is a subfamily of flavor enzymes that catalyze stereoselective reduction of activated C=C bonds in the presence of nicotinamide cofactor. Old Yellow Enzyme (OYE, EC 1.6.99.1) was first discovered in 1933 by Christian and Warburg during their investigation on biological oxidations. It was isolated from brewers' bottom yeast and identified as the first flavin-dependent enzyme [10]. Since then, OYE from *Saccharomyces carlsbergensis* has given rise to an ever growing family of enzymes sharing similar characteristics but displaying variable reactivity, and that have been found among yeasts, bacteria, higher plants [11, 12] and most surprisingly in parasites [13]. An OYE homolog was identified in a non-yeast organism for the first time in 1979, in the cytosol fraction of *Gluconobacter suboxydans* [14]. Since then, multiple homologs have been discovered, identified, and characterized. Members of this family of flavoproteins so far include OYE from *Saccharomyces carlsbergensis* [15], OYE2-3 from *Saccharomyces cerevisiae*, KYE1 from *Kluyveromyces lactis* [16-18], OYE from *Candida macedoniensis* [19], *trans*-2-enoyl-coenzyme A reductase and *N*-ethlymaleimide reductase (NemA) from *Escherichia coli* [20-22], estrogen-binding protein (EBP1) from *Candida albicans* [23], YqjM from *Bacillus subtilis* [24], NCR from *Zymomonas mobilis* [25], SYE1-4 from *Shewanella oneidensis* [26], Yers-ER from *Yersinia bercovieri* [17], morphinone reductase from *Pseudomonas putida* M10 [27], pentaerythritol tetranitrate (PETN) reductase from *Enterobacter cloacae* PB2 [28],

xenobiotic reductases XenA from *Pseudomonas putida* II-B and XenB from *Pseudomonas fluorescens* I-C resp. [29, 30], glycerol trinitrate reductase (NerA) from *Agrobacterium radiobacter* [31], 12-oxophytodienoate reductases OPR1-3 from *Arabidopsis thaliana* and *Lycopersicon esculentum* [32, 33], as well as OPRs from pea, maize and rice [34-37]. Enoate reductase activity has also been detected in a number of additional microorganisms and plants: *Aspergillus niger* [38, 39], *Rhodotorula rubra* [40], *Burkholderia sp.* WS [41], *Catharanthus roseus* [42], *Nicotiana tabacum* [43], *Peptostreptococcus productus* [44], *Synechococcus sp*. [45], *Glycine max* [46], *Astasia longa* [47], *Marchantia polymorpha* [48], *Acetobacterium woodii* [49, 50] and more [51, 52]; but most of the corresponding enzymes have not been identified yet (in the case of *Glycine max*, *Astasia longa* and *Nicotiana tabacum*, purified enzymes were described as enone reductases [46, 47, 53, 54]). A phylogenetic tree of the OYE family shows the sequence relationship between enzymes of this family (Fig. 1.3).

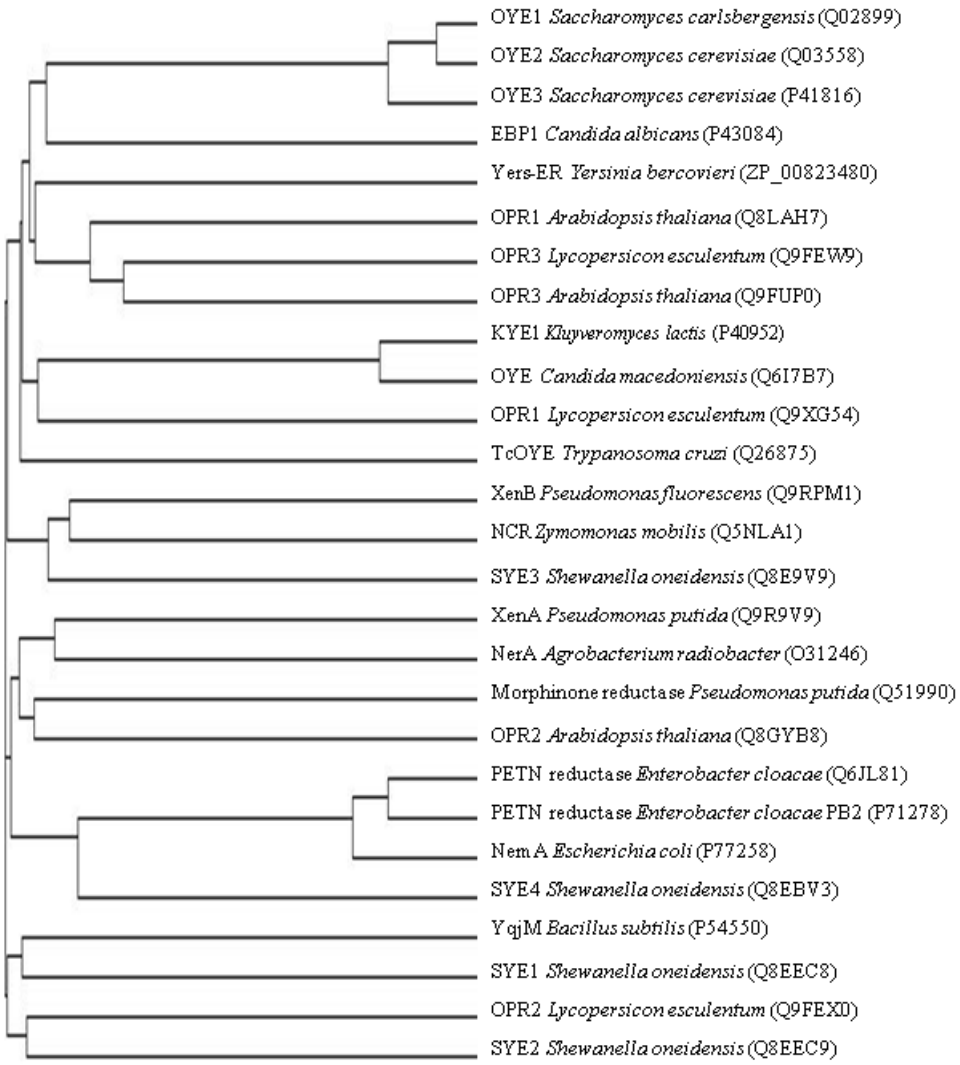

Figure 1.3. Phylogenetic tree of OYE family (constructed using ClustalW2 [55]). The names of the proteins are indicated to the right of the tree with the UniProtKB Accession Nos. given in parentheses (clustering NJ method used).

The use of OYE as a reducing agent was first demonstrated by Warburg while he was investigating the reaction between glucose-6-phosphate, $NADP^+$, an enzyme ("Zwischenferment"), and a substance called "Gelbe Ferment", later identified as OYE and permitting the system to form a complete respiratory chain reacting with molecular oxygen [56]. Theorell showed much later that the yellow color was due to flavin mononucleotide (FMN) [57].

Extensive studies have been conducted since then in an attempt to identify the physiological function of OYE, all rather inconclusive, but a general consensus arose on the likely role of OYE in oxidative stress response [26, 58]. Furthermore, the enzyme demonstrated the ability to reduce different types of substrate, most notably C=C bonds (Fig 1.4) [7, 59, 60], but also more complex compounds such as nitrate esters and nitro aromatic molecules [61-65]. The reaction mechanism for the reduction of α,β-unsaturated compounds has been extensively studied, however, less is known about mechanistic details and residues involved in nitro reduction.

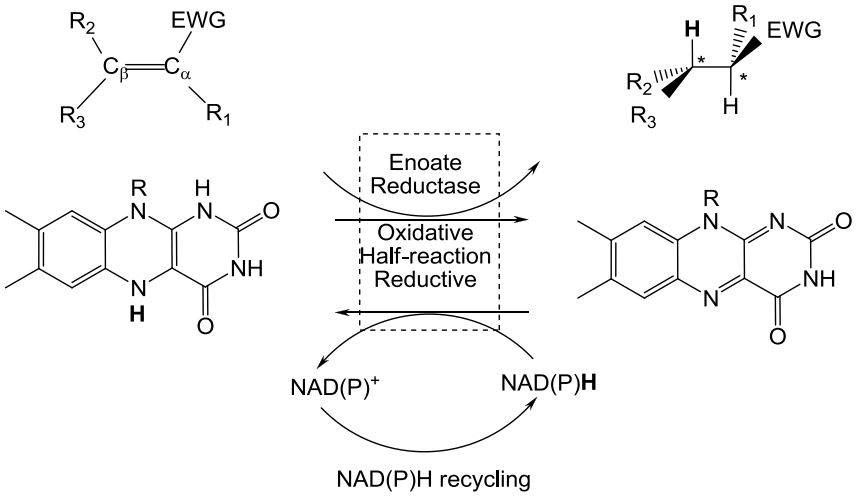

Figure 1.4. Asymmetric bioreduction of activated alkenes bearing an electron-withdrawing group (EWG) by enoate reductases (the hydride being transferred is shown in bold) [60].

At the time when studies on OYE were starting to give insight in this new chemistry, Simon *et al.* published their work on enoate reductases (EC 1.3.1.31) from anaerobic *Clostridium* species (*Clostridium kluyveri*, *Clostridium tyrobutyricum* and *Clostridium sporogenes*) catalyzing the reduction of carbon-carbon double bond of α,β-unsaturated carboxylate anions (hence the nomenclature) [66, 67]. However, despite

sequence similarities, these enzymes differ from the OYE family as they are iron-sulfur NADH-dependent flavoproteins [68, 69]. They have been shown to catalyze the reduction of carbon-carbon double bonds of (weakly activated) 2-enoates as well as of α,β-unsaturated aldehydes, cyclic ketones, methylketones and recently β,β-disubstituted aromatic nitroalkenes [70, 71].

1.2 Reactions catalyzed by enoate reductases

Members of the 'Old Yellow Enzyme' family share common catalytic properties as they are able to reduce a variety of different substrates such as nitro esters, nitro aromatics, and α,β-unsaturated compounds (activated by an electron withdrawing group such as aldehyde, ketone, imide, nitro, nitrile, carboxylic acid or ester) at the expense of a nicotinamide cofactor (Fig 1.4, Fig 1.5) [12, 72-74]. The physiological oxidant of OYE has not been clearly identified yet but common electron acceptors include molecular oxygen, methylene blue, cyanides, quinones, and the olefinic bond of α,β-unsaturated carbonyl and carboxylic compounds [59]. OYE characteristically interacts with phenolic compounds to yield long wavelength charge transfer bands in the region of 500-800 nm, which were attributed to the formation of OYE-phenolate complex [7, 75].

1.2.1 Asymmetric reduction of carbon carbon double and triple bonds

The asymmetric bioreduction of C=C bonds using enoate reductases was initially performed using whole cell fermentation with baker's yeast [76, 77]. However, the whole cell reactions were generally impeded by the presence of endogeneous ketoreductases in the host cells, which also require the same nicotinamide cofactor for bioreduction of C=O bonds. The competing reduction of C=C- and C=O- bonds by enoate reductases and alcohol dehydrogenases often resulted in poor chemoselectivity in the overall reaction and produced the corresponding alcohols of the saturated products [78]. In the case of

conjugated enals, the *prim*-alcohol dehydrogenases often over-reduced the substrate to the corresponding *prim*-alcohols [51, 52]. This competing side reaction was less observed in the case of conjugated enones as the reduction of ketone by *sec*-alcohol dehydrogenases is slower compared to the enoate reductase activity [12, 79].

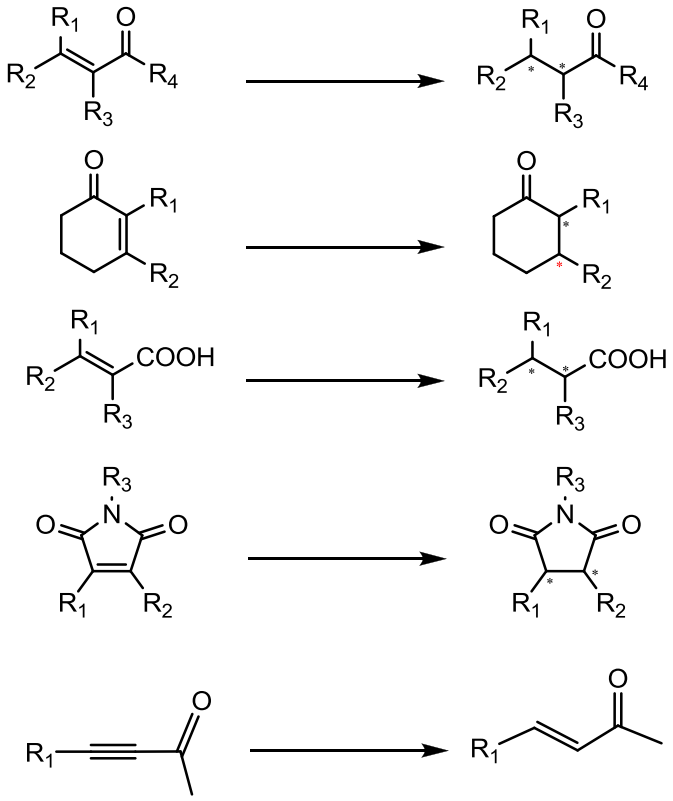

Figure 1.5. Asymmetric bioreduction of α,β-unsaturated carbonyl compounds (aldehydes and ketones), α,β-unsaturated carboxylic acids, imides and ynones [12, 80].

Besides the asymmetric bioreduction of C=C bonds, OYE also showed ability to reduce C-C triple bonds, converting ynones to α,β-saturated ketones *via* the formation of the intermediate enones. OYE1-3 from yeast catalyzed the reduction of 4-phenyl-3-butyne-2-one to (*E*)-4-phenyl-3-butene-2-one (only the *trans* isomer was produced), and subsequently produced 4-phenyl-2-butanone in the presence of NAD(P)H [80]. OYE was also shown to promote aromatization of α,β-unsaturated cyclic enones such as 2-cyclohexenone and 3-oxodecalin-4-ene. The aromatization of cyclic enones follows the *trans*-dehydrogenation of the 1β,2α-hydrogens, and is accompanied by a dismutation

reaction in which the olefinic bond of a second molecule of each substrate is reduced to give the saturated cyclic ketone [59]. The energetically favorable product aromatization drives the desaturation. Thus, two molecules of 2-cyclohexenone yielded one molecule of phenol and cyclohexane each (Fig. 1.6). The desaturation of cyclohexanone into cyclohexenone and further into phenol was recently reported using an OYE homolog from *Geobacillus kaustophilus*. Similarly, the enzyme was shown to introduce C-C double bonds adjacent to carbonyl groups in compounds such as dihydrocarvone (yielding carvone) and testosterone (yielding boldenone).

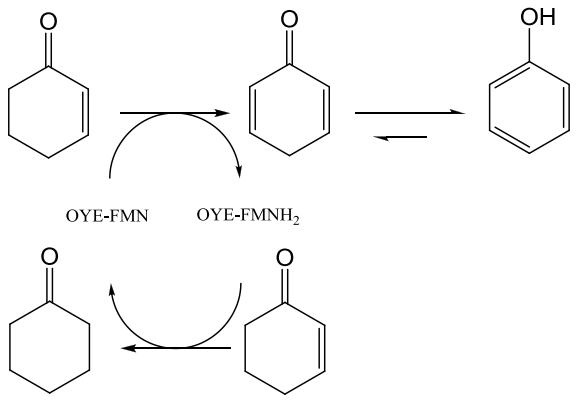

Figure 1.6. Dismutation reaction of cyclohexenone catalyzed by OYE. Adapted from [16, 59].

α,β-Unsaturated carboxylic acids and derivatives such as esters, lactones, cyclic anhydrides, and imides are also good substrates for enoate reductases [12, 60, 81]. The overall bioreduction also showed excellent stereoselectivities. In the case of substrates bearing two cumulated C=C double bonds, OYE only reduced the targeted α,β-bond, but not the γ,δ-bond [82]. Lactones were also shown to be reduced efficiently with baker's yeast with high stereoselectivities [83]. Acid anhydrides and imides were also reported to be good substrates for enoate reductases. *N*-phenyl-2-methylmaleimide was reduced completely by isolated enzymes of OYE1-3 from yeast in the presence of NAD(P)H [60].

Controlling the stereochemical outcome of the reduction of α,β-unsaturated compounds can be achieved *via* substrate- and/or enzyme-based stereocontrol (Fig. 1.7). The reduction of (*E*)- and (*Z*)-enoates and enals to opposite enantiomers constitutes an example of substrate-based stereocontrol. The *R/S*- configuration of the reduced products were shown to depend on the *E/Z*-configuration of the original substrates, as observed in the reduction of methyl 2-chloro-2-alkenoates by fermentation with baker's yeast (the actual substrates were the corresponding acid forms obtained after hydrolysis of the esters by unspecific esterases) [84]. The same effect was observed in the reduction of citral with OYE1 [25]. Furthermore, whereas one isomer can be accepted by OYEs, the oppositely configured substrate is not, leading to dramatic substrate recognition, as observed with citraconic acid and its *Z*-configured analog mesaconic acid, with OPR1 and YqjM. Their corresponding esters, however, were both accepted but led to strictly opposite enantiomers upon reduction with YqjM [85]. On the contrary, the reduction of (*E*)- and (*Z*)-isomers of various nitroolefins proceeded in a stereoconvergent manner using PETN reductase from *Enterobacter cloacae* PB2 [86].

Another possibility to control the enantiopurity of the product is to use different enzymes (enzyme-based stereocontrol). The most striking example was reported with two isozymes from *Lycopersicon esculentum*, OPR1 and OPR3. Despite high sequence identity, their stereoselectivities were opposite in the reduction of 1-nitro-2-phenylpropene and this striking result was explained by subtle changes in the active site geometry [81, 87].

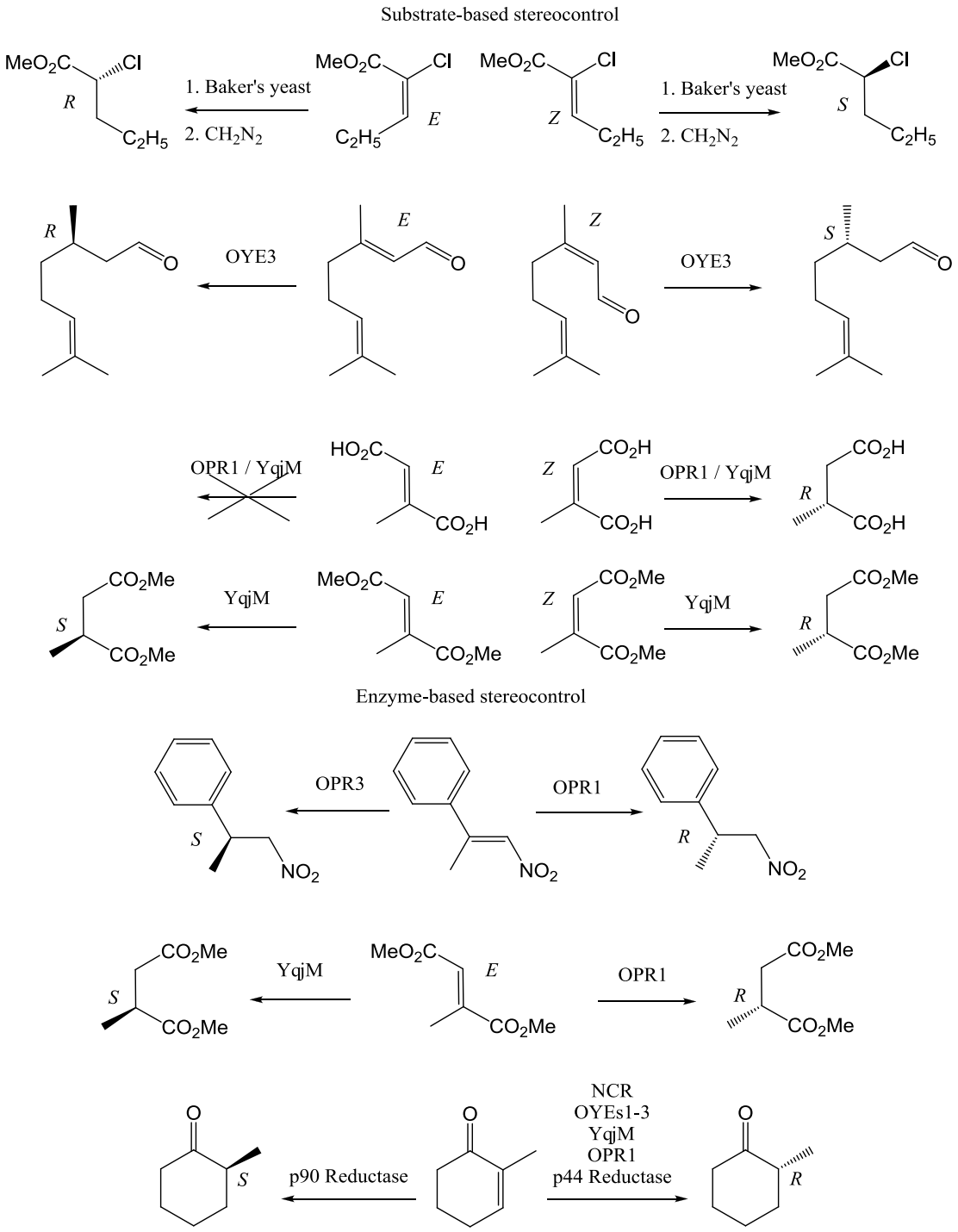

Figure 1.7. Examples of stereocontrol in the reduction of C=C bonds using OYE homologs (reduction of methyl 2-chloro-2-alkenoates proceeded at the acid stage, therefore diazomethane was used to recover the ester form after reduction with baker's yeast) [25, 53, 60, 81, 88].

1.2.2 Bioreduction of nitro compounds

Over the last few years, there has been significant development in the biodegradation and mineralization of explosives from the two world wars [89-91]. The main enzymes involved are nitroreductases, which reduce a wide range of aromatic nitro compounds such as nitrofurazones, nitrobenzenes, nitrophenols, and various explosives including trinitrotoluene (TNT) and pentaerythritol tetranitrate (PETN), as well as nitrate esters such as glycerin trinitrate (GTN). Nitroreductases have been grouped into two subfamilies according to their mechanism: oxygen-insensitive type I nitroreductase and oxygen-sensitive type II nitroreductase. Most nitroreductases were identified in bacterial strains, such as NfsA and NfsB from *E. coli* [92], SnrA and Cnr from *Salmonella enterica serovar Typhimurium* [93] or PnrA and PnrB from *Pseudomonas putida* [94]. Similarly to OYE, those nitroreductases contain FMN as the coenzyme and require NAD(P)H as physiological reductant [95].

The OYE family is also known for its nitroreductase activity on explosives such as PETN and TNT. Several well characterized members of the OYE family displaying nitroreductase activity include for instance XenA and XenB from *Pseudomonas sp.* [29], PETN reductase from *Enterobacter cloacae* [96], NemA from *E. coli* [97], morphinone reductase from *Pseudomonas putida* M10 [27], OYEs from *Saccharomyces sp.* [98] and YqjM from *Bacillus subtilis* [24]. PETN reductase, for example, was shown to be able to grow on TNT as nitrogen source and converted TNT to yield monohydride-Meisenheimer complex (H^--TNT) and dihydride-Meisenheimer complex ($2H^-$-TNT, Fig. 1.8) [99], which was shown to release nitrite upon rearomatization to 2-hydroxylamino-6-nitrotoluene in a slow abiotic process [100]. These reactions correspond to two different types of aromatic nitroreduction: reducing activity involving the reduction of the nitro group of TNT leading to hydroxylaminodinitrotoluene *via* the nitroso intermediate, possibly followed by further reduction to the corresponding amine, and reducing activity involving the reduction of the aromatic ring by the OYE to produce the corresponding

Meisenheimer complex, ultimately followed by the liberation of nitrite (recently described as type I, resp. type II hydride transferase [61, 62], despite the fact that transferases are not reductases). All enzymes of the OYE family are able to perform reduction of the nitro group, while the reduction of the aromatic ring is only catalyzed by PETN reductase, XenB, and NemA with the formation of H^--TNT followed by $2H^-$-TNT [101]. The dimerization of the Meisenheimer dihydride complex with hydroxylaminodinitrotoluenes was recently reported for enzymes displaying both types of reducing activity, leading to secondary diarylamines [61, 102].

Nitrate esters such as GTN or PETN were also reported to be reduced by the OYE family, *via* the cleavage of the ester bond leading to the liberation of nitrite and the formation of the corresponding alcohol. XenA and XenB, PETN reductase, NerA, and OYEs have all been shown to catalyze the reduction of GTN in the presence of NAD(P)H [103]. 1-2 mol of nitrite is removed from GTN while 2 mol of nitrite are usually removed from PETN during the reaction [28, 98, 104]. Several other organic nitroesters with explosives properties were also reduced by PETN reductase, with kinetic parameters depending on their log P_{ow} values (generally, the higher the log P_{ow} value, the higher the apparent rate constant k_{cat}/K_m) [105].

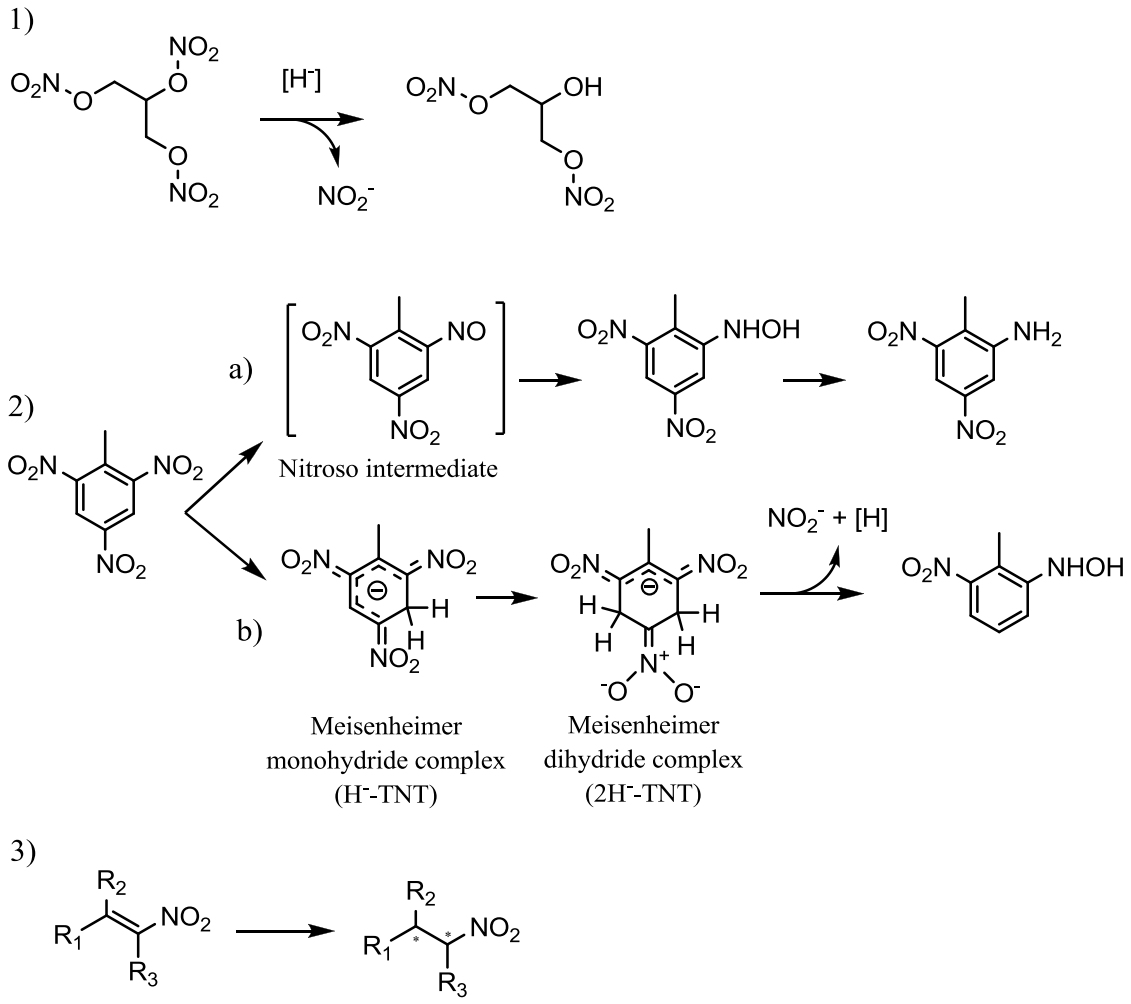

Figure 1.8. Reduction of nitro compounds by OYE family: (1) Reduction of nitroester (GTN) with liberation of nitrite, (2a) Reduction of the nitro group of TNT to the corresponding aromatic amine, (2b) Reduction of the aromatic ring of TNT to the corresponding hydroxylamino product *via* Meisenheimer complex formation, (3) Asymmetric reduction of nitroalkenes to nitroalkanes (* chiral center) [62, 87, 98, 100].

Besides, several other members of OYE family are also capable of catalyzing the hydrogenation of 1-nitrocyclohexene. The enzymes first catalyze the formation of nitronate as intermediate, followed by protonation of the nitronate toward the corresponding nitrocyclohexane (Fig. 1.9) [101]. Meah and Massey demonstrated the possibility to accumulate nitronate with a single mutant of OYE (Y196F), providing a possible biocatalytic route for the production of nitronate [106].

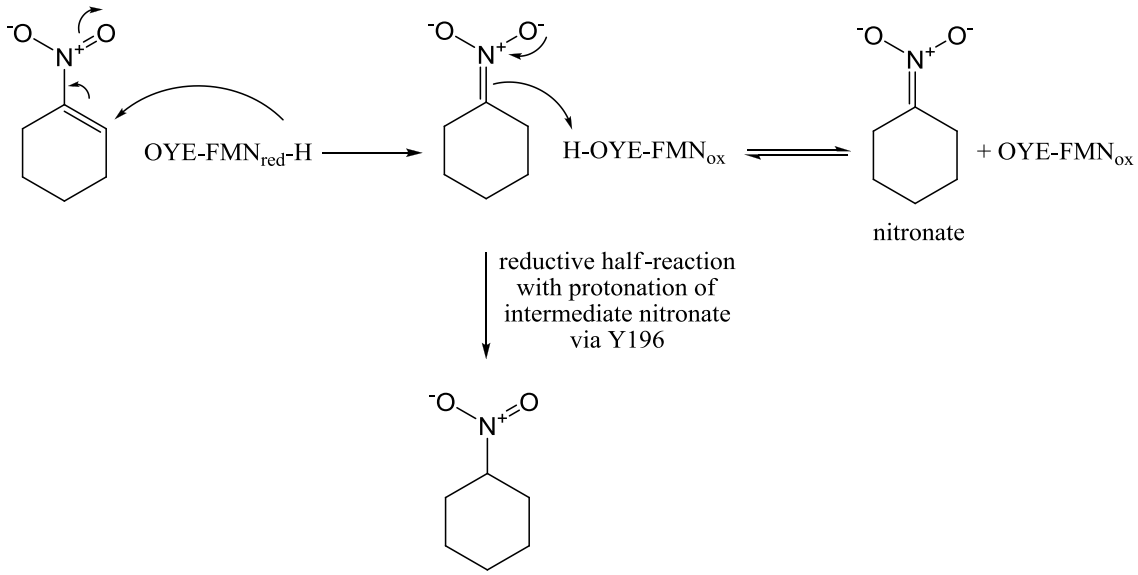

Figure 1.9. OYE-catalyzed reduction of nitrocyclohexene and formation of nitronate. Adapted from [106].

Last, the asymmetric bioreduction of aliphatic nitroalkenes does not affect the nitro group, rather it affords the chemoselective reduction of the C=C bond. Such activity was observed with OYE1-3 from yeast, OPR1 and OPR3 from *Lycopersicon esculentum*, YqjM from *Bacillus subtilis*, NCR reductase from *Zymomonas mobilis*, PETN reductase from *Enterobacter cloacae* PB2 and whole cells of *Clostridium sporogenes*, which all demonstrated excellent activities along with great stereoselectivities [60, 71, 74, 81, 86]. Recently, PETN reductase was shown to display activity on nitrogen analogues from organic nitrates (*N*-nitramines), e.g. RDX (hexahydro-1,3,5-trinitro-1,3,5-triazine) and HMX (octahydro-1,3,5,7-tetranitro-1,3,5,7-tetrazocine). However, reactivity on those compounds was three orders of magnitude lower than that on aliphatic nitroesters [105].

1.3 Biochemistry of Old Yellow Enzyme

1.3.1. Mechanism and structure

The asymmetric reduction of activated C=C bonds using members of the 'Old Yellow Enzyme' family resembles a *trans* Michael addition of [2H]. The mechanism

involved was studied extensively and good understanding on the molecular level has been reached [16, 107-109]. Besides, the access to a number of crystal structures (including those of enzymes complexed with various types of ligand [110-116]), together with mutational studies, allowed the identification of crucial (and conserved) residues.

The reaction occurs *via* a Ping Pong Bi Bi mechanism, where the flavin coenzyme is reduced by NAD(P)H *via* the transfer of the 4-pro-*R* hydridic hydrogen [59] in what is described as the 'reductive half-reaction'. A hydride is then transferred from the reduced flavin (from the N5 atom) onto the C_β of the activated α,β-unsaturated substrate ('oxidative half-reaction') followed by the addition of a proton on the C_α from the other side of the substrate. The reaction is thus strictly *trans*-specific, differing from its pure synthetic equivalent in homogeneous catalysis (*cis*-hydrogenation using transition metal-based catalysts [117-119]). As the prosthetic group is re-oxidized during the oxidative half-reaction (completion of catalytic turnover), the enzyme is ready for another cycle, provided sufficient amount of nicotinamide cofactor is present.

OYE is a dimer of ~45 kDa subunits with one non-covalently bound FMN per subunit. It folds into a single domain based on a TIM barrel ($(\alpha/\beta)_8$ barrel) with the FMN binding within the barrel near the carboxy-terminal ends of the β-strands [112] (Fig. 1.10). Fitzpatrick *et al.* classified YqjM as the first representative of a new bacterial subfamily of OYE homologs based on structural differences with OYE [24]. This is of special relevance as structure impacts activity and therefore would also affect subsequent attempts at predicting and investigating corresponding substrate spectrum.

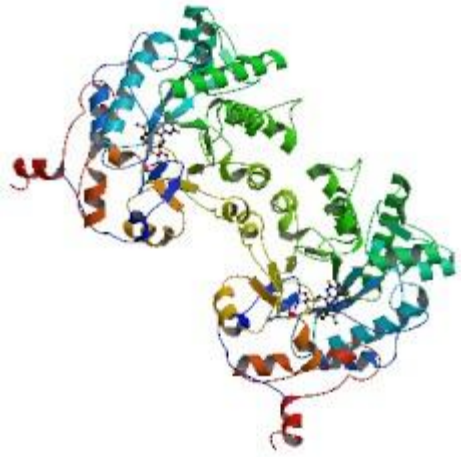

Figure 1.10. Ribbon diagram of the structure of OYE with FMN cofactor (deposited as 1oya in the Protein Databank. PDB: http://www.rcsb.org/ [112]).

The residues involved in substrate binding were identified in OYE as H191 and N194, and are conserved along the family (N194 is replaced by H in some cases), hydrogen bonding with the activating group (e.g. carbonyl). Interestingly, H184N mutation in PETN reductase (equivalent to OYE N194) prevented the hydride addition onto the aromatic ring of TNT, whereas H^--TNT was still a substrate for the mutant. This led to the conclusion that H/N184 might be crucial in determining the fate of TNT, i.e. aromatic ring-reduction vs. nitro-reduction (cf. section 2.2) [101]. Y196, positioned as an active site acid, was shown to be the proton donor in OYE [107], and is also conserved. This residue is replaced by C191 in morphinone reductase and was shown not to be crucial for reduction of olefinic bonds; in this specific case, the proton was inferred to be coming from the solvent [110, 120]. Similarly, Y186 was shown not to be a key proton donor in the reduction of α,β-unsaturated carbonyl compounds by PETN reductase [121]. Depicted in Figure 1.11 is a sequence alignment of residues 164-221 of OYE and its homologs, including the substrate binding site (H191 and N194) and the active site acid (Y196). In the NerA-catalyzed reduction of GTN, Y183 (equivalent to OYE Y196) was shown to play a role in substrate binding, whereas N181 (equivalent to N194 in OYE)

and a second N238 that lies close to Y183 (equivalent to Y196 in OYE) in the NerA model structure may influence substrate specificity [31].

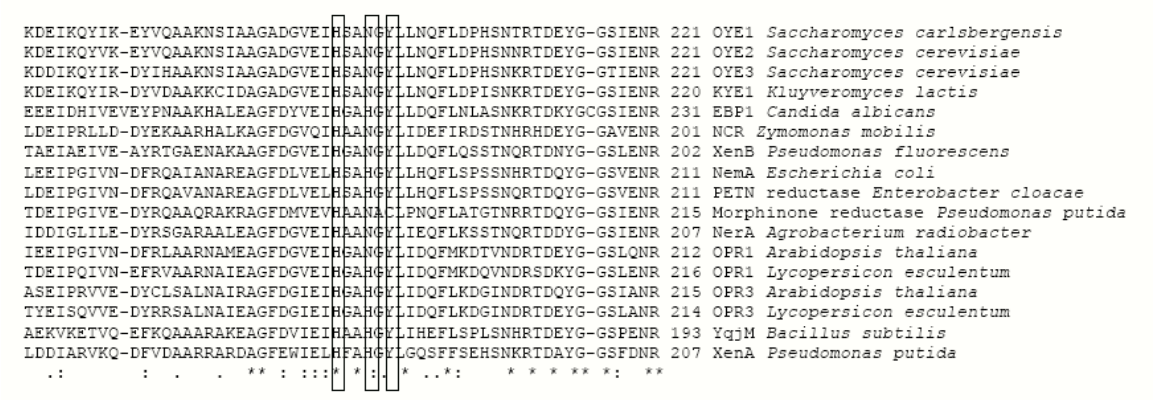

Figure 1.11. Partial amino acid sequence alignment of members of the OYE family (generated using ClustalW2 [55]). PDB Accession Nos. are a follows: Q02899 for OYE1 from *Saccharomyces carlsbergensis*; Q03558 for OYE2 from *Saccharomyces cerevisiae*; P41816 for OYE3 from *Saccharomyces cerevisiae*; P40952 for KYE1 from *Kluyveromyces lactis*; P43084 for EBP1 from *Candida albicans*; Q5NLA1 for NCR from *Zymomonas mobilis*; Q9RPM1 for XenB from *Pseudomonas fluorescens*; P77258 for NemA from *Escherichia coli*; P71278 for PETN reductase from *Enterobacter cloacae*; Q51990 for morphinone reductase from *Pseudomonas putida*; O31246 for GTN reductase from *Agrobacterium tumefaciens* (NerA)*;* Q8LAH7 for OPR1 from *Arabidopsis thaliana*; Q9XG54 for OPR1 from *Lycopersicon esculentum*; Q9FUP0 for OPR3 from *Arabidopsis thaliana*; Q9FEW9 for OPR3 from *Lycopersicon esculentum*; P54550 for YqjM from *Bacillus subtilis*; Q9R9V9 for XenA from *Pseudomonas putida* (H191, N194 and Y196 from OYE1 from *Saccharomyces carlsbergensis* and equivalents are highlighted in boxes).

The nature of the physiological reductant cannot be generalized across the OYE flavoproteins. Whereas NADPH is considered as OYE favored cofactor, morphinone reductase clearly shows a strong preference for NADH (NADPH/NADH ratio of 0.2 vs 10, resp. [101]), as does NerA (specific activity 11-fold lower for NADPH) [65], while OYE from *Candida macedoniensis* does not differentiate between the two nicotinamide forms [19] and the four SYEs of *Shewanella oneidensis* display different cofactor preferences [26]. In recent conversion studies, a number of OYEs showed ability to convert various substrates similarly fast, independently from the cofactor [60, 81]. Since

the reactions were run over extended periods of time, an analogy could be drawn with thermodynamic vs. kinetic reaction control. Cofactor specificity was also shown to be dependent on the substrate [17].

Massey *et al.* proposed to classify an enzyme as an OYE homolog under the condition that it contains FMN as coenzyme, shows NADPH oxidase activity and furthermore shares similar spectral properties, i.e. phenol binding leading to the formation of characteristic absorption changes [16]. The development of charge transfer, however, has not been reported for all the suspected members of the OYE family, which would thus result in a reorganization of the OYE family [14] (changes in absorption spectrum obtained on complex formation between Old Yellow Enzyme and phenolic compounds such as *p*-hydroxybenzaldehyde were shown to arise due to charge-transfer interactions [122]).

Enoate reductases from anaerobic *Clostridia*, despite sharing identical activities with members of the OYE family (reduction of the C=C bond in α,β-unsaturated compounds), belong to a different class of enzymes. Enoate reductase from *C. tyrobutyricum*, for instance, is a homododecamer with each subunit comprising a Fe_4S_4 cluster as well as one molecule each of FMN and FAD. These enzymes catalyze the transfer of the pro-*S* hydrogen from NADPH to the β-position of the substrate in contrast to OYEs [70, 123, 124], and also operate in a strictly *trans* stereospecific fashion [125].

1.3.2. Physiological role

The identification of one single physiological role within the whole family of OYE could not be achieved so far. One certainty concerns OPRs, where the enzymes are involved in the biosynthesis of jasmonic acid, by reducing the 10,11-double bond of 12-oxophytodienoic acid (OPDA) to 3-oxo-2-(2'-pentenyl)cyclopentaneoctanoic acid (OPC-8:0), a precursor of this plant hormone. Surprisingly, only OPR3 isoforms (both from

Arabidopsis thaliana and *Lycopersicon esculentum*) are involved in the synthesis of jasmonate. They accept (9*S*,13*S*)-OPDA as a substrate and yield (9*S*,13*S*)-OPC-8:0, the precursor of the biologically active jasmonate isomer, whereas other isoenzymes are strictly specific for the (9*R*,13*R*)-enantiomer (Fig. 1.12) [33, 126, 127]. Morphinone reductase was shown to be involved in the metabolism of morphine and codeine, by reducing morphinone and codeinone to hydromorphone (dihydromorphinone) and hydrocodone (dihydrocodeinone), respectively [27, 128]. Implication in the metabolism of unsaturated fatty acids has been also proposed for *trans*-2-enoyl-CoA reductase of *Escherichia coli* [22, 129]. Overall, OYEs are often linked to oxidative stress response and modulation [26, 58]. It was suggested that natural physiological substrates may be lipid peroxidation breakdown products often toxic for cells [107, 130]. Recently, OYE3 was indeed proven to be linked with Bax-induced lipid peroxidation [131]. Also, OYE2 was shown to protect against small reactive α,β-unsaturated carbonyl compounds such as acrolein (a major breakdown product of lipid peroxidation process), in vivo [132]. Furthermore, OYE was suggested to control the redox state of actin (thereby maintaining the proper plasticity of the actin cytoskeleton and protecting it from oxidative stress) and be involved in programmed cell death processes (apoptosis) [133, 134]. Besides, investigations on SYE1-4 from *Shewanella oneidensis* suggested multiple physiological roles existing for the different OYE homologs within a single organism [26].

Combining those findings with the wide substrate spectrum of OYEs and their xenobiotic reductase activity, an implication of OYEs in antioxidant defense system and detoxification is most probable [24, 135].

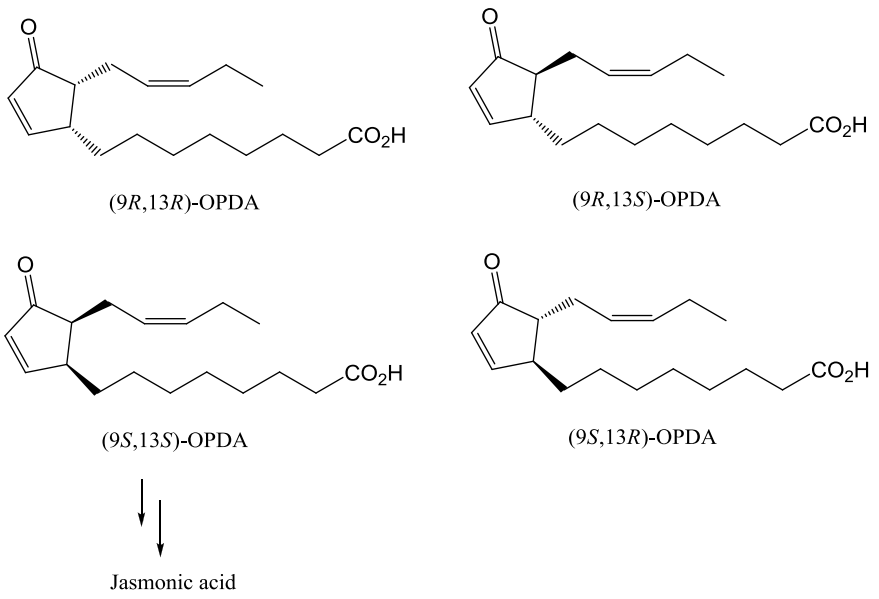

Figure 1.12. 12-Oxophytodienoic acid stereoisomers. Only (9*S*,13*S*)-isomer leads to biologically active jasmonic acid by OPR3 [126].

1.4 Biotechnological Applications

1.4.1. Whole cell systems

The use of whole cell systems has dominated the field of biocatalysis in its early development, mostly due to the lack of efficient methods for protein purification and apparent ease of use [136, 137]. However, this is cause for multiple issues, as whole cell biocatalysts not only contain the enzyme of choice (enoate reductase) but also various others, naturally expressed by the microorganism. The use of such systems where enoate reductase activity is present suffers mostly from side activities, leading to substrate and/or product depletion [12]. Competing alcohol dehydrogenase (ADH) for instance prevented isolation of the desired product (citronellal) in the reduction of citral with whole cells [52]. However, use of organic solvents could prevent further reduction of the product, and ADH activity was lowered by implementing the biphasic system with EDTA [51]. Besides, the presence of stereocomplementary enoate reductases within the same organism [53] or possibly racemase activity might lead to a loss of optical purity of the product, or more dramatically even to racemic mixtures. Therefore, most often

nowadays, the use of isolated enzymes and/or recombinant proteins in hosts lacking those side activities is favored (in a number of cases, it is still possible to obtain enantiopure products out of whole cell systems using wild-type organisms [51]).

1.4.2. Cofactor regeneration systems

Nicotinamide cofactor-dependent bioreduction of alkenes catalyzed by enoate reductases has started to emerge as a highly valuable technique for the production of optically active compounds; however, prohibitive costs of NAD(P)H render the process so far industrially not competitive with efficient metal-based catalytic hydrogenation. The key step to be studied before running large-scale synthesis using isolated enoate reductases is the recycling of the expensive redox cofactor. This can be performed *via* chemical, electrochemical, photochemical, microbial, or enzymatic reaction. The latter technique has been traditionally performed *via* "coupled-substrate" or "coupled-enzyme" approaches (Fig. 1.13, 1.14).

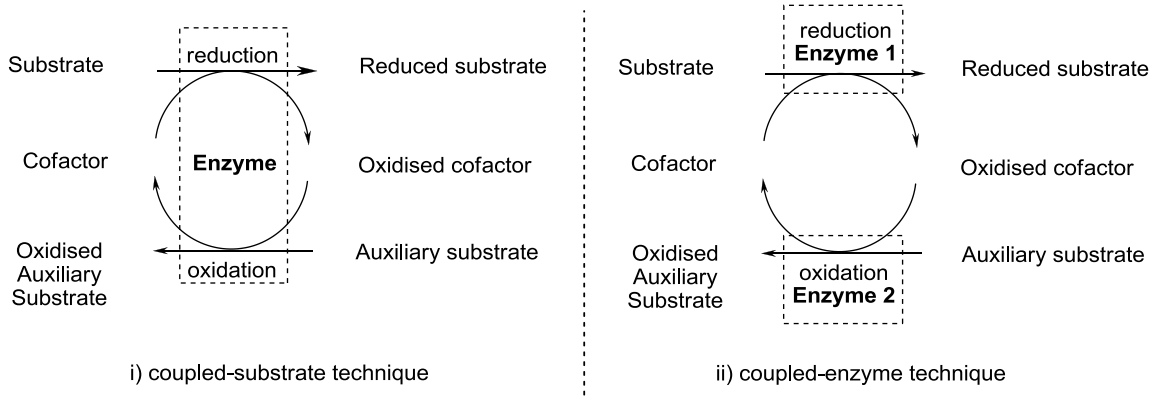

Figure 1.13. Enzymatic recycling of nicotinamide cofactors.

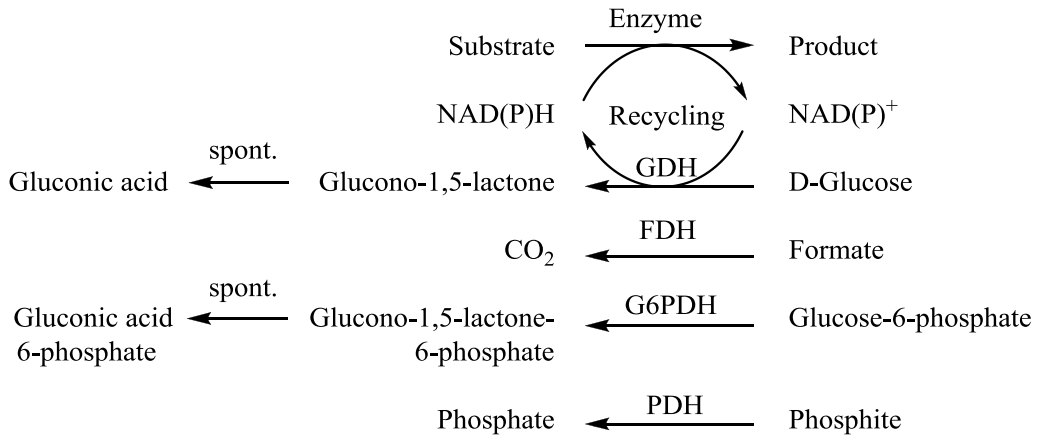

Figure 1.14. Recycling of NAD(P)H *via* coupled-enzyme method (GDH = glucose dehydrogenase, FDH = formate dehydrogenase, G6PDH = glucose-6-phosphate dehydrogenase, PDH = phosphite dehydrogenase).

Cofactor recycling in biotransformations employing enoate reductases hitherto has been performed by either complex electro-microbial or -enzymatic cofactor recycling systems, based on toxic mediators, such as methylviologen Paraquat^{TM} [66, 70, 82, 138], or the traditional "coupled-enzyme" approach using FDH, GDH, G6PDH and more recently phosphite dehydrogenase [17, 25, 74, 87, 88, 139, 140].

Simon *et al.* used H_2 as the electron donor in conjunction with anaerobic enoate reductase from *Clostridia*. They introduced a new recycling system, where cheap and stable methylviologen is oxidized by enoate reductases to its dicationic form upon reduction of the substrate (Fig. 1.15). The dication could be continuously reduced at an electrode and the system used for electro-enzymatic reduction (isolated enoate reductase), or in the form of bacterial cells (electro-microbial reduction). (2*R*)-2-Methyl-3-phenylpropionate was prepared in 95% yield using the enoate reductase from *Clostridium* La 1. Care must be however taken that the unsaturated compounds do not react spontaneously at the electrode nor with the reduced mediator [138].

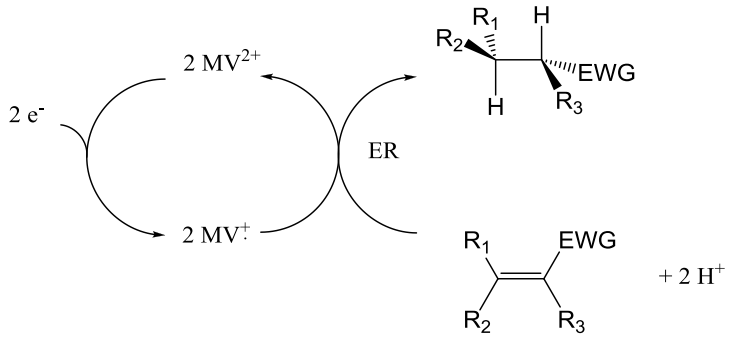

Figure 1.15. Reduction of C=C bond using methylviologen (MV) and an electrode as recycling system (EWG: electron withdrawing group, e^-: electron from a cathode, ER: enoate reductase) [138].

As members of the OYE family tend to accept both cofactors equally well, no need for a specific nicotinamide enzyme is required [60, 81]. In some cases, the use of FDH was impacted by competitive carbonyl reduction, observed when an aldehyde moiety was present in the substrate. *Prim*-ADH activity in the commercial crude FDH preparation was inferred [87]. Furthermore, the need for additional divalent metal ions in the reaction mixture was recently reported to be necessary in the reduction of dicarboxylic acids to render the cofactor recycling feasible [85]. Despite those good results, limitations appear in the use of such systems. By coupling Yers-ER with glucose dehydrogenase (GDH) to recycle NADP(H), conversion of >99% within one hour was obtained for the reduction of 2-cyclohexenone. However, upon lowering the loadings of Yers-ER and GDH, rapid deactivation of either enzyme was observed due to the presence of enone substrate, rather than oxygen or elevated temperature. The stability limitations need to be overcome to envision large-scale use of enoate reductases in synthesis [17]. Enone toxicity was circumvented *via* the use of *E. coli* whole cells expressing the enoate reductase, along with a NADPH regeneration system [88].

Most recently, the combination of YqjM from *Bacillus subtilis* with visible light was used for the reductive regeneration of flavin, as flavins can be photochemically reduced by using simple sacrificial electron donors such as amines (e.g. EDTA). This

light-driven direct regeneration system was successfully employed for the reduction of ketoisophorone, yielding quantitatively (6*R*)-levodione with decent enantioselectivity (88% ee) but only very modest turnover number and frequency (TON = 383; TOF = 194 h^{-1}) [141].

1.4.3. Examples of industrial synthesis

Enoate reductases selectively catalyze the reduction of C=C bonds in a strict *trans*-fashion, leading to the creation of up to two new stereogenic centers and thus constituting a valuable tool in asymmetric synthesis. Their exquisite chemo- and regio-selectivity contributes to promote their use in industrial applications, as enantiopure compounds are becoming the standard, especially in the manufacturing of pharmaceuticals. 66% of the new drugs introduced in 2000 were indeed single enantiomers, compared with 21% in 1991 [142]. In 2001, single-enantiomer drugs represented 36% of the total drug market [143]. Currently, applications in non-food industries favor the use of recombinant enoate reductases and isolated enzymes over whole cells of wild-type microorganisms.

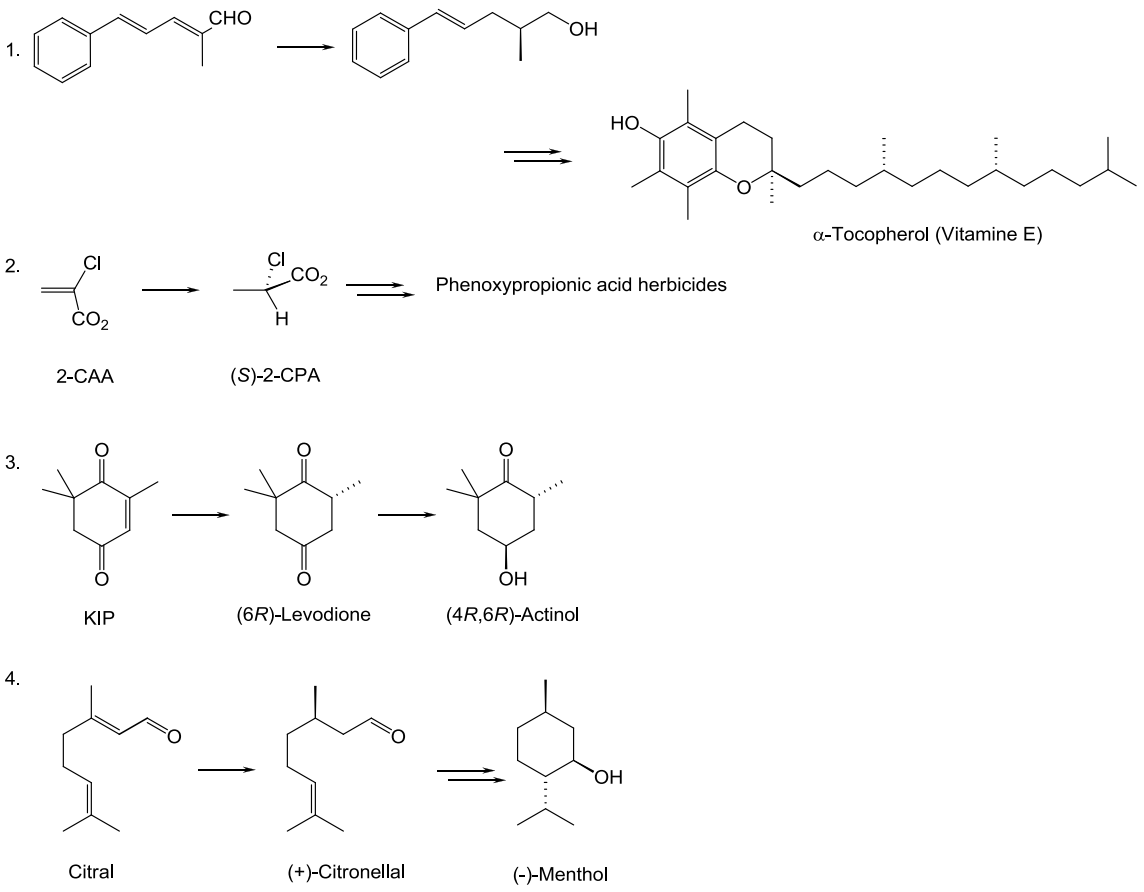

Figure 1.16. Examples of industrial syntheses implying reduction of C=C bonds (1. 2-Methyl-5-phenyl-2,4-pentadienal to (*S*)-2-Methyl-5-phenyl-4-penten-1-ol; 2. 2-CAA: 2-Chloroacrylic acid to 2-CPA: 2-Chloropropionic acid; 3. KIP: ketoisophorone to (6*R*)-levodione; 4. Citral to (+)-citronellal) [41, 144-147].

The synthesis of α-tocopherol (vitamin E) represents a challenge for synthetic chemists due to the presence of three stereocenters in the C_{29} framework of the molecule. One early method for the production of natural α-tocopherol involved the asymmetric transformation of non-conventional substrates by baker's yeast starting from derivatives of 5-phenylpenta-2,4-dienal and clearly involving enoate reductase activity [144] (Fig. 1.16-1).

(*R*)-2-Chloropropionic acid (CPA) is used as a building block for the synthesis of phenoxypropionic acid herbicides (activity due to their (*R*)-isomers). The industrial synthesis of this class of herbicide involves the resolution of a racemic 2-CPA mixture,

via the enantioselective degradation of (*R*)-2-CPA by (*R*)-2-haloacid dehalogenase [148]. This kinetic resolution allows a maximum of 50% yield; therefore, asymmetric synthesis leading directly to the (*R*)-enantiomer would be valuable. A reductase from *Burkholderia sp.* WS has been shown to display activity in the asymmetric reduction of the carbon–carbon double bond in 2-chloroacrylic acid (2-CAA), yielding (*R*)-2-CPA [41]. However, this enzyme was later identified as a 2-haloacrylate reductase [149]. Using recombinant *E. coli* cells coexpressing 2-haloacrylate reductase and a glucose dehydrogenase for NADPH regeneration, 37.4 g/l of enantiopure (*S*)-2-CPA were produced after 30 h, starting at a relatively high 2-CAA concentration of 385 mM [150] (Fig 1.16-2).

(4*R*,6*R*)-Actinol ((4*R*,6*R*)-4-hydroxy-2,2,6-trimethylcyclohexanone) is a useful intermediate for the synthesis of carotenoids, such as zeaxanthin, cryptoxanthin and xanthoxin [151-153]. Common synthetic strategies use ketoisophorone (KIP; 2,6,6-trimethyl-2-cyclohexen-1,4-dione) as starting material, which upon asymmetric hydrogenation of the C=C bond forms (6*R*)-levodione (2,2,6-trimethylcyclohexane-1,4-dione). Levodione is subsequently converted to enantiopure actinol *via* the asymmetric reduction of the carbonyl group (Fig 1.16-3).

One early (partially) microbial method referred to the stereoselective fermentative hydrogenation of KIP using baker's yeast and subsequent reduction of (6*R*)-levodione in the presence of $Al(CHMe_2)_3$ or a Ni catalyst. More than two weeks were required to produce 60 mg/ml of (6*R*)-levodione (with the necessity of adding KIP continuously to prevent substrate inhibition) [151].

The first successful report of a full enzymatic system was made of a two-step enzymatic asymmetric reduction system in which OYE2 from *Saccharomyces cerevisiae* expressed in *E. coli* was used to stereospecifically reduce KIP to levodione, which was thereafter converted to the optically pure corresponding alcohol by levodione reductase from *Corynebacterium aquaticum* M-13, also expressed in *E. coli*. A glucose dehydrogenase was used in both steps for cofactor (NADH) recycling. Full conversion of

a 1% (wt/v) KIP aqueous solution was achieved within 2.5 h, yielding 9.5 mg of (4*R*,6*R*)-actinol (94% ee) [145]. The microbial reduction of KIP to (6*R*)-levodione using growing cells of *Saccharomyces cerevisiae* was reported later, where *in situ* product crystallization (ISPC) was applied to prevent further degradation of levodione to unwanted by-products. A concentration of 100 g/l of enantiopure product was reached, corresponding to 85% yield (volumetric productivity of 0.92 g/l/h) [154]. The asymmetric reduction of KIP to (6*R*)-levodione has been also accomplished using *E. coli* cells co-expressing both OYE from *Candida macedoniensis* and a glucose dehydrogenase, rendering this synthesis of levodione highly advantageous. A 10% (wt/v) KIP solution was thus almost stoichiometrically converted to (6*R*)-levodione within 5.5 h (production efficiency of 18 g/l/h) [155].

The production of flavor and fragrances represents a promising market for biocatalysis, as products labeled 'natural' are more appreciated by consumers. As flavor-bearing chiral molecules usually occur as single enantiomers and different enantiomers often have different organoleptic properties, it is crucial to produce the right stereoisomer of the molecule [156]. Menthol is one of the most important flavoring chemicals due to its wide utilization (only (-)-menthol has the desired properties). Its estimated world production reached 19,000 metric tons in 2007 [152]. The Takasago process employs myrcene as starting material and a chiral rhodium phosphine catalyst (rhodium BINAP) for the asymmetric synthesis of (*R*)-(+)-citronellal, followed by cyclisation and hydrogenation reactions to yield (-)-menthol [146] (Fig. 1.16-4). Enoate reductases could potentially be introduced in the process as they reduce the α,β-unsaturated bond of citral, an antimicrobial terpene, to produce citronellal [51, 52] (one example of a pure synthetic route from citral exists but mixtures of menthol enantiomers were obtained [147]). This reducing activity is well spread among microorganisms and both enantiomers can be obtained in pure form [51]. When using whole cells, a two liquid phase system was employed and suppressed the competing activities [25, 51] leading to both substrate and

product depletion observed [52]. This drawback was also circumvented by using isolated recombinant enzymes [60, 81]. The use of recombinant *E. coli* overexpressing *Zymomonas mobilis* NCR, coupled with a cofactor regeneration system ($NADP^+$/GDH) in a binary solvent system (10% isopropanol (v/v)), led to a productivity of 9 mM/h for (*S*)-citronellal, starting from 20 mM citral, without any by-products being detected [25].

1.5 References

[1] A. S.Bommarius and B. R. Riebel, *Biocatalysis: Fundamentals and Applications*: Wiley-VCH; 1 edition 2004.

[2] K. Faber, *Biotransformations in Organic Chemistry: A Textbook* 2004.

[3] D. Voet and J. G. Voet, *Biochemistry* vol. Wiley; 3 edition 2004.

[4] A. Schmid, *et al.*, "Industrial biocatalysis today and tomorrow," *Nature*, vol. 409, pp. 258-268, Jan 11 2001.

[5] H. E. Schoemaker, *et al.*, "Dispelling the myths - Biocatalysis in industrial synthesis," *Science*, vol. 299, pp. 1694-1697, Mar 14 2003.

[6] D. J. Pollard and J. M. Woodley, "Biocatalysis for pharmaceutical intermediates: the future is now," *Trends in Biotechnology*, vol. 25, pp. 66-73, Feb 2007.

[7] K. Stott, *et al.*, "Old Yellow Enzyme - the Discovery of Multiple Isozymes and a Family of Related Proteins," *Journal of Biological Chemistry*, vol. 268, pp. 6097-6106, Mar 25 1993.

[8] M. W. Fraaije and A. Mattevi, "Flavoenzymes: diverse catalysts with recurrent features," *Trends in Biochemical Sciences*, vol. 25, pp. 126-132, Mar 2000.

[9] V. Massey, "The chemical and biological versatility of riboflavin," *Biochemical Society Transactions*, vol. 28, pp. 283-296, Aug 2000.

[10] O. Warburg and W. Christian, "Yellow enzyme and its effects.," *Biochemische Zeitschrift*, vol. 266, pp. 377-411, 1933.

[11] R. E. Williams and N. C. Bruce, "'New uses for an Old Enzyme' - the Old Yellow Enzyme family of flavoenzymes," *Microbiology-Sgm*, vol. 148, pp. 1607-1614, Jun 2002.

[12] R. Stuermer, *et al.*, "Asymmetric bioreduction of activated C=C bonds using enoate reductases from the old yellow enzyme family," *Current Opinion in Chemical Biology*, vol. 11, pp. 203-213, Apr 2007.

[13] B. K. Kubata, *et al.*, "A key role for old yellow enzyme in the metabolism of drugs by Trypanosoma cruzi," *Journal of Experimental Medicine*, vol. 196, pp. 1241-1251, Nov 4 2002.

[14] O. Adachi, *et al.*, "Occurrence of Old Yellow Enzyme in Gluconobacter-Suboxydans, and the Cyclic Regeneration of Nadp," *Journal of Biochemistry*, vol. 86, pp. 699-709, 1979.

[15] K. Saito, *et al.*, "The Cloning and Expression of a Gene Encoding Old Yellow Enzyme from Saccharomyces-Carlsbergensis," *Journal of Biological Chemistry*, vol. 266, pp. 20720-20724, Nov 5 1991.

[16] P. A. Karplus, *et al.*, "Flavoprotein structure and mechanism .8. Structure-function relations for old yellow enzyme," *Faseb Journal*, vol. 9, pp. 1518-1526, Dec 1995.

[17] J. F. Chaparro-Riggers, *et al.*, "Comparison of three enoate reductases and their potential use for biotransformations," *Advanced Synthesis & Catalysis*, vol. 349, pp. 1521-1531, Jun 2007.

[18] M. Miranda, *et al.*, "Nucleotide-Sequence and Chromosomal Localization of the Gene Encoding the Old Yellow Enzyme from Kluyveromyces-Lactis," *Yeast*, vol. 11, pp. 459-465, Apr 30 1995.

[19] M. Kataoka, *et al.*, "Old Yellow Enzyme from Candida macedoniensis catalyzes the stereospecific reduction of the C=Cbond of ketoisophorone," *Bioscience Biotechnology and Biochemistry*, vol. 66, pp. 2651-2657, Dec 2002.

[20] M. Uchiyama, *et al.*, "Evidence of Hydrogenation of Cis-2 Double Bonding on a Way of Beta-Oxidation by Escherichia Coli," *Journal of Biochemistry*, vol. 65, pp. 977-&, 1969.

[21] M. Mizugaki, *et al.*, "Studies on the Metabolism of Unsaturated Fatty-Acids .4. N-Ethylmaleimide Reducing Activity in Escherichia-Coli K-12," *Chemical & Pharmaceutical Bulletin*, vol. 29, pp. 570-573, 1981.

[22] T. Nishimaki, *et al.*, "Studies on the Metabolism of Unsaturated Fatty-Acids .14. Purification and Properties of Nadph-Dependent Trans-2-Enoyl-Coa Reductase of Escherichia-Coli K-12," *Journal of Biochemistry*, vol. 95, pp. 1315-1321, 1984.

[23] N. D. Madani, *et al.*, "Candida-Albicans Estrogen-Binding Protein Gene Encodes an Oxidoreductase That Is Inhibited by Estradiol," *Proceedings of the National*

Academy of Sciences of the United States of America, vol. 91, pp. 922-926, Feb 1 1994.

[24] T. B. Fitzpatrick, *et al.*, "Characterization of YqjM, an old yellow enzyme homolog from Bacillus subtilis involved in the oxidative stress response," *Journal of Biological Chemistry*, vol. 278, pp. 19891-19897, May 30 2003.

[25] A. Muller, *et al.*, "Asymmetric alkene reduction by yeast old yellow enzymes and by a novel Zymomonas mobilis reductase," *Biotechnology and Bioengineering*, vol. 98, pp. 22-29, Sep 1 2007.

[26] A. Brige, *et al.*, "Comparative characterization and expression analysis of the four Old Yellow Enzyme homologues from Shewanella oneidensis indicate differences in physiological function," *Biochemical Journal*, vol. 394, pp. 335-344, Feb 15 2006.

[27] C. E. French and N. C. Bruce, "Bacterial morphinone reductase is related to Old Yellow Enzyme," *Biochemical Journal*, vol. 312, pp. 671-678, Dec 15 1995.

[28] C. E. French, *et al.*, "Sequence and properties of pentaerythritol tetranitrate reductase from Enterobacter cloacae PB2," *Journal of Bacteriology*, vol. 178, pp. 6623-6627, Nov 1996.

[29] D. S. Blehert, *et al.*, "Cloning and sequence analysis of two Pseudomonas flavoprotein xenobiotic reductases," *Journal of Bacteriology*, vol. 181, pp. 6254-6263, Oct 1999.

[30] J. J. Griese, *et al.*, "Xenobiotic reductase A in the degradation of quinoline by Pseudomonas putida 86: Physiological function, structure and mechanism of 8-hydroxycoumarin reduction," *Journal of Molecular Biology*, vol. 361, pp. 140-152, Aug 4 2006.

[31] S. J. Marshall, *et al.*, "Characterization of glycerol trinitrate reductase (NerA) and the catalytic role of active-site residues," *Journal of Bacteriology*, vol. 186, pp. 1802-1810, Mar 2004.

[32] F. Schaller, *et al.*, "12-oxophytodienoate-10,11-reductase: Occurrence of two isoenzymes of different specificity against stereoisomers of 12-oxophytodienoic acid," *Plant Physiology*, vol. 118, pp. 1345-1351, Dec 1998.

[33] J. Strassner, *et al.*, "Characterization and cDNA-microarray expression analysis of 12-oxophytodienoate reductases reveals differential roles for octadecanoid biosynthesis in the local versus the systemic wound response," *Plant Journal*, vol. 32, pp. 585-601, Nov 2002.

[34] H. Matsui, *et al.*, "Structure and expression of 12-oxophytodienoate reductase (subgroup I) genes in pea, and characterization of the oxidoreductase activities of

their recombinant products," *Molecular Genetics and Genomics,* vol. 271, pp. 1-10, Feb 2004.

[35] J. L. Zhang, *et al.*, "Genomic analysis of the 12-oxo-phytodienoic acid reductase gene family of Zea mays," *Plant Molecular Biology,* vol. 59, pp. 323-343, Sep 2005.

[36] H. Sobajima, *et al.*, "Cloning and characterization of a jasmonic acid-responsive gene encoding 12-oxophytodienoic acid reductase in suspension-cultured rice cells," *Planta,* vol. 216, pp. 692-698, Feb 2003.

[37] B. A. Vick and D. C. Zimmerman, "Characterization of 12-Oxo-Phytodienoic Acid Reductase in Corn - the Jasmonic Acid Pathway," *Plant Physiology,* vol. 80, pp. 202-205, Jan 1986.

[38] Y. Yamazaki, *et al.*, "Microbial Conversion of 4-Oxoisophorone by Aspergillus-Niger," *Agricultural and Biological Chemistry,* vol. 52, pp. 2919-2920, Nov 1988.

[39] A. Arnone, *et al.*, "Enantioselective Reduction of Racemic Abscisic-Acid by Aspergillus-Niger Cultures," *Journal of the Chemical Society-Perkin Transactions 1,* pp. 3061-3063, Nov 1990.

[40] B. C. C. Cantello, *et al.*, "Facile Biocatalytic Reduction of the Carbon-Carbon Double-Bond of 5-Benzylidenethiazolidine-2,4-Diones - Synthesis of (+/-)-5-(4-(2-[Methyl(2-Pyridyl)Amino]Ethoxy)Benzyl)Thiazolidine-2,4-Dione (Brl-49653), Its (R)-(+)-Enantiomer and Analogs," *Journal of the Chemical Society-Perkin Transactions 1,* pp. 3319-3324, Nov 21 1994.

[41] A. Kurata, *et al.*, "Asymmetric reduction of 2-chloroacrylic acid to (S)-2-chloropropionic acid by a novel reductase from Burkholderia sp WS," *Tetrahedron-Asymmetry,* vol. 15, pp. 2837-2839, Sep 20 2004.

[42] T. Hirata, *et al.*, "Asymmetric hydrogenation of N-substituted maleimides by cultured plant cells," *Tetrahedron-Asymmetry,* vol. 15, pp. 15-16, Jan 12 2004.

[43] K. Shimoda, *et al.*, "Asymmetric reduction of alpha,beta-unsaturated carbonyl compounds with reductases from Nicotiana tabacum," *Tetrahedron-Asymmetry,* vol. 15, pp. 2443-2446, Aug 9 2004.

[44] H. Korbekandi, *et al.*, "Reduction of aliphatic nitro groups using an obligately anaerobic whole cell biocatalyst," *Enzyme and Microbial Technology,* vol. 42, pp. 308-314, Mar 4 2008.

[45] K. Shimoda, *et al.*, "Asymmetric reduction of enones with Synechococcus sp PCC 7942," *Tetrahedron-Asymmetry,* vol. 15, pp. 1677-1679, Jun 7 2004.

[46] K. Shimoda, *et al.*, "Stereoselective reduction of 2-butenolides to chiral butanolides by reductases from cultured cells of Glycine max," *Tetrahedron Letters,* vol. 48, pp. 1345-1347, Feb 19 2007.

[47] K. Shimoda and T. Hirata, "Biotransformation of enones with biocatalysts - two enone reductases from Astasia longa," *Journal of Molecular Catalysis B-Enzymatic,* vol. 8, pp. 255-264, Feb 18 2000.

[48] M. E. F. Hegazy, *et al.*, "Asymmetric hydrogenation of the C-C double bond of 1- and 1,2-methylated maleimides with cultured suspension cells of Marchantia polymorpha," *Tetrahedron-Asymmetry,* vol. 17, pp. 1859-1862, Jul 31 2006.

[49] F. Foroughi, *et al.*, "Reduction of carbon-carbon double bonds using Acetobacterium woodii: Determination of the optimum inducer structure," *Enzyme and Microbial Technology,* vol. 39, pp. 1066-1071, Sep 4 2006.

[50] E. T. Davies and G. M. Stephens, "Efficient mediator-independent hydrogenation of carbon-carbon double bonds, using the obligate anaerobe, Acetobacterium woodii, with fructose as an electron donor," *Applied Microbiology and Biotechnology,* vol. 46, pp. 615-618, Dec 1996.

[51] A. Muller, *et al.*, "Enzymatic reduction of the alpha,beta-unsaturated carbon bond in citral," *Journal of Molecular Catalysis B-Enzymatic,* vol. 38, pp. 126-130, Mar 15 2006.

[52] M. Hall, *et al.*, "Asymmetric whole-cell bioreduction of an alpha,beta-unsaturated aldehyde (citral): competing prim-alcohol dehydrogenase and C-C lyase activities," *Tetrahedron-Asymmetry,* vol. 17, pp. 3058-3062, Nov 17 2006.

[53] T. Hirata, *et al.*, "Asymmetric hydrogenation of the C-C double bond of enones with the reductases from Nicotiana tabacum," *Chemistry Letters,* pp. 850-851, Aug 5 2000.

[54] A. Matsushima, *et al.*, "An enone reductase from Nicotiana tabacum: cDNA cloning, expression in Escherichia coli, and reduction of enones with the recombinant proteins," *Bioorganic Chemistry,* vol. 36, pp. 23-28, Feb-Jun 2008.

[55] M. A. Larkin, *et al.*, "Clustal W and clustal X version 2.0," *Bioinformatics,* vol. 23, pp. 2947-2948, Nov 1 2007.

[56] O. Warburg and W. Christian, "On the yellow oxidation-enzyme.," *Biochemische Zeitschrift,* vol. 257, pp. 492-492, 1933.

[57] H. Theorell and A. P. Nygaard, "The Linkages between Fmn and the Protein of the Old Yellow Enzyme Studied by Means of Fluorescence Measurements," *Arkiv for Kemi,* vol. 7, pp. 205-209, 1954.

[58] O. Odat, *et al.*, "Old yellow enzymes, highly homologous FMN oxidoreductases with modulating roles in oxidative stress and programmed cell death in yeast," *Journal of Biological Chemistry,* vol. 282, pp. 36010-36023, Dec 7 2007.

[59] A. D. N. Vaz, *et al.*, "Old Yellow Enzyme - Aromatization of Cyclic Enones and the Mechanism of a Novel Dismutation Reaction," *Biochemistry,* vol. 34, pp. 4246-4256, Apr 4 1995.

[60] M. Hall, *et al.*, "Asymmetric bioreduction of activated C = C bonds using Zymomonas mobilis NCR enoate reductase and old yellow enzymes OYE 1-3 from yeasts," *European Journal of Organic Chemistry,* pp. 1511-1516, Mar 2008.

[61] P. van Dillewijn, *et al.*, "Type II Hydride Transferases from Different Microorganisms Yield Nitrite and Diarylamines from Polynitroaromatic Compounds," *Applied and Environmental Microbiology,* vol. 74, pp. 6820-6823, Nov 2008.

[62] P. van Dillewijn, *et al.*, "Subfunctionality of Hydride Transferases of the Old Yellow Enzyme Family of Flavoproteins of Pseudomonas putida," *Applied and Environmental Microbiology,* vol. 74, pp. 6703-6708, Nov 2008.

[63] J. W. Pak, *et al.*, "Transformation of 2,4,6-trinitrotoluene by purified xenobiotic reductase B from Pseudomonas fluorescens I-C," *Applied and Environmental Microbiology,* vol. 66, pp. 4742-4750, Nov 2000.

[64] A. Basran, *et al.*, "Degradation of nitrate ester and nitroaromatic explosives by Enterobacter cloacae PB2," *Biochemical Society Transactions,* vol. 26, pp. 680-685, Nov 1998.

[65] J. R. Snape, *et al.*, "Purification, properties, and sequence of glycerol trinitrate reductase from Agrobacterium radiobacter," *Journal of Bacteriology,* vol. 179, pp. 7796-7802, Dec 1997.

[66] W. Tischer, *et al.*, "Purification and Some Properties of a Hitherto-Unknown Enzyme Reducing the Carbon-Carbon Double-Bond of Alpha,Beta-Unsaturated Carboxylate Anions," *European Journal of Biochemistry,* vol. 97, pp. 103-112, 1979.

[67] M. Buhler, *et al.*, "Occurrence and the Possible Physiological-Role of 2-Enoate Reductases," *Febs Letters,* vol. 109, pp. 244-246, 1980.

[68] W. Tischer, *et al.*, "2-Enoate-Reductase, an Iron-Sulfur Flavoprotein Reducing Non-Activated Delta-2-Carboxylic Acids," *Hoppe-Seylers Zeitschrift Fur Physiologische Chemie,* vol. 359, pp. 1157-1157, 1978.

[69] S. Kuno, *et al.*, "Structure of Enoate Reductase from a Clostridium-Tyrobutyricum (C Spec La1)," *Biological Chemistry Hoppe-Seyler,* vol. 366, pp. 463-472, 1985.

[70] F. Rohdich, *et al.*, "Enoate reductases of Clostridia - Cloning, sequencing, and expression," *Journal of Biological Chemistry,* vol. 276, pp. 5779-5787, Feb 23 2001.

[71] A. Fryszkowska, *et al.*, "Highly enantioselective reduction of beta,beta-disubstituted aromatic nitroalkenes catalyzed by Clostridium sporogenes," *Journal of Organic Chemistry,* vol. 73, pp. 4295-4298, Jun 6 2008.

[72] B. F. Smets, *et al.*, "TNT biotransformation: when chemistry confronts mineralization," *Appl Microbiol Biotechnol,* vol. 76, pp. 267-77, Aug 2007.

[73] R. Stuermer, *et al.*, "Asymmetric bioreduction of activated C=C bonds using enoate reductases from the old yellow enzyme family," *Curr Opin Chem Biol,* vol. 11, pp. 203-13, Apr 2007.

[74] B. Kosjek, *et al.*, "Asymmetric bioreduction of alpha,beta-unsaturated nitriles and ketones," *Tetrahedron-Asymmetry,* vol. 19, pp. 1403-1406, Jun 30 2008.

[75] V. Massey, "Activation of Molecular-Oxygen by Flavins and Flavoproteins," *Journal of Biological Chemistry,* vol. 269, pp. 22459-22462, Sep 9 1994.

[76] P. D'Arrigo, *et al.*, "Old and new synthetic capacities of baker's yeast," *Adv Appl Microbiol,* vol. 44, pp. 81-123, 1997.

[77] C. Fuganti and P. Grasselli, "Stereochemistry and synthetic applications of products of fermentation of alpha,beta-unsaturated aromatic aldehydes by baker's yeast," *Ciba Found Symp,* vol. 111, pp. 112-27, 1985.

[78] G. Fronza, *et al.*, "Stereochemical aspects of flavour biogeneration through baker's yeast mediated reduction of carbonyl-activated double bonds," *Pure and Applied Chemistry,* vol. 68, pp. 2065-2071, Nov 1996.

[79] Y. Kawai, *et al.*, "Asymmetric synthesis of alpha-chiral ketones by the reduction of enones with baker's yeast," *Tetrahedron-Asymmetry,* vol. 12, pp. 3007-3013, Nov 26 2001.

[80] A. Muller, *et al.*, "Stereospecific alkyne reduction: Novel activity of old yellow enzymes," *Angewandte Chemie-International Edition,* vol. 46, pp. 3316-3318, 2007.

[81] M. Hall, *et al.*, "Asymmetric bioreduction of C=C bonds using enoate reductases OPR1, OPR3 and YqjM: Enzyme-based stereocontrol," *Advanced Synthesis & Catalysis,* vol. 350, pp. 411-418, Feb 2008.

[82] R. Eck and H. Simon, "Preparation of (S)-2-Substituted Succinates by Stereospecific Reductions of Fumarate and Derivatives with Resting Cells of Clostridium-Formicoaceticum," *Tetrahedron,* vol. 50, pp. 13631-13640, Nov 28 1994.

[83] K. Takabe, *et al.*, "Bakers-Yeast Reduction of 3-Phenylthiomethyl-2-Butenolide and Its Derivatives - Synthesis of Versatile Chiral C5-Building Blocks for Terpenoid Synthesis," *Tetrahedron-Asymmetry,* vol. 3, pp. 1399-1400, Nov 1992.

[84] M. Utaka, *et al.*, "Asymmetric Reduction of the Prochiral Carbon Carbon Double-Bond of Methyl 2-Chloro-2-Alkenoates by Use of Fermenting Bakers-Yeast," *Journal of Organic Chemistry,* vol. 54, pp. 4989-4992, Oct 13 1989.

[85] C. Stueckler, *et al.*, "Stereocomplementary bioreduction of alpha,beta-unsaturated dicarboxylic acids and dimethyl esters using enoate reductases: Enzyme- and substrate-based stereocontrol," *Organic Letters,* vol. 9, pp. 5409-5411, Dec 20 2007.

[86] H. S. Toogood, *et al.*, "Structure-Based Insight into the Asymmetric Bioreduction of the C=C Double Bond of alpha,beta-Unsaturated Nitroalkenes by Pentaerythritol Tetranitrate Reductase," *Advanced Synthesis & Catalysis,* vol. 350, pp. 2789-2803, Nov 2008.

[87] M. Hall, *et al.*, "Asymmetric bioreduction of activated alkenes using cloned 12-oxophytodienoate reductase isoenzymes OPR-1 and OPR-3 from Lycopersicon esculentum (Tomato): A striking change of stereoselectivity," *Angewandte Chemie-International Edition,* vol. 46, pp. 3934-3937, 2007.

[88] M. A. Swiderska and J. D. Stewart, "Stereoselective enone reductions by Saccharomyces carlsbergensis old yellow enzyme," *Journal of Molecular Catalysis B-Enzymatic,* vol. 42, pp. 52-54, Oct 2 2006.

[89] J. Hawari, *et al.*, "Microbial degradation of explosives: biotransformation versus mineralization," *Applied Microbiology and Biotechnology,* vol. 54, pp. 605-618, Nov 2000.

[90] J. L. Ramos, *et al.*, "Bioremediation of polynitrated aromatic compounds: plants and microbes put up a fight," *Current Opinion in Biotechnology,* vol. 16, pp. 275-281, Jun 2005.

[91] Z. C. Symons and N. C. Bruce, "Bacterial pathways for degradation of nitroaromatics," *Natural Product Reports,* vol. 23, pp. 845-850, 2006.

[92] J. Rau and A. Stolz, "Oxygen-insensitive nitroreductases NfsA and NfsB of Escherichia coli function under anaerobic conditions as lawsone-dependent azo reductases," *Applied and Environmental Microbiology,* vol. 69, pp. 3448-3455, Jun 2003.

[93] M. R. Nokhbeh, *et al.*, "Identification and characterization of SnrA, an inducible oxygen-insensitive nitroreductase in Salmonella enterica serovar Typhimurium TA1535," *Mutation Research-Fundamental and Molecular Mechanisms of Mutagenesis,* vol. 508, pp. 59-70, Oct 31 2002.

[94] A. Caballero, *et al.*, "PnrA, a new nitroreductase-family enzyme in the TNT-degrading strain Pseudomonas putida JLR11," *Environmental Microbiology,* vol. 7, pp. 1211-1219, Aug 2005.

[95] B. F. Smets, *et al.*, "TNT biotransformation: when chemistry confronts mineralization," *Applied Microbiology and Biotechnology,* vol. 76, pp. 267-277, Aug 2007.

[96] C. E. French, *et al.*, "Biodegradation of explosives by transgenic plants expressing pentaerythritol tetranitrate reductase," *Nature Biotechnology,* vol. 17, pp. 491-494, May 1999.

[97] K. Miura, *et al.*, "Molecular cloning of the nemA gene encoding N-ethylmaleimide reductase from Escherichia coli," *Biological & Pharmaceutical Bulletin,* vol. 20, pp. 110-112, Jan 1997.

[98] Y. Meah, *et al.*, "Old yellow enzyme: Reduction of nitrate esters, glycerin trinitrate, and propylene 1,2-dinitrate," *Proceedings of the National Academy of Sciences of the United States of America,* vol. 98, pp. 8560-8565, Jul 17 2001.

[99] C. E. French, *et al.*, "Aerobic degradation of 2,4,6-trinitrotoluene by Enterobacter cloacae PB2 and by pentaerythritol tetranitrate reductase," *Applied and Environmental Microbiology,* vol. 64, pp. 2864-2868, Aug 1998.

[100] M. M. Gonzalez-Perez, *et al.*, "Escherichia coli has multiple enzymes that attack TNT and release nitrogen for growth," *Environmental Microbiology,* vol. 9, pp. 1535-1540, Jun 2007.

[101] R. E. Williams, *et al.*, "Biotransformation of explosives by the old yellow enzyme family of flavoproteins," *Applied and Environmental Microbiology,* vol. 70, pp. 3566-3574, Jun 2004.

[102] R. M. Wittich, *et al.*, "OYE flavoprotein reductases initiate the condensation of TNT-derived intermediates to secondary diarylamines and nitrite," *Environmental Science & Technology,* vol. 42, pp. 734-739, Feb 1 2008.

[103] H. Khan, *et al.*, "Kinetic and structural basis of reactivity of pentaerythritol tetranitrate reductase with NADPH, 2-cyclohexenone, nitroesters, and nitroaromatic explosives," *Journal of Biological Chemistry*, vol. 277, pp. 21906-21912, Jun 14 2002.

[104] D. S. Blehert, *et al.*, "Regioselectivity of nitroglycerin denitration by flavoprotein nitroester reductases purified from two Pseudomonas species," *Journal of Bacteriology*, vol. 179, pp. 6912-6920, Nov 1997.

[105] H. Nivinskas, *et al.*, "Reduction of aliphatic nitroesters and N-nitramines by Enterobacter cloacae PB2 pentaerythritol tetranitrate reductase," *Febs Journal*, vol. 275, pp. 6192-6203, Dec 2008.

[106] Y. Meah and V. Massey, "Old Yellow Enzyme: Stepwise reduction of nitro-olefins and catalysis of aci-nitro tautomerization," *Proceedings of the National Academy of Sciences of the United States of America*, vol. 97, pp. 10733-10738, Sep 26 2000.

[107] R. M. Kohli and V. Massey, "The oxidative half-reaction of old yellow enzyme - The role of tyrosine 196," *Journal of Biological Chemistry*, vol. 273, pp. 32763-32770, Dec 4 1998.

[108] D. Xu, *et al.*, "The role of threonine 37 in flavin reactivity of the old yellow enzyme," *Proceedings of the National Academy of Sciences of the United States of America*, vol. 96, pp. 3556-3561, Mar 30 1999.

[109] B. J. Brown, *et al.*, "The role of glutamine 114 in Old Yellow Enzyme," *Journal of Biological Chemistry*, vol. 277, pp. 2138-2145, Jan 18 2002.

[110] T. Barna, *et al.*, "Crystal structure of bacterial morphinone reductase and properties of the C191A mutant enzyme," *Journal of Biological Chemistry*, vol. 277, pp. 30976-30983, Aug 23 2002.

[111] T. M. Barna, *et al.*, "Crystal structure of pentaerythritol tetranitrate reductase: "Flipped" binding geometries for steroid substrates in different redox states of the enzyme," *Journal of Molecular Biology*, vol. 310, pp. 433-447, Jul 6 2001.

[112] K. M. Fox and P. A. Karplus, "Old Yellow Enzyme at 2-Angstrom Resolution - Overall Structure, Ligand-Binding, and Comparison with Related Flavoproteins," *Structure*, vol. 2, pp. 1089-1105, Nov 15 1994.

[113] C. Breithaupt, *et al.*, "Crystal structure of 12-oxophytodienoate reductase 3 from tomato: Self-inhibition by dimerization," *Proceedings of the National Academy of Sciences of the United States of America*, vol. 103, pp. 14337-14342, Sep 26 2006.

[114] K. Kitzing, *et al.*, "The 1.3 A crystal structure of the flavoprotein YqjM reveals a novel class of Old Yellow Enzymes," *Journal of Biological Chemistry*, vol. 280, pp. 27904-27913, Jul 29 2005.

[115] C. Breithaupt, *et al.*, "X-ray structure of 12-oxophytodienoate reductase 1 provides structural insight into substrate binding and specificity within the family of OYE," *Structure*, vol. 9, pp. 419-429, May 9 2001.

[116] A. M. Orville, *et al.*, "Crystallization and preliminary analysis of xenobiotic reductase B from Pseudomonas fluorescens I-C," *Acta Crystallographica Section D-Biological Crystallography*, vol. 60, pp. 1289-1291, Jul 2004.

[117] R. Noyori, "Asymmetric catalysis: Science and opportunities (Nobel lecture)," *Angewandte Chemie-International Edition*, vol. 41, pp. 2008-2022, 2002.

[118] R. Noyori, *et al.*, "Toward efficient asymmetric hydrogenation: Architectural and functional engineering of chiral molecular catalysts," *Proceedings of the National Academy of Sciences of the United States of America*, vol. 101, pp. 5356-5362, Apr 13 2004.

[119] W. S. Knowles, "Asymmetric hydrogenations (Nobel lecture)," *Angewandte Chemie-International Edition*, vol. 41, pp. 1999-2007, 2002.

[120] H. L. Messiha, *et al.*, "Role of active site residues and solvent in proton transfer and the modulation of flavin reduction potential in bacterial morphinone reductase," *Journal of Biological Chemistry*, vol. 280, pp. 27103-27110, Jul 22 2005.

[121] H. Khan, *et al.*, "Proton transfer in the oxidative half-reaction of pentaerythritol tetranitrate reductase," *Febs Journal*, vol. 272, pp. 4660-4671, Sep 2005.

[122] A. S. Abramovitz and V. Massey, "Interaction of Phenols with Old Yellow Enzyme - Physical Evidence for Charge-Transfer Complexes," *Journal of Biological Chemistry*, vol. 251, pp. 5327-5336, 1976.

[123] J. Caldeira, *et al.*, "EPR and Mossbauer spectroscopic studies on enoate reductase," *Journal of Biological Chemistry*, vol. 271, pp. 18743-18748, Aug 2 1996.

[124] W. Tischer, *et al.*, "Mechanism of Enoate Reductase," *Hoppe-Seylers Zeitschrift Fur Physiologische Chemie*, vol. 361, pp. 339-339, 1980.

[125] H. Simon, "Properties and Mechanistic Aspects of Newly Found Redox Enzymes from Anaerobes Suitable for Bioconversions on Preparatory Scale," *Pure and Applied Chemistry*, vol. 64, pp. 1181-1186, Aug 1992.

[126] F. Schaller, *et al.*, "12-oxophytodienoate reductase 3 (OPR3) is the isoenzyme involved in jasmonate biosynthesis," *Planta*, vol. 210, pp. 979-984, May 2000.

[127] B. A. Vick and D. C. Zimmerman, "Biosynthesis of Jasmonic Acid by Several Plant-Species," *Plant Physiology*, vol. 75, pp. 458-461, 1984.

[128] A. M. Hailes and N. C. Bruce, "Biological Synthesis of the Analgesic Hydromorphone, an Intermediate in the Metabolism of Morphine, by Pseudomonas-Putida M10," *Applied and Environmental Microbiology*, vol. 59, pp. 2166-2170, Jul 1993.

[129] M. Mizugaki, *et al.*, "Studies on the Metabolism of Unsaturated Fatty-Acids .9. Stereochemical Studies of the Reaction Catalyzed by Trans-2-Enoyl-Coenzyme-a Reductase of Escherichia-Coli," *Journal of Biochemistry*, vol. 92, pp. 1649-1654, 1982.

[130] H. Esterbauer, *et al.*, "Chemistry and Biochemistry of 4-Hydroxynonenal, Malonaldehyde and Related Aldehydes," *Free Radical Biology and Medicine*, vol. 11, pp. 81-128, 1991.

[131] R. Reekmans, *et al.*, "Old yellow enzyme interferes with Bax-induced NADPH loss and lipid peroxidation in yeast," *Fems Yeast Research*, vol. 5, pp. 711-725, May 2005.

[132] E. W. Trotter, *et al.*, "Old yellow enzymes protect against acrolein toxicity in the yeast Saccharomyces cerevisiae," *Applied and Environmental Microbiology*, vol. 72, pp. 4885-4892, Jul 2006.

[133] B. K. Haarer and D. C. Amberg, "Old yellow enzyme protects the actin cytoskeleton from oxidative stress," *Molecular Biology of the Cell*, vol. 15, pp. 4522-4531, Oct 2004.

[134] F. Amari, *et al.*, "Antioxidant Small Molecules Confer Variable Protection against Oxidative Damage in Yeast Mutants," *J Agric Food Chem*, Dec 2 2008.

[135] D. J. Opperman, *et al.*, "A novel chromate reductase from Thermus scotoductus SA-01 related to old yellow enzyme," *Journal of Bacteriology*, vol. 190, pp. 3076-3082, Apr 2008.

[136] C. Fuganti, "Bakers-Yeast Mediated Synthesis of Natural-Products," *Pure and Applied Chemistry*, vol. 62, pp. 1449-1452, Jul 1990.

[137] S. Servi, "Baker Yeast as a Reagent in Organic-Synthesis," *Synthesis-Stuttgart*, pp. 1-25, Jan 1990.

[138] H. Simon, *et al.*, "Electro-Enzymatic and Electro-Microbial Stereospecific Reductions," *Angewandte Chemie-International Edition in English*, vol. 20, pp. 861-863, 1981.

[139] J. M. Vrtis, *et al.*, "Phosphite dehydrogenase: A versatile cofactor-regeneration enzyme," *Angewandte Chemie-International Edition*, vol. 41, pp. 3257-+, 2002.

[140] T. W. Johannes, *et al.*, "Efficient regeneration of NADPH using an engineered phosphite dehydrogenase," *Biotechnology and Bioengineering*, vol. 96, pp. 18-26, Jan 1 2007.

[141] A. Taglieber, *et al.*, "Light-driven biocatalytic oxidation and reduction reactions: scope and limitations," *Chembiochem*, vol. 9, pp. 565-72, Mar 3 2008.

[142] I. Agranat, *et al.*, "Putting chirality to work: The strategy of chiral switches," *Nature Reviews Drug Discovery*, vol. 1, pp. 753-768, Oct 2002.

[143] A. M. Rouhi, "Chiral roundup - As pharmaceutical companies face bleak prospects, their suppliers diligently tend the fertile fields of chiral chemistry in varied ways," *Chemical & Engineering News*, vol. 80, pp. 43-+, Jun 10 2002.

[144] C. Fuganti and P. Grasselli, "Efficient Stereoselective Synthesis of Natural Alpha-Tocopherol (Vitamin-E)," *Journal of the Chemical Society-Chemical Communications*, pp. 995-997, 1979.

[145] M. Wada, *et al.*, "Production of a doubly chiral compound, (4R,6R)-4-hydroxy-2,2,6-trimethylcyclohexanone, by two-step enzymatic asymmetric reduction," *Applied and Environmental Microbiology*, vol. 69, pp. 933-937, Feb 2003.

[146] S. Akutagawa, "Enantioselective isomerization of allylamine to enamine: practical asymmetric synthesis of (-)-menthol by Rh-BINAP catalysts," *Topics in Catalysis*, vol. 4, pp. 271-274, 1997.

[147] P. Maki-Arvela, *et al.*, "One-pot citral transformation to menthol over bifunctional micro- and mesoporous metal modified catalysts: Effect of catalyst support and metal," *Journal of Molecular Catalysis a-Chemical*, vol. 240, pp. 72-81, Oct 3 2005.

[148] M. Breuer, *et al.*, "Industrial methods for the production of optically active intermediates," *Angewandte Chemie-International Edition*, vol. 43, pp. 788-824, 2004.

[149] A. Kurata, *et al.*, "2-Haloacrylate reductase, a novel enzyme of the medium chain dehydrogenase/reductase superfamily that catalyzes the reduction of a carbon-carbon double bond of unsaturated organohalogen compounds," *Journal of Biological Chemistry*, vol. 280, pp. 20286-20291, May 27 2005.

[150] A. Kurata, *et al.*, "Production of (S)-2-chloropropionate by asymmetric reduction of 2-chloroacrylate with 2-haloacrylate reductase coupled with glucose dehydrogenase," *Journal of Bioscience and Bioengineering*, vol. 105, pp. 429-431, Apr 2008.

[151] H. G. W. Leuenberger, *et al.*, "Synthesis of Optically-Active Natural Carotenoids and Structurally Related Compounds .1. Synthesis of Chiral Key Compound (4r,6r)-4-Hydroxy-2,2,6-Trimethylcyclohexanone," *Helvetica Chimica Acta*, vol. 59, pp. 1832-1849, 1976.

[152] R. Csuk and B. I. Glanzer, "Bakers-Yeast Mediated Transformations in Organic-Chemistry," *Chemical Reviews*, vol. 91, pp. 49-97, Jan-Feb 1991.

[153] R. S. Burden and H. F. Taylor, "Structure and Chemical Transformations of Xanthoxin," *Tetrahedron Letters*, pp. 4071-&, 1970.

[154] E. M. Buque-Taboada, *et al.*, "Microbial reduction and in situ product crystallization coupled with biocatalyst cultivation during the synthesis of 6R-dihydrooxoisophorone," *Advanced Synthesis & Catalysis*, vol. 347, pp. 1147-1154, Jun 2005.

[155] M. Kataoka, *et al.*, "Cloning and overexpression of the old yellow enzyme gene of Candida macedoniensis, and its application to the production of a chiral compound," *Journal of Biotechnology*, vol. 114, pp. 1-9, Oct 19 2004.

[156] E. Brenna, *et al.*, "Enantioselective perception of chiral odorants," *Tetrahedron-Asymmetry*, vol. 14, pp. 1-42, Jan 6 2003.

CHAPTER 2

INITIAL DEVELOPMENT & CHARACTERIZATION OF THREE ENOATE REDUCTASES IN THE GROUP

Enoate reductases (ERs) selectively reduce carbon-carbon double bonds in α,β-unsaturated carbonyl compounds and thus can be employed to prepare enantiomerically pure aldehydes, ketones, and esters. Most known ERs, most notably Old Yellow Enzyme (OYE), are biochemically very well characterized. Some ERs have only been used in whole-cell systems, with endogenous ketoreductases often interfering with the ER activity. Not many ERs are biocatalytically characterized as to specificity and stability. Here, the group cloned the genes and expressed three non-related ERs, two of them novel, in E. coli: XenA from *Pseudomonas putida*, KYE1 from *Kluyveromyces lactis*, and YersER from *Yersinia bercovieri*. All three proteins showed broad ER specificity and broad temperature and pH optima but different specificity patterns. All three proteins prefer NADPH as cofactor over NADH and are stable up to 40 ^{o}C. By coupling YersER with glucose dehydrogenase (GDH) to recycle NADP(H), conversion of >99% within one hour was obtained for the reduction of 2-cyclohexenone. Upon lowering the loadings of YersER and GDH, we discovered rapid deactivation of either enzyme, especially of the thermostable GDH. We found that the presence of enone substrate, rather than oxygen or elevated temperature, is responsible for deactivation. In summary, we successfully demonstrate the wide specificity of enoate reductases for a range of α,β-unsaturated carbonyl compounds as well as coupling to glucose dehydrogenase for recycling of NAD(P)(H); however, the stability limitations we found need to be overcome to envision large-scale use of ERs in synthesis.

2.1 Enoate Reductase Characterization & Purification

Three enoate reductase candidates were cloned and expressed in *E. coli*: xenobiotic reductase A (XenA) from *Pseudomonas putida*, KYE1 from *Kluyveromyces lactis*, and YersER from *Yersinia bercovieri*. Amino acid sequence identities and similarities between the three candidates with other known ERs were tabulated in Table 2.1. The three gene products were cloned into pET27 and pET28 for expression of ERs with and without N-terminal polyhistidine tag. Only XenA showed activity decrease in the presence of N-terminal histag. Both KYE1 and YersER showed same activity level with 2-cyclohexenone and were purified with Ni^{2+}-NTA bead protocol. XenA was purified according to published protocol with the combination of DEAE-column and Q-sepharose column.[1] Purification procedures of all three candidates were monitored with SDS-PAGE (Fig 2.1) to ensure the final purity before proceeding to substrate characterizations.

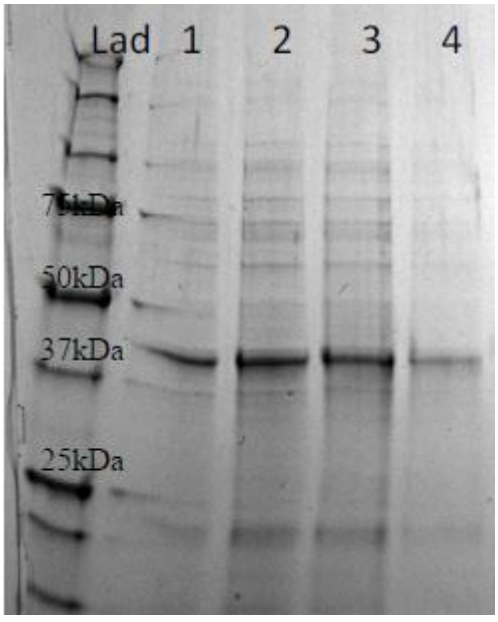

Figure 2.1. YersER purification SDS-PAGE. Lane 1: cell lysate lane 2: binding step flow through, lane 3: wash step flow through, lane 4: final eluted fraction.

The specific activity of the three ERs was calculated based on NADPH molar absorption coefficient of 6.22 $mM^{-1}cm^{-1}$ at 340 nm reading. The enzyme assay condition was standardized for substrate characterization: 200 mM sodium phosphate buffer pH 7.5, 10 mM of substrate, 0.2 mM NADPH, and 25 ^{o}C. The result showed all three candidates possessed broad substrate spectrum and successfully reduced almost all tested substrates with satisfactory specific activity (Table 2.2). The stability of the ERs was tested towards thermal deactivation at three different temperatures of 30, 37 and 45 ^{o}C, where YersER was proven to be the most thermo stable candidate with half-life of >13124 min at 45 ^{o}C. The collected data showed YersER possessed a broad substrate spectrum with overall high specific activity profiles even at high temperatures, so we decided to optimize its operating conditions by measuring activity-temperature profile and pH-activity profile. The result showed that highest activity of YersER was observed at 50 ^{o}C and pH 7. [2]

Table 2.1. Amino acid sequence identities and similarities between XenA, KYE1, and YersER with other published enoate reductases (Alligned with EMBOSS Pairwise Alignment Algorithms).

	KYE1	Yers-ER	XenA
CaMa	75/85	38/54	27/45
KYE1	-	36/53	28/48
OYE1	70/82	39/54	27/44
OYE2	70/81	38/54	29/44
OYE3	67/78	39/54	28/45
Yers-ER	36/53	-	31/47
PETN	38/51	76/85	27/41
ZYMM	32/49	41/57	32/48
XenA	28/48	31/47	-
Yqjm	30/48	32/48	39/52
OPR1	36/51	44/58	28/43
PrSa	29/47	38/54	30/45

Table 2.2. The specific activity on different α,β-unsaturated carbonyl compounds. nd = not determined

Substrate	Structure	Specific Activity [U/mg] KYE1	XenA	YersER
2-cyclohexenone	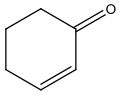	1.54	2.74	4.22
trans,trans-2,4-hexadienal	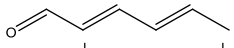	1.51	3.18	2.19
citral	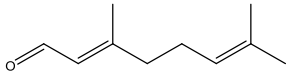	0.67	1.75	1.97
cinnamaldehyde	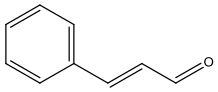	2.30	1.56	2.91
(R)-carvone	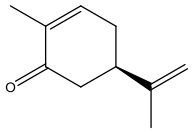	0.73	Nd	2.54
3-methyl-2-butenal	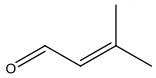	0.45	Nd	0.39
maleic anhydride	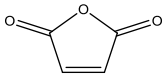	0.86	1.91	5.20
ketoisophorone	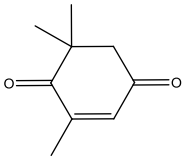	1.33	1.84	10.11
maleimide	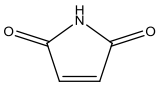	2.04	25.8	18.9
N-ethylmaleimide	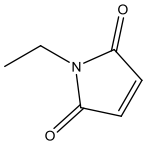	2.46	14.9	15.8
but-3-en-2-one	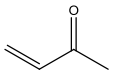	2.14	22.7	14.8
ethyl-3-(2-furyl)-propanoate	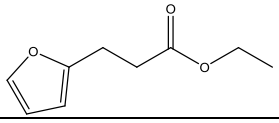	2.36	9.96	12.9

2.2 Cofactor Specificity of YersER, KYE1, and XenA

After testing substrate specificity, the cofactor preference of the three ERs was checked with four different enone substrates (Table 2.3). NADPH was always the preferred cofactor, and the enzymes showed very little or no activity with NADH. Interestingly, the choice of enone substrate seems to influence the NADPH/NADH specificity ratio. While NADPH did not react at all in the presence of 2-cyclohexen-1-one and rarely in presence of maleimide, all three ERs showed activity with NADH in presence of methyl vinyl ketone and ethyl-3-(2-furyl)propanoate. This phenomenon is all the more interesting, as ER is known to react according to a ping-pong mechanism, i.e., the reductive (substrate) and oxidative (FMN by NADPH) half-reactions occur independently, thus, the different enone substrates should not influence cofactor specificity.

Table 2.3. Cofactor preference for YersER, KYE1, and XenA

	Substrate	Specific Activity [U/mg] NADPH	Specific Activity [U/mg] NADH
Kluyveromyces	2-cyclohexen-1-one	1.54	nd
	maleimide	2.04	nd
	methyl vinyl ketone	2.14	0.30
	ethyl 3-(2-furyl)-propanoate	2.36	0.56
XenA	2-cyclohexen-1-one	2.74	nd
	maleimide	25.82	1.50
	methyl vinyl ketone	22.69	1.43
	ethyl 3-(2-furyl)-propanoate	9.96	1.08
Yersinia	2-cyclohexen-1-one	4.22	nd
	maleimide	18.88	nd
	methyl vinyl ketone	14.85	0.69
	ethyl 3-(2-furyl)-propanoate	12.87	0.56

2.3 Enzyme Stability at Different Temperatures

The lack of stability of enzymes against heat and organic solvents can hamper their economical application. We investigated the thermal tolerance of all three ERs by taking samples after various incubation times at three temperatures (30, 37, and 45 ^{o}C) and measuring residual activity at 25 ^{o}C. We always found deactivation to fit a first-order rate law. Although none of the three proteins is particularly thermostable, YersER at 37 ^{o}C was 25-fold and 7-fold more stable than XenA and KYE1, respectively (Table 2.4). YersER at 45 ^{o}C in degassed solution deactivates with a half-life of 129 min, compared with 117 min in air-saturated solution, which demonstrates that oxygen has no influence on stability. The half-life of XenA and KYE1 at that temperature was less than 5 min. Since sufficient stability is an important factor for biocatalysis, we chose the YersER for further characterization.

Table 2.4. Half-lives of enoate reductase and glucose dehydrogenase: (a) In the presence of 25 g/L of 2-cyclohexen-1-one. (b) In the presence of 25 g/L of 2-cyclohexanone. (c) Literature value from Pollard et al.

Enzyme	Temperature [°C]	Half-life [min]
XenA	30	600
XenA	37	99
XenA	45	<5
KYE1	30	1146
KYE1	37	210
KYE1	45	<5
Yers-ER	30	>2160
Yers-ER	37	1488
Yers-ER	45	117
Yers-ER[a]	30	78
Yers-ER[b]	30	2880
GDH-103[c]	30	~7800
GDH-103[a]	30	1.6
GDH-103[b]	30	564

2.4 Coupling of the ERs with the Cofactor Recycling System

The coupling of YersER with GDH was performed in the batch mode (Fig 2.2). Enoate reductase from *Yersinia bercovieri* and GDH-103 (a glucose dehydrogenase from Biocatalytics, Pasadena, CA) were added in different ratios to a 200 mM phosphate buffer of pH 7.5, 299 mM glucose and 1.2 mM of NADP+. The reaction was performed in the batch mode at 30 ^{o}C and substrate cyclohexen-1-one was added to a final concentration of 260 mM. The work was carried out at 125 mg scale (5 mL total volume), the temperature was maintained at 30 ^{o}C using a water bath, pH was adjusted manually using 2 M NaOH and agitation was achieved using a magnetic stirrer at 200 rpm. The conversion was determined *via* gas chromatography (GC) by measuring the substrate and product content of a reaction sample extracted with ethyl acetate using an Agilent GC-FID (model 6890) with a DB17 column (Agilent, Palo Alto, CA).

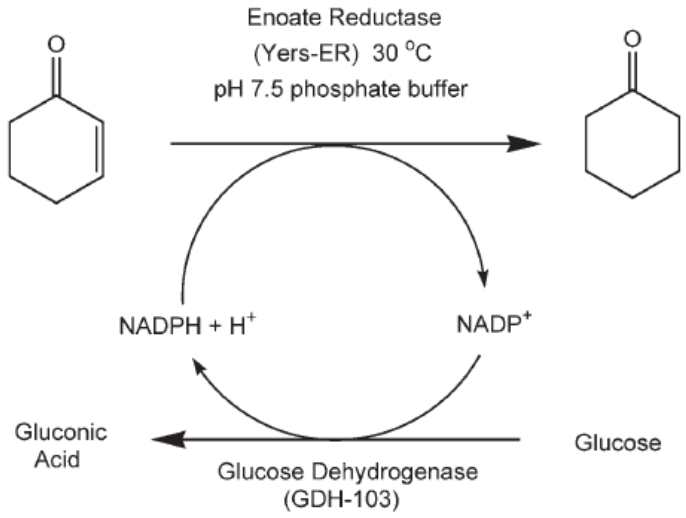

Figure 2.2. Enzyme-coupled cofactor regeneration system with enoate reductase from *Yersinia bercovieri* and glucose dehydrogenase (GDH-103).

All reactions were run at 30 ^{o}C in 200 mM phosphate buffer (pH 7.5) containing 25 g/L (260 mM) of the substrate 2-cyclohexen-1-one, 53.8 g/L (299 mM, 15% molar excess) of glucose, 1 g/L (1.2 mM) of cofactor $NADP^{+}$ and both enzymes at varying

ratios of kU/L. Four reactions were run at these conditions at 8:16, 8:8, 4:8, and 2:4 kU/L of YersER to GDH-103, respectively (Fig 2.3).

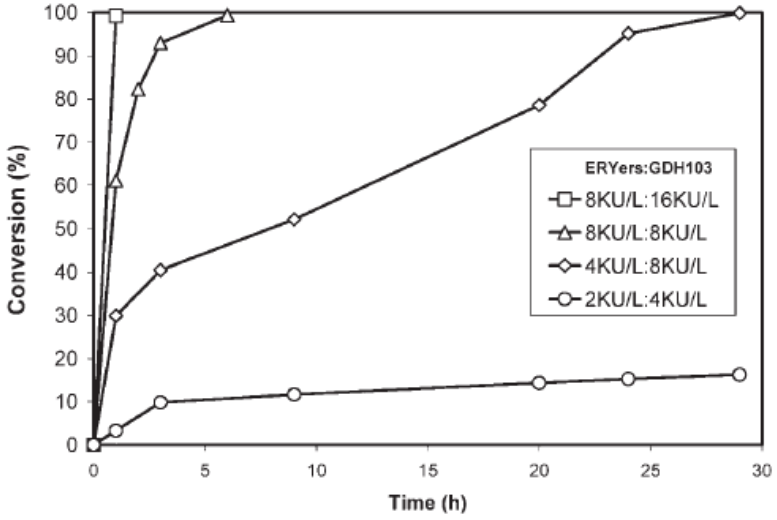

Figure 2.3. Enzymatic oxidation of 25 g/L of 2-cyclohexen-1-one to 2-cyclohexanone at 30 ^{o}C in 200 mM phosphate pH 7.5.

It is evident that enzyme loading had a significant effect on reaction rate. At 8:16 kU/L of YersER to GDH-103, the reaction reached >99% conversion within an hour (217 turnovers), while at a loading of 8:8 kU/L the reaction required 6 h for the same degree of conversion (>99%) (Fig 2.3). This difference in reaction rate might be explained by the increased supply of reduced cofactor achieved at a higher loading of GDH-103. At more diluted levels of YersER and GDH-103, 4:8 kU/L and 2:4 kU/L, >99% and >16% conversion were measured after 29 h, respectively. Such a dramatic difference in reaction rate between the 8:16 kU/L and the 4:8 kU/L enzyme loadings for YersER and GDH-103 suggests significant enzyme deactivation at the operating conditions.

To test this hypothesis, the residual activities of YersER and GDH-103 were monitored separately in batch experiments in the presence of reactant or product at the operating conditions (30 ^{o}C, 200 mM phosphate pH 7.5 and 25 g/L of 2-cyclohexen-1-one or 2-cyclohexanone) in the absence of cofactor. The residual activity was measured by monitoring NADP(H) depletion (YersER) or formation (GDH-103). Assuming first-

order deactivation (corroborated above for ER and independently verified for GDH from various organisms), half-lives were estimated for YersER to be 78 min and 48 h in the presence of reactant (2-cyclohexen-1-one) and product (2-cyclohexanone), respectively. For GDH-103, the half-lives were estimated to be 1.6 min and 9.4 h in the presence of reactant and product, respectively. The addition of 260 mM 2-cyclohexen-1-one leads to a more than 30-fold decrease of the half-life at 30 ^{o}C from >2160 min to 78 min for YersER. A high degree of precipitation was observed in both enzyme samples which contained 260 mM 2-cyclohexen-1-one.

2.4 References

[1] D. S. Blehert, *et al.*, "Regioselectivity of nitroglycerin denitration by flavoprotein nitroester reductases purified from two Pseudomonas species," *Journal of Bacteriology*, vol. 179, pp. 6912-6920, Nov 1997.

[2] J. F. Chaparro-Riggers, *et al.*, "Comparison of three enoate reductases and their potential use for biotransformations," *Advanced Synthesis & Catalysis*, vol. 349, pp. 1521-1531, Jun 2007.

CHAPTER 3

NITROREDUCTASE FROM SALMONELLA TYPHIMURIUM: CHARACTERIZATION AND CATALYTIC ACTIVITY

The biocatalytic activity of nitroreductase from *Salmonella typhimurium* (NRSal) was investigated for the reduction of α,β-unsaturated carbonyl compounds, nitroalkenes, and nitroaromatics. The synthesized gene was subcloned into a pET28 overexpression system in *E.coli* BL21 strain, and the corresponding expressed protein was purified to homogeneity with 15% protein mass yield and 41% of total activity recovery. NRSal showed broad substrate acceptance for various nitro compounds such as 1-nitrocyclohexene and aliphatic nitroalkenes (alkene reductase activity), as well as nitrobenzene (nitroreductase activity), with substrate conversion efficiency of > 95%. However, the reduction of enones was generally low, proceeding albeit with high stereoselectivity. The efficient biocatalytic reduction of substituted nitroalkenes provides a route for the preparation of the corresponding nitroalkanes. NRSal also demonstrated the first single isolated enzyme-catalyzed reduction of nitrobenzene to aniline through the formation of nitrosobenzene and phenylhydroxylamine as intermediates. However, chemical condensation of the two intermediates to produce azoxybenzene currently limits the yield of aniline.

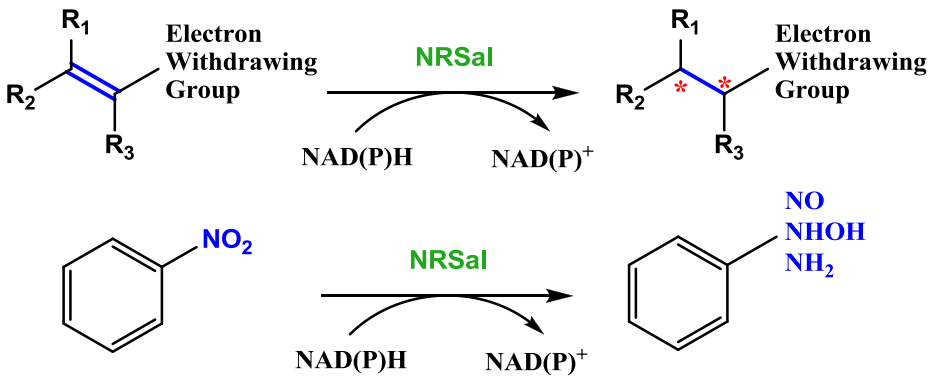

Fig 3.1. Nitroreductase NRSal from *Salmonella typhimurium* displays both nitroreductase and enoate reductase activity in the asymmetric reduction of C=C bonds and aromatic nitro compound. It also demonstrated the first single isolated enzyme-catalyzed reduction of nitrobenzene to aniline.

3.1 Introduction

Flavoenzymes are biocatalysts that catalyze a wide range of biochemical reactions ranging from dehydrogenation, one- and two-electron transfer redox reactions, oxygen activation during oxidation and hydroxylation reactions, to light emission in bioluminescent bacteria.[1, 2] As part of flavoenzymes, the recently growing "Old Yellow Enzyme" (OYE) family was reported to catalyze the reduction of various substrates such as α,β-unsaturated aldehydes, ketones, imides, esters, nitriles, and carboxylic acids.[3-6] The asymmetric bioreduction of C=C bonds employing OYE family proteins can create up to two chiral centers and therefore constitutes an interesting route towards enantiomerically pure compounds. The C=C bond reduction catalyzed by enoate reductases proceeds via a ping-pong mechanism, where the flavin is first reduced at the expense of a nicotinamide cofactor in the reductive half-reaction, followed by the asymmetric reduction of the substrates through *trans*-hydrogenation (oxidative half-reaction).[7-9] The OYE family also features nitroreductase activity through biodegradation of explosive compounds such as PETN, TNT, and nitroglycerin. Several members of the OYE family such as XenA and XenB from *Pseudomonas sp.*,[10, 11] PETN reductase from *Enterobacter cloacae*,[12, 13] OYEs from *Saccharomyces sp.*,[6,

14] YqjM from *Bacillus subtilis*,[15, 16] and OPRs from *Arabidopsis thaliana*[17, 18] have been characterized for their biocatalytic activity on both nitro-aromatics and aliphatic nitro compounds.

In our previous work, we have characterized three un-related enoate reductases: XenA from *Pseudomonas putida*, KYE1 from *Kluyveromyces lactis*, and YersER from *Yersinia bercovieri*. We have shown that these three enoate reductases feature broad substrate specificity but different substrate preferences on a set of various α,β-unsaturated carbonyl compounds.[3] Since enoate reductases often possess nitroreductase activity, we initiated a new search for a candidate that possesses broad substrate specificity for nitro compounds, however, applying a different strategy: the investigation of nitroreductases for their enoate reductase activity, with specific emphasis on the biocatalytic reduction of nitroalkenes to provide an efficient route for the synthesis of chiral substituted nitroalkanes. This strategy was based on the observation that some nitroreductases had shown reductase activity on quinones.[19-22]

3.1.1 Reduction of nitro compounds

Nitroalkanes are potential intermediates in the synthesis of amines, aldehydes, carboxylic acids or denitrated compounds.[23, 24] The traditional organic synthesis of enantiomerically pure nitroalkanes occurs through asymmetric conjugate addition to nitroalkenes,[25-27] reduction of nitroalkenes with transition metal catalyst,[28] hydrogenation with Jacobsen-type organocatalyst,[29] or addition of α,β-unsaturated bonds onto nitroalkanes.[30] Due to various restrictions on these organic synthesis processes (such as growing environmental restrictions on the type of catalyst used, narrow substrate acceptance), an efficient biocatalytic route for chiral nitroalkanes is highly desirable. Recently, several published works have demonstrated stereoselective reduction of nitroalkenes using: OPR1 and OPR3 from *Lycopersicon esculentum*,[15, 16] OYE from *Saccharomyces carlsbergensis* and OYE2-3 from *Saccharomyces*

cerevisiae,[6, 14] NCR from *Zymomonas mobilis*,[6, 14] YqjM from *Bacillus subtilis*,[15, 16] PETN reductase from *Enterobacter cloacae*,[12, 13] and crude enzyme preparation from *Clostridium sporogenes*.[31] These enzymatic processes are a valuable addition to the established synthetic toolbox and inspire the search for new candidates.

In this context, we came across a homolog of nitroreductase from *Enterobacter cloacae*: nitroreductase from *Salmonella typhimurium* (NRSal). NRSal was first discovered in 1989 from *Salmonella typhimurium* strain TA1538NR,[32] and represents a new class of flavin-dependent nitroreductase enzymes.[21, 33-35] The nucleotide sequence of this oxygen-insensitive FMN-containing NRSal encodes for 217 amino acids, with a calculated molecular weight of 23,955 Da. This enzyme has been shown to reduce some nitroaromatic compounds, such as *p*-nitrophenol or *p*-nitrobenzoic acid.[36] Since then however, there has been no published work about any further characterization of NRSal, and especially its catalytic activity, which renders it an interesting candidate for us to explore. In this paper, we examine the ability of NRSal to catalyze the reduction of α,β-unsaturated carbonyl compounds, nitroalkenes, and nitroaromatics.

3.2 Results & Discussion

3.2.1 Cloning, overexpression, and purification

The gene coding for NRSal was purchased from BioBasic Inc (Ontario, Canada) according to the published sequence (UnitProtKB accession # P15888).[32, 37] Sequence analysis revealed that NRSal from *Salmonella typhimurium* shares high amino acid identity and similarity with nitroreductase from *Enterobacter cloacae* with 89% identity and 93% similarity (Figure 3.2). The gene product was cloned into vector pET28a(+) (Novagen, San Diego, CA) at the following restriction sites: NcoI and HindIII with stop codon for expression of wild type NRSal, NcoI and HindII for expression of

NRSal with C-terminal polyhistidine tag, and NdeI and HindIII with stop codon for expression of NRSal with N-terminal polyhistidine tag. The addition of the polyhistidine tag was for ease of enzyme purification.

```
NR_SAL   1   MDIVSVALQRYSTKAFDPSKKLTAEEADKIKTLLQYSPSSTNSQPWHFIV    50
             |||:||||:|:||||||.|||||||||:||||||||||||||||||||
NR_ENT   1   MDIISVALKRHSTKAFDASKKLTAEEAEKIKTLLQYSPSSTNSQPWHFIV    50
NR_SAL  51   ASTEEGKARVAKSAAGNYTFNERKMLDASHVVVFCAKTAMDDAWLERVVD   100
             ||||||||||||||||.|.||||||||||||||||||||||||||||||||
NR_ENT  51   ASTEEGKARVAKSAAGTYVFNERKMLDASHVVVFCAKTAMDDAWLERVVD   100
NR_SAL 101   QEDADGRFATPEAKAANDKGRRFFADMHRVSLKDDHQWMAKQVYLNVGNF   150
             ||:|||||.||||||||.|||.:|||||||.||||.|||||||||||||||
NR_ENT 101   QEEADGRFNTPEAKAANHKGRTYFADMHRVDLKDDDQWMAKQVYLNVGNF   150
NR_SAL 151   LLGVAAMGLDAVPIEGFDAEVLDAEFGLKEKGYTSLVVVPVGHHSVEDFN   200
             ||||.|||||||||||||.:||.||||||||:||||||||||||||||||
NR_ENT 151   LLGVGAMGLDAVPIEGFDAAILDEEFGLKEKGFTSLVVVPVGHHSVEDFN   200
NR_SAL 201   AGLPKSRLPLETTLTEV    217
             |.||||||||.|.:||.
NR_ENT 201   ATLPKSRLPLSTIVTEC    217
```

Figure 3.2. Amino acid alignment of nitroreductase NRSal from *Salmonella typhimurium* (P15888, NR_Sal) and nitroreductase from *Enterobacter cloacae* (Q01234, NR_ENT) using EMBOSS Pairwise Alignment Needle Algorithm (http://www.ebi.ac.uk).

The purification of wild-type NRSal was optimized compared to previously published method.[36] The original six steps of NRSal purification were reduced to two steps, with first ammonium sulfate precipitation to remove the majority of non-proteinaceous biological material, followed by anion exchange column chromatography with DEAE-Sepharose column to isolate pure NRSal with 15% protein mass recovery from the cell lysate sample, and with total activity recovery of 41%. The purification of wild-type NRSal was monitored with the standard activity assay on nitrofurazone[36] (Table 3.1) followed by SDS-PAGE analysis (Figure 3.3). The final elution showed a single band upon SDS-PAGE analysis. The NRSal with N- or C-terminal polyhistidine tag was purified according to the standard Ni^{2+}-NTA bead protocol from Qiagen (Valencia, CA). However, the activity of NRSal with polyhistidine tag was found to be much lower compared to the wild type. Activity check was performed by monitoring the reduction of nitrofurazone (known substrate for NRSal[36]) and cyclohexenone (common substrate for enoate reductases). NRSal with N- or C-terminal polyhistidine tag showed

specific activity of 4.40 U/mg and 3.27 U/mg respectively for nitrofurazone reduction, which was much lower compared to wild type specific activity of 14.2 U/mg. An analogous pattern was observed for the reduction of cyclohexenone, where wild type NRSal showed significantly higher specific activity (0.39 U/mg) compared to NRSal with N-terminal (0.16 U/mg) and C-terminal (0.17 U/mg) polyhistidine tag. Since the presence of the polyhistidine tag considerably decreased enzymatic activity of NRSal, further characterization was continued only with wild-type, untagged-NRSal.

Table 3.1. Purification of wild type NRSal monitored with nitrofurazone activity. [a]

Purification step	Total protein [mg] [b]	Total activity [U]	Specific activity [U/mg]	Yield %
Lysate	53.3	285	5.34	100
$(NH_4)_2SO_4$	22.4	136	5.02	48
Dialysis	22.0	149	6.78	52
DEAE	8.20	116	14.2	41

[a] Dry cell weight 1.1 g/L.
[b] Nitrofurazone activity assay: 50 mM TrisHCl buffer pH 7.2, 0.05 mM Nitrofurazone, 0.1 μM NRSal, GDH recycling system: (8 μM NADPH, 2 mM Glucose, 10 U GDH). The activity was calculated by monitoring the decrease of nitrofurazone wavelength at 375 nm with extinction coefficient of ε_{375nm} = 15,000 $(M\ cm)^{-1}$.[38]

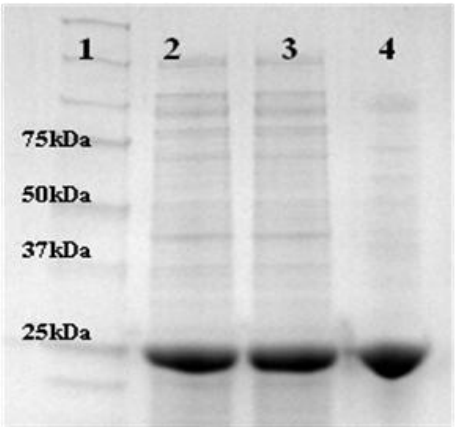

Figure 3.3. SDS-PAGE analysis for purification of wild type NRSal: Lane 1 protein ladder, lane 2 cell lysate sample, lane 3 70% $(NH_4)_2SO_4$ precipitation, lane 4 DEAE-Sepharose column.

3.2.2 Enzymatic activity and stability study

We first investigated the effect of temperature and pH on NRSal by monitoring the change of enzymatic activity over the range of 10 – 60 ℃ (Figure 3.4), and pH range of 4 – 9 (Figure 3.5). The activity-temperature profile showed maximum specific activity of 13.6 U/mg for reduction of nitrofurazone at 45 ℃ and pH 7.5, which was 3.2-fold higher than the activity at room temperature (20 ℃). Arrhenius plots yield an activation energy E_a of 42.7 kJ/mol for the temperature range of 10 – 45 ℃ (r^2 = 0.963), and a deactivation energy E_d of -31.5 kJ/mol for the temperature range of 45 – 60 ℃ (r^2 = 0.965). The activity-pH profile showed an optimum pH at 7.2 with highest specific activity of 8.10 U/mg for reduction of nitrofurazone at 20 ℃ in 50 mM TrisHCl buffer. We also found that NRSal had lower activity (but similar activity–pH pattern with a maximum activity at pH 7.2) in 50 mM phosphate buffer compared to 50 mM TrisHCl buffer. The activity of NRSal is therefore buffer dependent and TrisHCl is the optimum buffer for reactions run between pH 6 – 7.5. Additionally, NRSal considerably lost its activity beyond pH 8.

Since thermal stability of enzymes is a key consideration for application in larger scale processes, we investigated the kinetic stability of NRSal by measuring its half-life

at three different temperature points of 37, 45, and 50 ℃ (Table 3.2). The deactivation of NRSal at all temperatures followed first order deactivation kinetic (data not shown). Also, NRSal seemed reasonably stable with shortest half-life of 2.3 hours measured at 50 ℃, and half-life decreased exponentially with increasing temperatures.

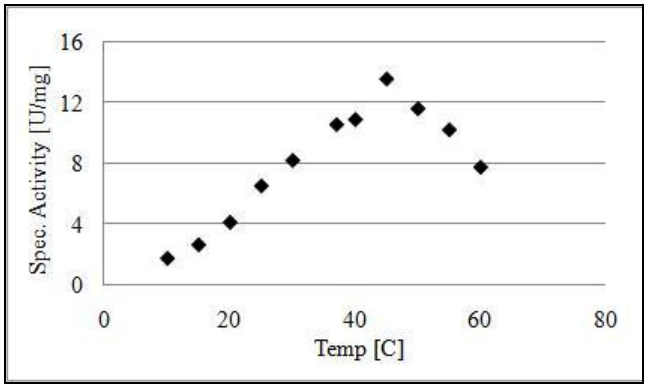

Figure 3.4. Activity – temperature profile of NRSal. Activity was measured with standard nitrofurazone activity assay in 50 mM phosphate buffer at pH 7.5.

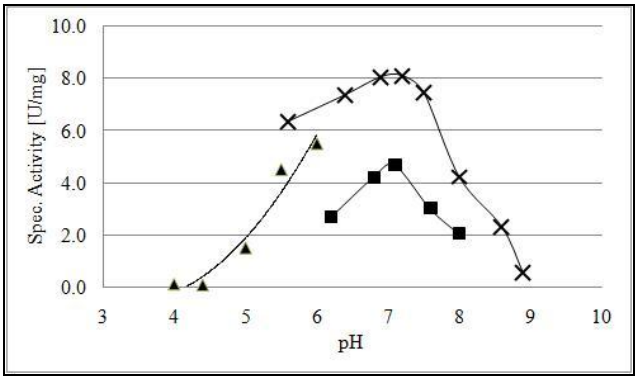

Figure 3.5. Activity – pH profile of NRSal in three different buffers: 50 mM TrisHCl (**x**), 20 mM citrate buffer (▲), and 50 mM phosphate buffer (■). Activity was measured with standard nitrofurazone activity assay at 20 ℃.

Table 3.2. Half-life of NRSal measured at various temperatures using 1-nitrocyclohexene as substrate

Temperature [^{o}C]	Half-life	$k_{d,obs}$[a]
37	365 hours	0.0019 hour^{-1}
45	17.9 hours	0.0388 hour^{-1}
50	2.3 hours	0.3100 hour^{-1}

[a] $k_{d,obs}$ is the observed deactivation rate constant

3.2.3 Substrate spectrum characterization

With finding of a broad enoate reductase activity in a nitroreductase as one of our goals, we investigated the catalytic activity of purified NRSal with several common α,β-unsaturated carbonyl substrates for enoate reductases (Table 3.3. Entries #**1**–**4**). We first tested NRSal activity on cyclohex-2-enone (**1)** and related substrate 3-methyl-2-cyclohexenone (**2**).[39-41] The nitroreductase enzyme displayed enoate reductase activity on both substrates. Both compounds **1** and **2** were reduced, albeit with maximum substrate conversion of only 12% and 5.2% respectively. NRSal showed strong stereospecificity in the reduction of **2** and yielded (*R*)-3-methyl-2-cyclohexanone with 84% e.e.. Substrates ketoisophorone (**3**) and citral (**4**) were also tested due to their large-scale industry application to produce the corresponding levodione and citronellal, respectively.[42-45] NRSal showed modest maximum conversion of 12% with **3** to produce (*R*)-levodione with 87% e.e, and did not show any biocatalytic reduction of aldehyde **4**. This remarkable stereoselectivity for a nitroreductase in reducing C=C bonds may point at a mechanism similar to that of OYEs, as OYEs proceed via a ping pong Bi Bi mechanism, as do nitroreductases in the reduction of the nitro group.[7-9, 20, 21]

Despite the low conversions with α,β-unsaturated carbonyl substrates, we hypothesized that NRSal, as a nitroreductase, would display stronger alkene reductase activity in the presence of a nitro group. Indeed, NRSal showed broader substrate acceptance for nitro related compounds (Table 3.3. Entries #**5**-**8**). First, we observed the

reduction of C=C bond on nitro compounds **5** to **7**. Maximum conversion of 1-nitrocyclohexene (**5**) was 97% to produce the reduced product 1-nitrocyclohexane. Aliphatic nitroalkenes (**6**-**7**) were also shown to be favored substrates of NRSal with overall conversion efficiency of > 95%. Both compounds **6** and **7** were reduced to the corresponding alkanes, with compound **7** being reduced to the racemic product; either the enzyme was not stereoselective for that compound, or alternatively the potential enantiomeric product could have racemized due to the acidity of the proton on C_{α}. Finally, we observed a more typical behavior for a nitroreductase in the reduction of aromatic nitro compound such as nitrobenzene (**8**), which was reduced with conversion of > 99% to produce nitrosobenzene, phenylhydroxylamine, but also aniline and the chemical condensation product azoxybenzene. To our knowledge, this is the first report of a single enzyme-catalyzed reduction of nitrobenzene to aniline (reaction detailed in the next section).

Overall, NRSal accepts both cofactors NADPH / NADH equally well, with higher substrate acceptance for compounds containing the electron withdrawing nitro group. Importantly, the diverse catalytic activity of NRSal was reflected in the broad substrate spectrum and range of conversion efficiency.

Table 3.3**.** Biocatalytic conversion of various α,β-unsaturated carbonyl compounds, nitroalkenes, and nitroaromatic substrates with NRSal (* represents a chiral center).

Entry	Substrate	Product	Conversion (NADPH/ NADH)
1	 2-Cyclohexen-1-one	 2-Cyclohexanone	12% / 12%
2	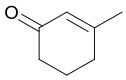 3-Methyl-2-cyclohexenone	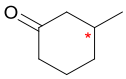 3-Methyl-2-cyclohexanone	5.2% / 4.8% (*R*) 84% e.e
3	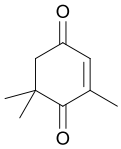 Ketoisophorone	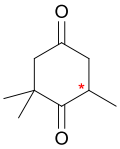 Levodione	12% / 10% (*R*) 87% e.e
4	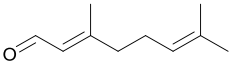 Citral	N/A	No conversion
5	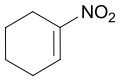 1-Nitrocyclohexene	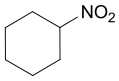 1-Nitrocyclohexane	95% / 97%
6	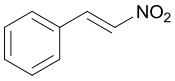 Trans-β-nitrostyrene	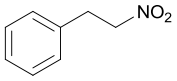 Phenylnitroethane	95% / 95%
7	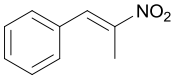 1-Phenyl-2nitropropene	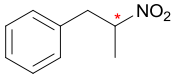 1-Phenyl-2nitropropane	Both >99% Racemic mixture
8	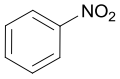 Nitrobenzene	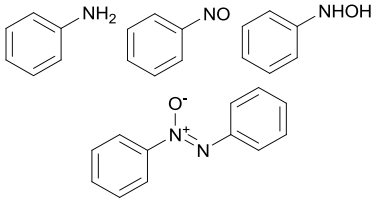 Aniline / Nitrosobenzene / Phenyl-hydroxylamine / Azoxybenzene	Both >99%

3.2.4 Enzymatic reduction of nitrobenzene to aniline

The enzymatic reduction of nitroaromatic compounds can follow two pathways: the reduction of the nitro group or the reduction of the aromatic ring. The nitro group reduction is either a one-electron or two-electron reduction mechanism.[46] Both mechanisms involve the reduction of the nitro group to the amine through highly reactive nitroso and hydroxylamino intermediates. The aromatic ring in nitroaromatic compounds can also be reduced, resulting into the corresponding Meisenheimer complex, followed by subsequent release of nitrite.[47, 48] The formation of the Meisenheimer complex has been observed for several members of the OYE family such as PETN reductase from *Enterobacter cloacae*,[49] XenB from *Pseudomonas fluorescens*,[50] and NemA from *Escherichia coli*,[51] which also display nitroreductase activity on the nitro group.

Published work on the reduction of nitrobenzene to aniline was mainly accomplished with metal support catalysts (e.g Ru/SBA, Ni, Pt/C catalysts) or whole-cell biocatalysts (e.g *Rhodotorula mucilaginosa*, *Arracacia xanthorrhiza*, *Candida guilliermondii*, *Saccharomyces cerevisiae*).[52-57] The single enzyme-catalyzed reduction of nitrobenzene (e.g with nitrobenzene nitroreductase from *Pseudomonas pseudoalcaligenes* JS45) was reported to produce phenylhydroxylamine, a highly reactive intermediate.[58, 59] To the best of our knowledge, the discovery of NRSal reduction of nitrobenzene represents the first single isolated enzyme-catalyzed reduction of nitrobenzene to aniline. The mechanism for NRSal nitrobenzene reduction was shown to follow the two-electron reduction pathway of the nitro-group: nitrobenzene was reduced to form nitrosobenzene first and phenylhydroxylamine next, followed by subsequent reduction of phenylhydroxylamine to aniline. At the same time, chemical condensation between the nitrosobenzene and phenylhydroxylamine resulted in the production of azoxybenzene (Figure 3.6).[60, 61] Control experiments were performed to demonstrate the condensation reaction by mixing of these standards under similar reaction conditions but without enzyme present. Real-time analysis was performed to quantify the reduction

of 1 mM nitrobenzene over time course of 160 min: nitrobenzene was completely converted within 40 minutes (with conversion of > 99%), along with the formation of 0.26 mM nitrosobenzene, 0.09 mM phenylhydroxylamine, 0.06 mM aniline, and 0.35 mM azoxybenzene (Figure 3.7). Nitrobenzene and phenyl-hydroxylamine were found to be chemically unstable and were completely degraded after 6 hours, with no further increase of aniline as final product. In an effort to boost the percentage formation of aniline in the overall reaction, one possible method was to limit the condensation between nitrosobenzene and phenylhydroxylamine. Experiments were performed to remove molecular oxygen from the reaction system as initial hypothesis that O_2 was essential in the condensation reaction. However, azoxybenzene formation was still detected at similar concentration level, implying that its formation is a condensation reaction without oxidation.

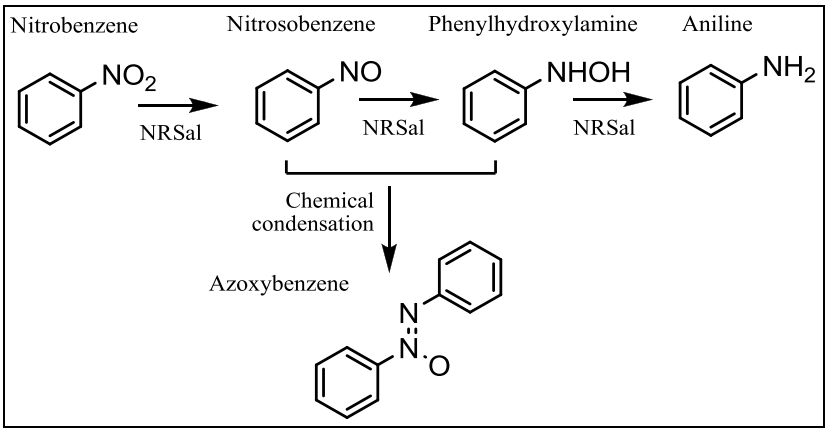

Figure 3.6**.** Proposed nitrobenzene reduction pathway to aniline and azoxybenzene by NRSal.

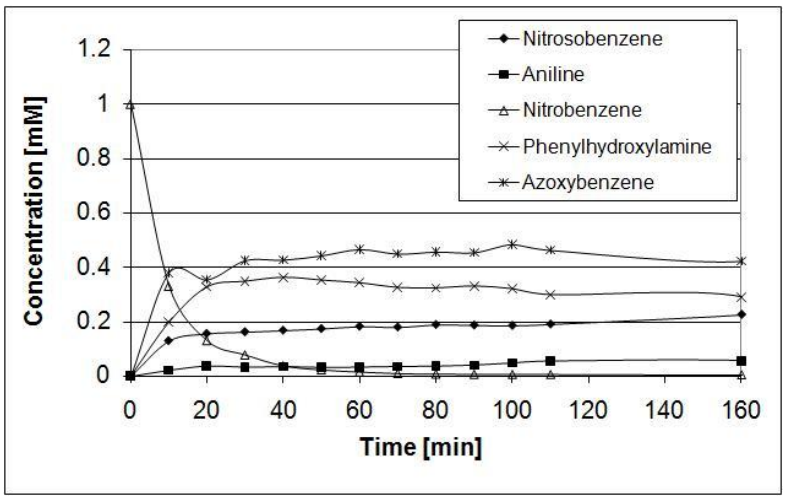

Figure 3.7. Conversion-time plot for the reduction of nitrobenzene by NRSal in the presence of NADH.

3.3 Conclusion

In summary, nitroreductase NRSal from *Salmonella typhimurium* is a versatile biocatalyst that displays both nitroreductase and enoate reductase activity. The enzyme showed strong preference in the reduction of C=C bonds for nitro-containing substrates, with less satisfactory biocatalytic activity towards the reduction of C=C bonds in enones, still with a high stereoselectivity. It is interesting that a true nitroreductase presents strong enoate reductase activity with substrate stereopreference, is an FMN-bound enzyme and is still not associated with OYE family. The feasibility of biocatalytic reduction of nitroalkenes to nitroalkanes provides an addition as part of the synthetic toolbox to obtain various intermediates of interest. This is also the first isolated single enzyme-catalyzed reduction of nitrobenzene to aniline, which provides a possible perspective for a green production process of anilines other than traditional synthesis through chemical hydrogenation and metal-supported catalyst.[46] Although overall aniline formation is still limited due to condensation reaction in the system, we are currently investigating for optimized reaction conditions and larger scale reaction system.

Acknowledgements: We thank the Eckert-Liotta Research Group (especially Ryan Hart) at the Georgia Institute of Technology for access and help with GC-MS and Jim Spain's Research Group (especially Shirley F Nishino) at the Georgia Institute of Technology for help in phenylhydroxylamine analysis with HPLC.

3.4 Meterials & Methods

3.4.1 NRSal orimer sequences, cloning, and expression

The DNA sequence of NRSal from *Salmonella typhimurium* was synthesized by BioBasic Inc (Ontario, Canada) according to UnitProtKB accession # P15888. The corresponding specific 5'- and 3'-primers were synthesized at Eurofins-mwg|operon Biosciences (Huntville, AL). The primers contain a gene-encoding segment (italic), a restriction site (underlined), and an overhang. The 5'-primers of wild type and C-terminal polyhistidine tagged introduced a NcoI restriction site (5'-CAT GCC ATG *GCA ATG GAT ATT GTT TCC GTA GCT CTG C*-3'), and N-terminal tagged introduced a NdeI restriction site (5'-GGG AAT TCC ATA *TGA TGG ATA TTG TTT CCG TAG CTC TGC*-3') into the PCR fragment. The 3'-primer introduced a HindIII restriction site in to the PCR fragment (with stop codon: 5'-CCC AAG CTT *TTA CAC TTC AGT CAG GGT GGT TTC CA*-3', and without stop codon: 5'- CCC AAG CTT CAC TTC AGT CAG GGT GGT TTC CA-3').

DNA amplification was performed with standard PCR protocol with Pfu polymerase from New England Biolabs (Marlborough, MA) and PCR buffer from Stratagene (La Jolla, CA). DNA was amplified for 30 cycles in an Eppendorf Gradient Thermocycler (Eppendorf, Hamburg, Germany) followed by gel purification with standard Qiagen gel kit (Qiagen, Valencia, CA). PCR assay: 100 ng of DNA, 200 µM of each dNTP, 10 µM of each primers, 1 U of Pfu polymerase, and 5 µL of Pfu buffer in a

final volume of 50 µL. Each DNA amplification cycle: 1 min denaturation at 95 ℃, 1 min annealing step at 50, 55, and 60 ℃, 3.5 min extension step at 68 ℃. The final PCR products were digested with restriction enzymes and ligated into pET28a (+) (Novagen, San Diego) and transformed into competent *E. coli* XL1-Blue cells. The NRSal genes were sent for DNA sequencing at Eurofins-mwg|operon Biosciences (Huntville, AL).

The NRSal genes were transformed into *E. coli* BL21 for protein expression. Starter culture consisted of 5 ml LB_{Kan} inoculated from frozen stock and grown overnight at 37 ℃. The starter culture were used for inoculation of 300 ml culture (0.1% v/v), which was gently aerated until OD_{600} reached 0.5 for addition of 0.1 mM of IPTG and left overnight for protein expression. Harvested cell pellets were kept for -80 ℃ for protein purification.

3.4.2 Purification of NRSal

The cell pellets of wild type NRSal were re-suspended in 50 mM TrisHCl buffer pH 7.5 (buffer A) and disrupted by sonication. The supernatant was separated after centrifugation, where NRSal was precipitated between 40-70% of saturated ammonium sulfate. The precipitate was dissolved again in buffer A and dialyzed over 6 hours. The dialyzed sample was applied to DEAE-Sepharose^{TM} FF (GE Healthcare, Sweden) column and washed with 25 mM step increment of NaCl in buffer A. Purified NRSal was collected at elution of 150 mM NaCl with 0.1 mM of free FMN added to account for the loss of FMN during the purification (only 20% FMN occupancy measured before addition of free FMN). Although experiments were performed to measure for the FMN occupancy at the end of purification, free FMN in the sample seemed to saturate the spectrophotometer measurement even with multiple wash cycles. The NRSal with N- or C-terminal polyhistidine tag were purified with Ni^{2+}-NTA beads according to the standard protocols of Qiagen (Valencia, CA). The protein concentration was determined by the Bradford method with Coomassie Plus Protein assay reagent and BSA assay

(Pierce Chemical) as the calibration curve. SDS-PAGE analysis was performed with 50 µg protein sample elution into each well. The protein samples were mixed with 2X sample buffer (125mM TrisHCl, pH 6.8, 4% SDS, 50% glycerol. 0.02% bromophenol blue, and 10% 2-mercaptoethanol). The mixed samples were incubated at 100 ℃ for 5 min and loaded onto 12% PAGE^{TM} Gold precast gel and run in BioRad Mini Protean chamber (BioRad, Hercules CA) at 150 V for 45 min with Tris-HEPES-SDS running buffer (12.1 g/L Tris, 23.8 g/L HEPES, 1 g/L SDS). Biorad Precision Plus protein ladder was used as standards in the gel analysis. GelCode® Blue Stain Reagent (Pierce, Rockford IL) was used for final gel staining.

3.4.3 Enzyme assay

NRSal kinetic measurement were performed by monitoring the oxidation of NAD(P)H at 340 nm using ε_{340nm} of 6.22 $mM^{-1}cm^{-1}$. Reaction assays were analyzed with Shimadzu GC-2010 using RT-BDEXcsf chiral column (30 m 0.32 mm 0.25 µm, Restek) for entry # **1** – **4**; Cyclosil-B chiral column (30 m 0.32 mm 0.25 µm, J&W Scientific) for entry # **6** – **8**; and SHRX5 column (15m 0.25 mm 0.25 µm Shimadzu) for entry # **5**. All substrates and products were purchased commercially from Sigma Aldrich or VWR with highest purity available except products of entry #**6** - **8**, and phenyl-hydroxylamine. Prof. Jim Spain Research Group (Georgia Institute of Technology) kindly provided synthesized phenylhydroxylamine.[62] Products of **6** – **7** were synthesized according to previous published protocols.[31]

3.5 Publication Information

The work presented in Chapter 3 of this dissertation was published in the *Organic & Biomolecular Chemistry* volume 8 pages 1826-1932, 2010; with Mélanie Hall and my thesis advisor Andreas S. Bommarius as co-authors.

3.5 References

[1] M. W. Fraaije and A. Mattevi, "Flavoenzymes: diverse catalysts with recurrent features," *Trends in Biochemical Sciences*, vol. 25, pp. 126-132, Mar 2000.

[2] V. Massey, "The chemical and biological versatility of riboflavin," *Biochemical Society Transactions*, vol. 28, pp. 283-296, Aug 2000.

[3] J. F. Chaparro-Riggers, *et al.*, "Comparison of three enoate reductases and their potential use for biotransformations," *Advanced Synthesis & Catalysis*, vol. 349, pp. 1521-1531, Jun 2007.

[4] B. Kosjek, *et al.*, "Asymmetric bioreduction of alpha,beta-unsaturated nitriles and ketones," *Tetrahedron-Asymmetry*, vol. 19, pp. 1403-1406, Jun 30 2008.

[5] R. Stuermer, *et al.*, "Asymmetric bioreduction of activated C=C bonds using enoate reductases from the old yellow enzyme family," *Current Opinion in Chemical Biology*, vol. 11, pp. 203-213, Apr 2007.

[6] R. E. Williams, *et al.*, "Biotransformation of explosives by the old yellow enzyme family of flavoproteins," *Applied and Environmental Microbiology*, vol. 70, pp. 3566-3574, Jun 2004.

[7] B. J. Brown, *et al.*, "The role of glutamine 114 in Old Yellow Enzyme," *Journal of Biological Chemistry*, vol. 277, pp. 2138-2145, Jan 18 2002.

[8] C. E. French, *et al.*, "Biological Production of Semisynthetic Opiates Using Genetically-Engineered Bacteria," *Bio-Technology*, vol. 13, pp. 674-676, Jul 1995.

[9] K. Stott, *et al.*, "Old Yellow Enzyme - the Discovery of Multiple Isozymes and a Family of Related Proteins," *Journal of Biological Chemistry*, vol. 268, pp. 6097-6106, Mar 25 1993.

[10] D. S. Blehert, *et al.*, "Cloning and sequence analysis of two Pseudomonas flavoprotein xenobiotic reductases," *Journal of Bacteriology*, vol. 181, pp. 6254-6263, Oct 1999.

[11] J. J. Griese, *et al.*, "Xenobiotic reductase A in the degradation of quinoline by Pseudomonas putida 86: Physiological function, structure and mechanism of 8-hydroxycoumarin reduction," *Journal of Molecular Biology,* vol. 361, pp. 140-152, Aug 4 2006.

[12] H. Nivinskas, *et al.*, "Reduction of aliphatic nitroesters and N-nitramines by Enterobacter cloacae PB2 pentaerythritol tetranitrate reductase," *Febs Journal,* vol. 275, pp. 6192-6203, Dec 2008.

[13] H. S. Toogood, *et al.*, "Structure-Based Insight into the Asymmetric Bioreduction of the C=C Double Bond of alpha,beta-Unsaturated Nitroalkenes by Pentaerythritol Tetranitrate Reductase," *Advanced Synthesis & Catalysis,* vol. 350, pp. 2789-2803, Nov 2008.

[14] M. Hall, *et al.*, "Asymmetric bioreduction of activated C = C bonds using Zymomonas mobilis NCR enoate reductase and old yellow enzymes OYE 1-3 from yeasts," *European Journal of Organic Chemistry,* pp. 1511-1516, Mar 2008.

[15] T. B. Fitzpatrick, *et al.*, "Characterization of YqjM, an old yellow enzyme homolog from Bacillus subtilis involved in the oxidative stress response," *Journal of Biological Chemistry,* vol. 278, pp. 19891-19897, May 30 2003.

[16] M. Hall, *et al.*, "Asymmetric bioreduction of C=C bonds using enoate reductases OPR1, OPR3 and YqjM: Enzyme-based stereocontrol," *Advanced Synthesis & Catalysis,* vol. 350, pp. 411-418, Feb 2008.

[17] E. R. Beynon, *et al.*, "The Role of Oxophytodienoate Reductases in the Detoxification of the Explosive 2,4,6-Trinitrotoluene by Arabidopsis," *Plant Physiology,* vol. 151, pp. 253-261, Sep 2009.

[18] J. Strassner, *et al.*, "A homolog of old yellow enzyme in tomato - Spectral properties and substrate specificity of the recombinant protein," *Journal of Biological Chemistry,* vol. 274, pp. 35067-35073, Dec 3 1999.

[19] H. Nivinskas, *et al.*, "Two-electron reduction of quinones by Enterobacter cloacae NAD(P)H : nitroreductase: quantitative structure-activity relationships," *Archives of Biochemistry and Biophysics,* vol. 403, pp. 249-258, Jul 15 2002.

[20] S. Zenno, *et al.*, "Biochemical characterization of NfsA, the Escherichia coli major nitroreductase exhibiting a high amino acid sequence homology to Frp, a Vibrio harveyi flavin oxidoreductase," *Journal of Bacteriology,* vol. 178, pp. 4508-4514, Aug 1996.

[21] S. Zenno, *et al.*, "Gene cloning, purification, and characterization of NfsB, a minor oxygen-insensitive nitroreductase from Escherichia coli, similar in

biochemical properties to FRase I, the major flavin reductase in Vibrio fischeri," *Journal of Biochemistry,* vol. 120, pp. 736-744, Oct 1996.

[22] S. H. Zenno, *et al.*, "Conversion of NfsB, a minor Escherichia coli nitroreductase, to a flavin reductase similar in biochemical properties to FRase I, the major flavin reductase in Vibrio fischeri, by a single amino acid substitution," *Journal of Bacteriology,* vol. 178, pp. 4731-4733, Aug 1996.

[23] R. Ballini, *et al.*, "One-pot synthesis of polyfunctionalized alpha,beta-unsaturated nitriles from nitroalkanes (vol 44, pg 9033, 2003)," *Tetrahedron Letters,* vol. 45, pp. 1311-1311, Feb 2 2004.

[24] R. Ballini, *et al.*, "Nitroalkanes and ethyl glyoxalate as common precursors for the preparation of both beta-keto esters and alpha,beta-unsaturated esters," *Tetrahedron Letters,* vol. 45, pp. 7027-7029, Sep 13 2004.

[25] A. Cote, *et al.*, "Application of the chiral bis(phosphine) monoxide ligand to catalytic enantioselective addition of dialkylzinc reagents to beta-nitroalkenes," *Organic Letters,* vol. 9, pp. 85-87, Jan 4 2007.

[26] D. M. Mampreian and A. H. Hoveyda, "Efficient Cu-catalyzed asymmetric conjugate additions of alkylzinc reagents to aromatic and aliphatic acyclic nitroalkenes," *Organic Letters,* vol. 6, pp. 2829-2832, Aug 5 2004.

[27] J. Wu, *et al.*, "Enantioselective synthesis of nitroalkanes bearing all-carbon quaternary stereogenic centers through Cu-catalyzed asymmetric conjugate additions," *Journal of the American Chemical Society,* vol. 127, pp. 4584-4585, Apr 6 2005.

[28] C. Czekelius and E. M. Carreira, "Convenient transformation of optically active nitroalkanes into chiral aldoximes and nitriles," *Angewandte Chemie-International Edition,* vol. 44, pp. 612-615, 2005.

[29] N. J. A. Martin, *et al.*, "Organocatalytic asymmetric transfer hydrogenation of nitroolefins," *Journal of the American Chemical Society,* vol. 129, pp. 8976-+, Jul 25 2007.

[30] R. Ballini, *et al.*, "Conjugate additions of nitroalkanes to electron-poor alkenes: Recent results," *Chemical Reviews,* vol. 105, pp. 933-971, Mar 2005.

[31] A. Fryszkowska, *et al.*, "Highly enantioselective reduction of beta,beta-disubstituted aromatic nitroalkenes catalyzed by Clostridium sporogenes," *Journal of Organic Chemistry,* vol. 73, pp. 4295-4298, Jun 6 2008.

[32] M. Watanabe, *et al.*, "Nucleotide-Sequence of Salmonella-Typhimurium Nitroreductase Gene," *Nucleic Acids Research*, vol. 18, pp. 1059-1059, Feb 25 1990.

[33] C. Bryant and M. Deluca, "Purification and Characterization of an Oxygen-Insensitive Nad(P)H Nitroreductase from Enterobacter-Cloacae," *Journal of Biological Chemistry*, vol. 266, pp. 4119-4125, Mar 5 1991.

[34] M. R. Nokhbeh, *et al.*, "Identification and characterization of SnrA, an inducible oxygen-insensitive nitroreductase in Salmonella enterica serovar Typhimurium TA1535," *Mutation Research-Fundamental and Molecular Mechanisms of Mutagenesis*, vol. 508, pp. 59-70, Oct 31 2002.

[35] R. E. Williams, *et al.*, "Degradation of explosives by nitrate ester reductases," *From Protein Folding to New Enzymes*, pp. 143-153, 2001.

[36] M. Watanabe, *et al.*, "Purification and characterization of wild-type and mutant "Classical" nitroreductases of Salmonella typhimurium - L33R mutation greatly diminishes binding of FMN to the nitroreductase of S-typhimurium," *Journal of Biological Chemistry*, vol. 273, pp. 23922-23928, Sep 11 1998.

[37] M. McClelland, *et al.*, "Complete genome sequence of Salmonella enterica serovar typhimurium LT2," *Nature*, vol. 413, pp. 852-856, Oct 25 2001.

[38] F. J. Peterson, *et al.*, "Induction of Superoxide-Dismutase in Escherichia-Coli by Nitrofurazone," *Pharmacologist*, vol. 20, pp. 157-157, 1978.

[39] K. M. Fox and P. A. Karplus, "Old Yellow Enzyme at 2-Angstrom Resolution - Overall Structure, Ligand-Binding, and Comparison with Related Flavoproteins," *Structure*, vol. 2, pp. 1089-1105, Nov 15 1994.

[40] P. A. Karplus, *et al.*, "Flavoprotein structure and mechanism .8. Structure-function relations for old yellow enzyme," *Faseb Journal*, vol. 9, pp. 1518-1526, Dec 1995.

[41] A. D. N. Vaz, *et al.*, "Old Yellow Enzyme - Aromatization of Cyclic Enones and the Mechanism of a Novel Dismutation Reaction," *Biochemistry*, vol. 34, pp. 4246-4256, Apr 4 1995.

[42] E. M. Buque-Taboada, *et al.*, "Microbial reduction and in situ product crystallization coupled with biocatalyst cultivation during the synthesis of 6R-dihydrooxoisophorone," *Advanced Synthesis & Catalysis*, vol. 347, pp. 1147-1154, Jun 2005.

[43] A. Muller, *et al.*, "Enzymatic reduction of the alpha,beta-unsaturated carbon bond in citral," *Journal of Molecular Catalysis B-Enzymatic,* vol. 38, pp. 126-130, Mar 15 2006.

[44] A. Muller, *et al.*, "Asymmetric alkene reduction by yeast old yellow enzymes and by a novel Zymomonas mobilis reductase," *Biotechnology and Bioengineering,* vol. 98, pp. 22-29, Sep 1 2007.

[45] M. Wada, *et al.*, "Production of a doubly chiral compound, (4R,6R)-4-hydroxy-2,2,6-trimethylcyclohexanone, by two-step enzymatic asymmetric reduction," *Applied and Environmental Microbiology,* vol. 69, pp. 933-937, Feb 2003.

[46] J. C. Spain, "Biodegradation of Nitroaromatic Compounds," *Annual Review of Microbiology,* vol. 49, pp. 523-555, 1995.

[47] C. E. French, *et al.*, "Aerobic degradation of 2,4,6-trinitrotoluene by Enterobacter cloacae PB2 and by pentaerythritol tetranitrate reductase," *Applied and Environmental Microbiology,* vol. 64, pp. 2864-2868, Aug 1998.

[48] P. van Dillewijn, *et al.*, "Subfunctionality of Hydride Transferases of the Old Yellow Enzyme Family of Flavoproteins of Pseudomonas putida," *Applied and Environmental Microbiology,* vol. 74, pp. 6703-6708, Nov 2008.

[49] C. E. French, *et al.*, "Biodegradation of explosives by transgenic plants expressing pentaerythritol tetranitrate reductase," *Nature Biotechnology,* vol. 17, pp. 491-494, May 1999.

[50] J. W. Pak, *et al.*, "Transformation of 2,4,6-trinitrotoluene by purified xenobiotic reductase B from Pseudomonas fluorescens I-C," *Applied and Environmental Microbiology,* vol. 66, pp. 4742-4750, Nov 2000.

[51] M. M. Gonzalez-Perez, *et al.*, "Escherichia coli has multiple enzymes that attack TNT and release nitrogen for growth," *Environmental Microbiology,* vol. 9, pp. 1535-1540, Jun 2007.

[52] A. Agrawal and P. G. Tratnyek, "Reduction of nitro aromatic compounds by zero-valent iron metal," *Environmental Science & Technology,* vol. 30, pp. 153-160, Jan 1996.

[53] K. Chary and C. Srikanth, "Selective Hydrogenation of Nitrobenzene to Aniline over Ru/SBA-15 Catalysts," *Catalysis Letters,* vol. 128, pp. 164-170, Mar 2009.

[54] A. F. Cunha, *et al.*, "Catalytic decomposition of methane on Raney-type catalysts," *Applied Catalysis a-General,* vol. 348, pp. 103-112, Sep 30 2008.

[55] V. Holler, *et al.*, "Three-phase nitrobenzene hydrogenation over supported glass fiber catalysts: Reaction kinetics study," *Chemical Engineering & Technology*, vol. 23, pp. 251-255, Mar 2000.

[56] C. L. Zheng, *et al.*, "Isolation and characterization of a novel nitrobenzene-degrading bacterium with high salinity tolerance: Micrococcus luteus," *Journal of Hazardous Materials*, vol. 165, pp. 1152-1158, Jun 15 2009.

[57] C. L. Zheng, *et al.*, "Isolation and characterization of a nitrobenzene degrading yeast strain from activated sludge," *Journal of Hazardous Materials*, vol. 160, pp. 194-199, Dec 15 2008.

[58] L. J. Nadeau, *et al.*, "Production of 2-amino-5-phenoxyphenol from 4-nitrobiphenyl ether using nitrobenzene nitroreductase and hydroxylaminobenzene mutase from Pseudomonas pseudoalcaligenes JS45," *Journal of Industrial Microbiology & Biotechnology*, vol. 24, pp. 301-305, Apr 2000.

[59] A. Schenzle, *et al.*, "Chemoselective nitro group reduction and reductive dechlorination initiate degradation of 2-chloro-5-nitrophenol by Ralstonia eutropha JMP134," *Applied and Environmental Microbiology*, vol. 65, pp. 2317-2323, Jun 1999.

[60] A. Agrawal, *et al.*, "Processes Affecting Nitro Reduction by Iron - Mineralogical Consequences of Precipitation in Aqueous Carbonate Environments," *Abstracts of Papers of the American Chemical Society*, vol. 209, pp. 143-ENVR, Apr 2 1995.

[61] W. Baik, *et al.*, "Selective Reduction of Aromatic Nitro-Compounds to Aromatic-Amines by Bakers-Yeast in Basic Solution," *Tetrahedron Letters*, vol. 35, pp. 3965-3966, Jun 6 1994.

[62] J. K. Davis, *et al.*, "Sequence analysis and initial characterization of two isozymes of hydroxylaminobenzene mutase from Pseudomonas pseudoalcaligenes JS45," *Applied and Environmental Microbiology*, vol. 66, pp. 2965-2971, Jul 2000.

CHAPTER 4

CHARACTERIZATION OF XENOBIOTIC REDUCTASE A: STUDY OF ACTIVE SITE RESIDUES, SUBSTRATE SPECTRUM, AND STABILITY

Xenobiotic reductase A (XenA) has broad catalytic activity and reduces various α,β-unsaturated and nitro compounds with moderate to excellent stereoselectivity. Single mutants C25G and C25V are able to reduce nitrobenzene, a non-active substrate for the wild type, to produce aniline. Total turnover is dominated by chemical rather than thermal instability.

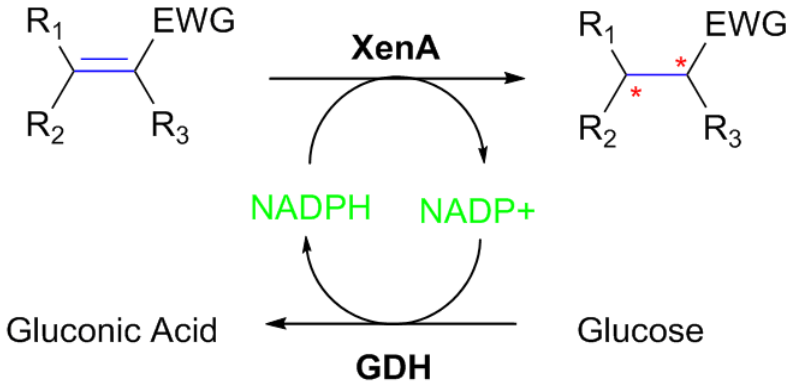

Figure 4.1. Asymmetric *trans*-bioreduction of C=C bonds coupling XenA with cofactor recycling system through half-oxidative and half-reductive reaction (EWG = electron withdrawing group, GDH = glucose dehydrogenase, * = center of chirality).

4.1 Introduction

The Old Yellow Enzyme (OYE) family is a class of flavin-dependent enzymes that catalyze the stereoselective reduction of activated C=C bonds at the expense of nicotinamide cofactors. This asymmetric bioreduction creates up to two new stereogenic centers and thus has gained increasing interest as a new tool in chiral intermediates synthesis.[1-3] Members of the OYE family were reported to catalyze the bioreduction of a variety of different substrates such as α,β-unsaturated aldehydes, ketones, imides, nitro groups, nitriles, carboxylic acids, nitro esters, and nitro aromatics.[4-6]

4.1.1 Background on xenobiotic reductase A

The catalytic activity of xenobiotic reductase A (XenA) from *Pseudomonas putida* was first reported for the reduction of nitroglycerin (reductive denitration), TNT (reduction of nitro group) and 2-cyclohexen-1-one (reduction of olefinic bond),[7] and later for nitroreductase activity for Research Department Explosive (RDX) and a series of nitroaromatic and nitramine explosive compounds.[8] This FMN containing enzyme was also shown to display broad enoate reductase activity over various α,β-unsaturated carbonyl compounds such as citral, ketoisophorone, maleimide,[9] 8-hydroxycoumarin, and coumarin.[10] XenA shares a generally low amino acid sequence identity and similarity with other OYE enzymes and structural variation was observed in the active site of XenA compared to the OYE family. A recently published study focused on XenA active site residue C25, which replaces the highly conserved threonine residue in OYE enzymes. This important residue interacts with FMN and was shown to modulate the flavin reduction potential and thus influence substrate binding in XenA.[11] An analogous residue C26 in YqjM from *Bacillus subtilis* (OYE enzyme that shares the highest sequence identity and similarity with XenA: 40.1% identity and 53.8% similarity, respectively), was shown to act as redox sensor that controls the reduction potential of FMN in YqjM, and mutation C26D and C26G changed the enzyme stereoselectivity in

the reduction of α,β-unsaturated ketones.[12] Overall, only few mutation studies have been published for OYEs[12, 13] to improve their catalytic properties and we wish to report efforts toward this goal.

4.2 Results & Discussion

In this work, the substrate spectrum, stereoselectivity, and stability of XenA were characterized. The selection of mutants was based on the results of iterative saturation mutagenesis (ISM) around the binding pocket of YqjM, which implied both residues C25 and A59 in substrate binding.[12] The QuikChange® mutagenesis protocol was used to generate C25G, C25V, and A59V mutants. We analyzed wild type XenA (WT) and the effect of mutations on thermal and chemical stability, enzyme activity, and regio- and stereoselectivity with various α,β-unsaturated compounds and nitro compounds (Table 4.2). Constant cofactor concentration was maintained using a recycling system with glucose dehydrogenase (GDH) in conversion study (Fig 4.1). The reaction products were extracted and analyzed by gas chromatography to determine substrate conversion and product enantiopurity. Enzyme activities were monitored on a spectrophotometer for specific activity, half-life at 37℃, and total turnover number (TTN) studies (Table 4.1).

Table 4.1. XenA specific activity and stability study.

XenA Constructs	WT	C25G	C25V	A59V
Substrate	Specific Activity [U/mg]			
1-Nitrocyclohexene	5.87	0.86	0.35	0.16
2-Cyclohexenone	3.84	0.80	0.47	0.05
Ketoisophorone	1.34	0.21	0.70	0.02
2-Methylfuran	0.15	0.16	0.07	0.02
T_m [°C]	50.4	52.7	48.0	63.5
$t_{1/2}$ at 37°C [h]	63	49.5	44.7	>112
$k_{d,obs}$ [h^{-1}]	0.0119	0.0136	0.0155	<0.0062
TTN_{chem}	1959	1073	280	38
$TTN_{thermal}$ (37°C)	8.3×10^5	1.4×10^5	7.2×10^4	1.9×10^4

Specific activity assay: 200 mM phosphate buffer pH 7.5, 1 mM substrate, 0.2 mM NADPH, 10 µg.mL^{-1} (0.25 µM) enzyme, 37 ^{o}C. $t_{1/2}$ assay: Enzymes incubated at 37 ^{o}C and residual activity measured with 2-cyclohexenone at different time points.

4.2.1 Specific activity study of XenA

The enzymatic activity of XenA and mutants was first investigated on four different substrates: 1-nitrocyclohexene, 2-cyclohexenone, ketoisophorone, and 2-methylfuran. WT showed highest specific activity compared to all other mutants on the four compounds. Both C25 mutants showed significantly lower reactivity for all substrates with < 1 U.mg^{-1} specific activities observed. Mutation on the C25 residue was previously shown to strongly affect both oxidative half reaction towards the substrate and reductive half reaction towards the cofactor.[11] Our results confirmed the importance of C25 in the overall reaction as shown by the much lower specific activity of the mutants compared to the wild type. Mutation of A59V had a dramatic effect on XenA, as it almost led to disappearance of any enoate reductivity. We also observed uncompetitive substrate inhibition with 2-cyclohexenone; inhibition has never been observed with XenA before.[10, 11] A non-linear fit of the Michaelis-Menten equation yielded k_{cat} of 25.7 s^{-1}, K_M of 0.19 mM, and inhibition constant K_I of 0.15 mM.

Substrate inhibition was observed with substrate 2-cyclohexenone with uncompetitive inhibition pattern. Concentration activity profile range (0 - 2.5 mM) was fitted with Matlab to determine the inhibition constant, K_I:

Michaelis-Menten equation for uncompetitive inhibition: $$v_0 = \frac{V_{max}[S]}{K_M + \alpha'[S]}$$

where $$\alpha' = 1 + \frac{[I]}{K_I}$$

Note: v_0 is the initial reaction rate at substrate concentration [S], V_{max} is the maximum rate, Michaelis constant K_M measures the substrate concentration at half V_{max}, K_I is the inhibition constant, and [I] is the inhibitor concentration.

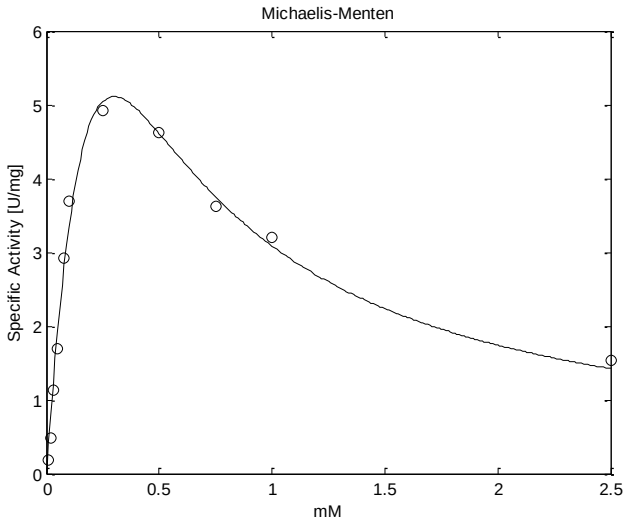

Figure 4.2. Michaelis-Menten fit for 2-cyclohexenone (0 – 2.5 mM) substrate inhibition with XenA.
The fitted parameters were: k_{cat} = 25.7 s^{-1}, K_M = 0.19 mM, K_I = 0.15 mM, R^2 = 0.9843

4.2.2 Kinetics and thermal deactivation

XenA kinetic measurement was performed by monitoring the oxidation of cofactor NADPH at 340 nm using spectrophotometer (Beckman Coulter DU800, Brea, CA), with extinction coefficient ε_{340nm} of 6.22 $mM^{-1}.cm^{-1}$. Assay condition: 200 mM phosphate buffer pH 7.5, 1 mM substrate, 0.2 mM cofactor NADPH, 10 $\mu g.mL^{-1}$ enzyme, at 37 ℃. Enzyme thermostability study (half-life $t_{1/2}$) was performed with incubation of purified enzyme at 37 ℃, and monitoring the residual activity with 2-cyclohexenone kinetic assay over time. The collected data was fitted with 1st order deactivation kinetic to determine the deactivation constant, $k_{d,obs}$. The half-life $t_{1/2}$ at 37 ℃ results: wild type 63 h, C25G 49.5 h, C25V 44.5 h, A59V >112 h. The deactivation constant $k_{d,obs}$ results: wild type 0.0119 h^{-1}, C25G 0.0136 h^{-1}, C25V 0.0155 h^{-1}, A59V 0.0062 h^{-1}.

1st order deactivation equation: $$[A] = [A]_0 e^{-k_{d,obs}t}$$

Linearization: $$\ln\left(\frac{[A]}{[A]_0}\right) = -k_{d,obs}t$$

Half life equation: $$t_{1/2} = \frac{\ln(2)}{k_{d,obs}}$$

Note: [A] is the enzyme concentration at time t, $[A]_0$ is the original enzyme concentration, t is time measurement, $t_{1/2}$ is the half-life, and $k_{d,obs}$ is the deactivation constant.

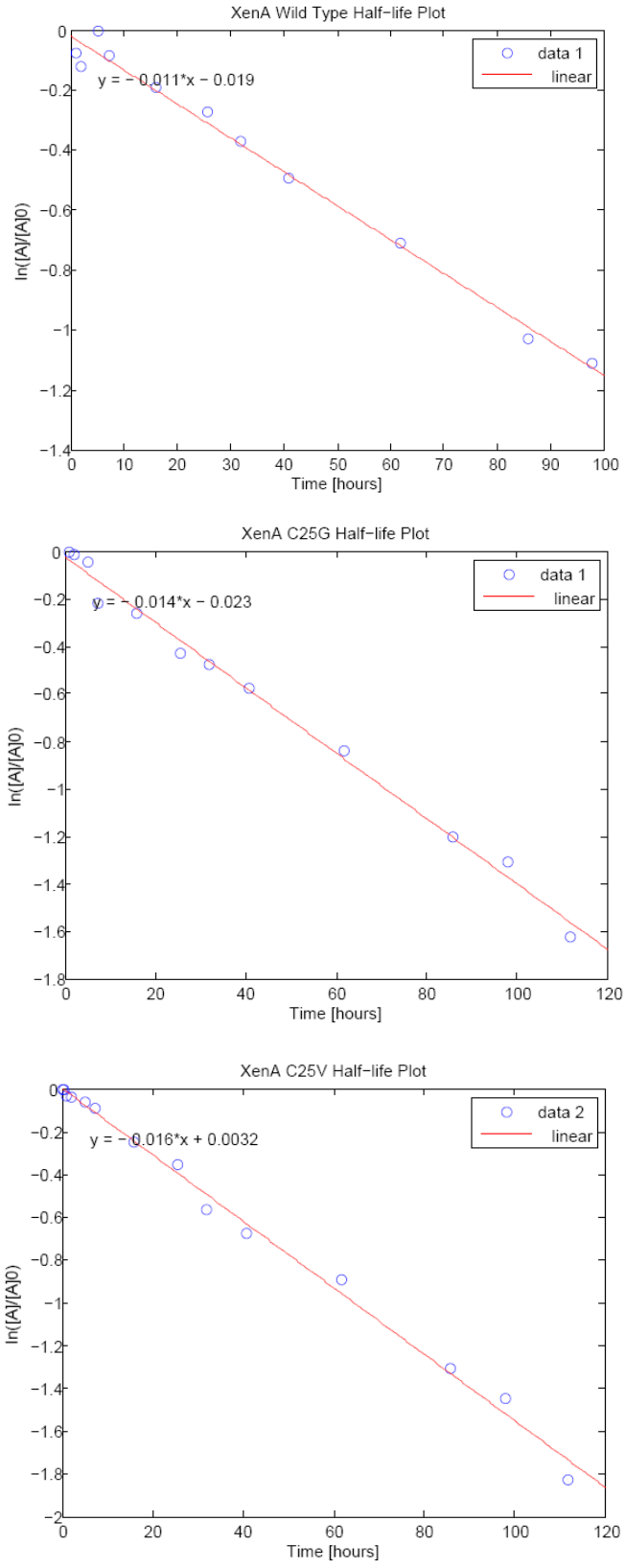

Figure 4.3**.** Thermal deactivation study of XenA wild type, C25G, and C25V mutants.

Due to its relatively high sequence identity with YqjM, XenA belongs to the same subclass of OYEs that has been proposed to contain "thermostable-like" enzymes along with recently identified thermostable OYE from *T. pseudethanolicus*,[14] and chromate reductase from the thermophile *T. scotoductus*.[15] One characteristic of this subclass is the conservation of C25, which was observed in both XenA and YqjM. We investigated the effect of C25 mutation on the thermal stability by measuring both the melting temperature (T_m) and the half-life ($t_{1/2}$) 37 ℃. The T_m of WT was determined to be 50.4 ℃ with $t_{1/2}$ of 58.2 hours at 37 ℃. C25G displayed a slightly higher T_m (52.7 ℃) but a lower $t_{1/2}$ (50.9 h), whereas C25V showed opposite behavior with T_m (reduced to 48.0℃) and a significantly lower $t_{1/2}$ of 44.7 hours. (Table 4.1) Surprisingly, A59V mutant showed major improvement in T_m to 63.5 ℃ and consequently higher $t_{1/2}$ at 37 ℃. XenA and YqjM were proposed to be stabilized through simple salt bridges involving single pairs of charged amino acids.[16] However, the single A59V mutation showed significant influence on thermostability (although as an uncharged residue, it cannot form any salt bridge), while the C25 residue did not show significant influence on thermostability.

The melting temperature T_m was determined with Circular Dichroism Spectropolarimeter (Jasco-810, Easton, MD) using 6Q quartz cuvette by analyzing the change in ellipticity at 220 nm. CD measurement assay: enzyme concentration at 50 $\mu g.mL^{-1}$ with temperature ramp of 1 $℃.min^{-1}$ from 20 – 90 ℃. The data was interpreted employing a two-state model with a native and a denaturated state.

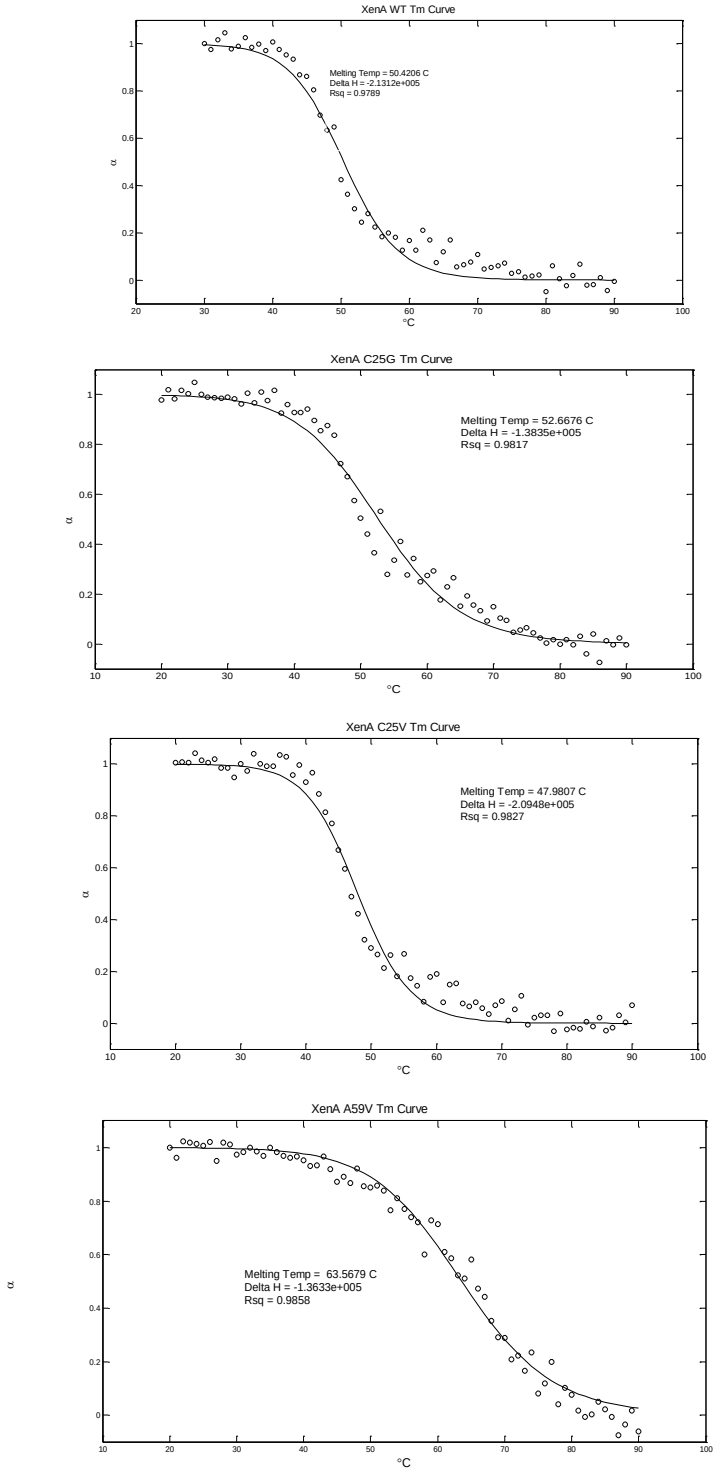

Figure 4.4. Tm curve for XenA WT, C25G, C25V, and A59V mutants.
α = 1 represents enzyme was at native state, α = 0 represents enzyme at denatured state.
The T_m result: wild type 50.4 ℃, C25G 52.7 ℃, C25V 48.0 ℃, and A59V 63.5 ℃.

4.2.3 Total turnover number study

The total turnover number (TTN) is an indicator of lifetime biocatalyst productivity and is defined as the maximum number of molecules of substrate that an enzyme active site can convert over its life cycle. The chemical TTN (TTN_{chem})[17, 18] was experimentally determined by measuring the maximum amount of substrate 2-cyclohexenone that can be reduced with a set amount of purified enzyme before the enzyme is chemically deactivated. The thermal TTN ($TTN_{thermal}$) was based on the thermal deactivation of enzyme, calculated from the ratio $k_{cat}/k_{d,obs}$, valid for enzymes with 1^{st} order thermal deactivation,[19] such as XenA. The WT showed the highest TTN values compared to all other variants. Mutant A59V showed the lowest TTN_{chem} of 38 and $TTN_{thermal}$ of 1.9×10^{4}. Overall, the results showed that XenA enzyme reactivity was dominated by chemical rather than thermal deactivation, and that single point mutations on C25 and A59 led to significant decrease in TTN. The cause for the chemical turnover-dependent deactivation is under investigation. Turnover-driven stability limits have also been observed in D-amino acid oxidase in connection with the mutation of the C108 residue.[20]

Chemical TTN was determined by varying the enzyme concentration and observing NADPH turnover until no more turnover (i.e. change in NADPH concentration) was observed.

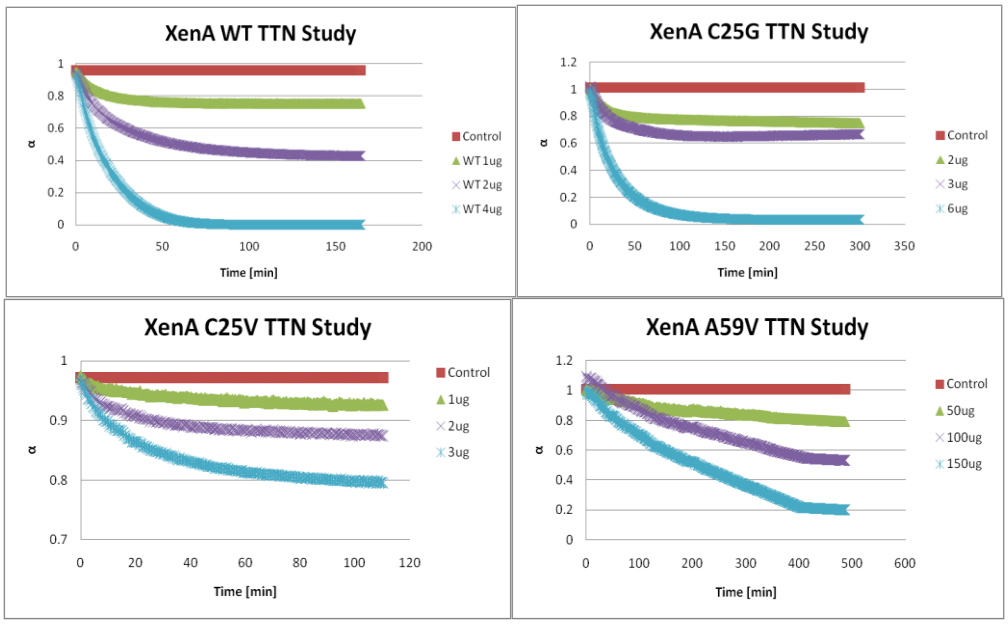

Figure 4.5. TTN Data for XenA WT and mutants. α defined as the amount of cofactor in the system. Assay: 200 mM phosphate buffer pH 7.5, 0.2 mM NADPH, 2 mM 2-cyclohexenone, and varying amount of enzyme at 37 °C. The TTN_{chem} results: wild type 1959, C25G 1073, C25V 280, and A59V 38 (Table 4.1). Note: TTN_{chem} for A59V is an approximation, this mutant still show activity even after >10 h of measurement.

Thermal TTN was estimated from readily measured biochemical quantities, namely the specific activity and the deactivation half-life, measured under identical conditions at 37 °C. This method was established and proved in recent work for enzymes whose thermal deactivation followed the 1st order deactivation.[19] This estimation method requires two parameters, namely $k_{d,obs}$, the observed first-order deactivation rate constant; and $k_{cat,obs}$, the observed turnover number.

The process yield during the life time of a biocatalyst: $yield = \int_0^{\infty} V_{\max}(t)dt$

where we define: $V_{max} = k_{cat,obv}[E]_0 e^{-k_{d,obs}t}$

The integrated result gave: $TTN = \frac{k_{cat,obs}}{k_{d,obs}}$

where $k_{cat,obs}(s^{-1}) = \frac{specific\ activity\ (\frac{U}{mg}) \times enzyme\ MW\ (\frac{g}{mol})}{60{,}000}$

and $k_{d,obs}(s^{-1}) = \frac{\ln(2)}{t_{1/2}\ (s)}$

Note: $[E]_0$ is the original enzyme concentration, $k_{cat,obs}$ is the observed catalytic constant, and $k_{d,obs}$ is the observed deactivation constant. The $TTN_{thermal}$ result: wild type 8.3×10^5, C25G 1.4×10^5, C25V 7.2×10^4, A59V 1.9×10^4 (Table 4.1)

4.2.4 Biocatalytic conversion of various α,β-unsaturated carbonyl, nitrostyrene, nitroaromatic, and nitrofuran substrates

The conversion study of XenA was performed over 12 hours with multiple sets of substrate: α,β-unsaturated carbonyl compounds (**1** - **5**), α,β-unsaturated nitro compounds (**6** – **9**), nitro aromatic compounds (**10** – **11**), and nitrofuran-like substrate (**12** – **14**) (Table 4.2). This is the first study where nitrofuran type substrates are tested with true OYE enzymes. The WT showed high conversion efficiency in C=C reduction of substrate **2**, **4**, and **9**; and modest conversion for substrate **2**, **10**, and **12**. The WT also showed moderate to excellent stereoselectivity for reduction of **2** (78.5% *R*), **5** (99.5% *R*), and **6** (69.9% *S*), although a racemic product was obtained in the reduction of **4** (2.25% *S*).[21] Overall, the WT seems to show preference for cyclic compounds (except **2** and **3**). Mutation C25G improved the conversion and stereoselectivity with various substrates compared to the wild type: conversion of **3** was increased to 6.4% from 0.4% with product e.e >99.9% (*R);* conversion of **5** was increased fourfold with similar product e.e;

conversion of **6** was also improved by 4-fold to 33.3% with slight improved product e.e. Most importantly, one single mutation was able to significantly increase the conversion of **11** (5 mM) from 1.1% to 54.3% to produce nitrosobenzene (0.18 mM), aniline (0.15 mM), and azobenzene (2.6mM). C25V mutant showed higher conversion efficiency of substrate **2** and **5** with similar or slightly enhanced product e.e; conversion of substrate **6** was slightly improved, the product was however nearly racemic with e.e of 2.7% (*S)*; C25V also catalyzed the reduction of **11** and produced similar products as C25G mutant, including aniline. Mutant A59V showed lower conversion for most of the tested substrates. However, the stereoselectivity in the reduction of **6** was significantly improved to 98% (*S*) while maintaining similar conversion efficiency as WT. Upon this result, we analyzed the reduction of **6** with the double mutant C25G/A59V. However, C25G/A59V showed negligible activity, even with 2-cyclohexenone as substrate. All mutants showed highly reduced enzymatic activity towards the reduction of nitrofurans (**12** – **14**), except for A59V that retained activity towards **13**.

Both single mutants C25G and C25V surprisingly catalyzed the reduction of **6** to produce aniline, while WT was nearly inactive. A similar reduction pattern was also reported for NRSal from *S. typhimurium*.[22] We propose the removal of the C25 residue changes the binding conformation of **6** in the catalytic pocket, thus allowing the subsequent reduction of the nitro group *via* two-electron reduction pathway and the formation of aniline. Traces of phenylhydroxylamine were also observed along the enzyme-catalyzed formation of aniline. Formation of azobenzene as side product was detected likely due to the chemical condensation reaction between nitrosobenzene and phenylhydoxylamine.[23]

Table 4.2. Biocatalytic conversion of various α,β-unsaturated carbonyl, nitrostyrene, nitroaromatic, and nitrofuran substrates.

Substrate	XenA WT		C25G		C25V		A59V	
	Conv.	e.e	Conv.	e.e	Conv.	e.e	Conv.	e.e
1. 2-Cyclohexenone	96.4%	-	99.1%	-	21.5%	-	7.1%	-
2. 2-Methyl-2-cyclopentenone	19.7%	78.5% (*R*)	12.9%	59.9% (*R*)	32.4%	86.1% (*R*)	0.5%	-
3. 3-Methyl-2-cyclohexenone	0.4%	n.d[c]	6.4%	>99.9% (*R*)	0.9%	n.d	no conv.	-
4. Ketoisophorone	98.9%	2.25% (*S*)	54.1%	37.7% (*S*)	87.7%	14.9% (*S*)	3.8%	25.6% (*S*)
5. Citral	8.1%	99.5% (*R*)	33.5%	99.5% (*R*)	18.5%	99.3% (*R*)	18.4%	68.0% (*R*)
6. 1-Nitro-2-phenyl-propene[a]	7.1%	69.9% (*S*)	33.3%	72.9% (*S*)	11.7%	2.7% (*S*)	6.3%	98% (*S*)
7. Trans-β-nitrostyrene	10.1%	-	15.6%	-	no conv.	-	5.0%	-
8. Trans-β-methyl-β-nitrostyrene	13.6%	-	36.1%	-	2.7%	-	3.6%	-
9. 1-Nitrocyclohexene	91.2%	-	29.3%	-	53.2%	-	no conv.	-
10. 2,4-Dinitrotoluene	60.2%	-	59.9%	-	23.2%	-	6.6%	-
11. Nitrobenzene[b]	1.1%	-	54.3%	-	5.9%	-	no conv.	-
12. 2-Nitrofuran	47.0%	-	0.7%	-	1.3%	-	5.8%	-
13. 2-Methyl-5-nitrofuran	17.4%	-	5.8%	-	7.0%	-	22.9%	-
14. 2-(2-Nitrovinyl)-furan	8.3%	-	7.9%	-	9.3%	-	5.8%	-

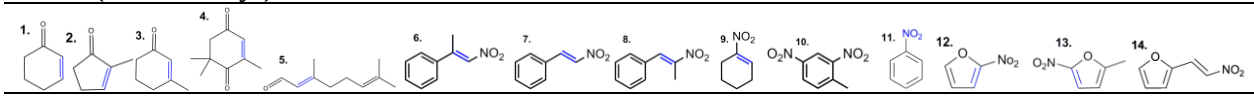

Conversion assay: 200 mM phosphate buffer pH 7.5, 5mM substrate, 20µg.mL^{-1} (0.5 µM) enzyme, 0.2 mM NADP^{+}, 20 mM glucose, 10U.mL^{-1} GDH. [a.]The conversion of **6** showed side products other than 1-nitro-2-phenyl-propane, which are possibly the corresponding carbonyl compounds similar to Nef-reaction products.[24] [b.]Conversion of **11** with C25G and C25V produced nitrosobenzene, aniline, and azobenzene. [c.]n.d: not determined.

4.3 Conclusion

In conclusion, we have characterized the substrate spectrum of WT XenA and mutants. The enzyme showed a high degree of conversion and marked stereoselectivy and was able to reduce C=C bonds as well as nitro compounds. Mutations on C25 interestingly showed significantly stronger nitroreductase activity to produce the corresponding amino product. We also studied both chemical and thermal enzyme stability, melting temperature, and TTN as an indicator for biocatalyst productivity. The results showed the effect of chemical instability is more significant than thermal instability.

4.4 Materials & Methods

4.4.1 XenA expression and purification

The gene of XenA from *Pseudomonas putida* was kindly provided by Prof. Brian Fox (University of Wisconsin, Madison, WI).[1] The *xenA* gene was transformed into *E. coli* BL21 for protein expression. The culture was started in a 5 mL LB_{Kan} medium inoculated from frozen glycerol stock and grown overnight at 37 ℃. The preculture was used for inoculation of a 1 L culture (0.1% v/v), which was gently aerated until OD600 reached 0.6 before addition of 0.1 mM of IPTG. The induced culture was incubated overnight for protein expression at 37 ℃. Harvested cell pellets were kept at -80 ℃ before protein purification.

XenA was purified with a two-step column purification process: HiTrap Q-XL anion chromatography and HiPrep Sephacryl S-100 gel filtration chromatography on an ÄKTAexplorer™ system (all by GE Healthcare, Sweden). The harvested XenA pellet was first resuspended in 20 mM pH 8.0 bis-tris buffer and disrupted by sonication. The cell debris were discarded by centrifugation, and the supernatant was washed with a

gradient of 0 - 500 mM KCl in 20 mM bis-tris buffer on a Q-XL column at a flow rate of 1 mL/min. The majority of XenA eluted at 300 mM KCl and was applied to the Sephacryl S-100 column. 50 mM sodium phosphate buffer with 300 mM NaCl at pH 7.5 was used as the running buffer with flow rate set at 0.5 mL/min, where pure XenA was collected at 60 – 70 mL elution range (total column volume is 120 mL). The protein concentration was determined by the Bradford method using Coomassie Plus Protein assay reagent with BSA assay (Pierce Chemical) as the calibration curve standard. SDS-PAGE analysis was performed with 50 µg protein loaded into each well (Figure 4.6). The protein samples were mixed with 2X sample buffer (125 mM TrisHCl, pH 6.8, 4% SDS, 50% glycerol. 0.02% bromophenol blue, and 10% 2-mercaptoethanol). The mixed samples were incubated at 100℃ for 5min and loaded onto 12% PAGE^{TM} Gold precast gel and run in BioRad Mini Protean chamber (BioRad,Hercules CA) at 150 V for 45 min with Tris-HEPES-SDS running buffer (12.1 g/L Tris, 23.8 g/L HEPES, 1 g/L SDS). Biorad Precision Plus protein ladder was used as standards in the gel analysis. GelCodeR Blue Stain Reagent (Pierce, Rockford IL) was used for final gel staining. Lastly, we measured the FMN occupancy of the purified XenA (all purified XenA wild type and variants showed full FMN occupancy) and checked the enzymatic activity with 2-cyclohexenone as substrate (Table 4.3). The FMN occupancy study was performed by observing the changes in XenA at both 360 nm and 450 nm wavelength for native and unfolded states. The changes in absorbance were used to compute the FMN concentration with extinction coefficient of 12,500 $M^{-1}.cm^{-1}$. The occupancy of FMN was determined by comparing the calculated FMN concentration with pure enzyme concentration.

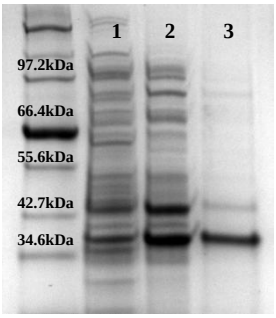

Figure 4.6. SDS-PAGE analysis for wild type XenA purification. Lane #1 lysate, #2 Q-XL fraction, #3 S-100 fraction.

Table 4.3. XenA purification table.

XenA Purification	Total Protein [mg]	% Recovery	Specific Activity [U/mg]	Total Activity [U]	% Yield
Lysate	38.4	100	2.56	98.3	100
QXL Fraction	13.3	34.6	2.97	39.5	40.2
S-100 Fraction	3.81	9.91	3.84	14.6	14.9

Assay: 200 mM phosphate buffer pH 7.5, 1 mM 2-cyclohexenone, 0.2 mM NADPH, 37℃, and 10 µg of enzyme.

4.4.2 QuikChange® mutagenesis protocol

The mutations on XenA were accomplished with the QuikChange® mutagenesis protocol with the following PCR primers design (red letters indicate the changes to the wild type):

C25G: Forward: 5' CGCCATTCCGCCCATGGGCCAGTACATGGCCGAGGAT 3'

C25V: Forward: 5' CATCGCCATTCCGCCCATGGTGCAGTACATGGCCGAGGATGG 3'

A59V: Forward: 5' TGGTGGTCGAAGCCACGGTGGTGGCACCGGAAGGGC 3'

The *xenA* gene from *Pseudomonas putida* in pET27 vector was used as the template for mutations. Failsafe buffer J (EPICENTER® Biotechnology, Madison, WI) was used in the standard PCR protocol with Pfu polymerase from New England Biolabs (Marlborough, MA). PCR assay: 25 µL of Failsafe buffer J, 125 ng *xenA* DNA plasmid template, 0.25 µM each of both forward and reverse primers, and sterile water to 50 µL in total volume. The mixed sample was first denatured at 98 ℃ for 5 minutes,

supplemented with 1 µL of Pfu buffer, followed by denaturation at 98 ℃ for another 30 seconds. The annealing temperature was set at 55 ℃ for 1 minute, extension at 72 ℃ for 16 minutes, and repeated for total of 18 cycles. The final extension was set at 72 ℃ for 25 minutes, and finished with temperature hold at 4 ℃. All mutants were sequenced with Eurofins MWG Operon (Birmingham, AL) service and transformed into *E. coli* BL21 strain for protein expression and purification as described in Section 1.1.

4.4.3 Gas chromatography analytical procedures

GC-FID analyses were performed on a Shimadzu GC-2010 instrument with helium (ultra high purity grade, Airgas South, Atlanta, GA) as carrier gas. Conversions of compounds **1–14** and e.e. values of the corresponding products were determined with the columns and methods described below. All the substrates and the corresponding products were purchased from Sigma Aldrich unless stated otherwise with literature resources provided.

2-Cyclohexen-1-one (**1**), *trans*-β-nitrostyrene (**7**), *trans*-β-methyl-β-nitrostyrene (**8**), 1-nitro-1-cyclohexene (**9**), 2,4-dinitrotoluene (**10**), nitrobenzene (**11**), 2-nitrofuran (**12**), 2-methyl-5-nitrofuran (**13**), and 2-(2-nitrovinyl)-furan (**14**) were analyzed using a SHRX5 column (15 m, 0.25 mm, 0.25 µm) (Shimadzu, Kyoto, Japan). Temperature program for **1**: injector and detector temperature at 220 ℃; split ratio 25:1; start at 100 ℃, hold 2 min, 10 ℃.min^{-1} to 160 ℃, hold 2 min. Retention time: 2-cyclohexen-1-one 1.4 min, cyclohexanone 1.3 min. Temperature program for **7**: injector and detector temperature at 320 ℃; split ratio 25:1; start at 100 ℃, hold 2 min, 10 ℃.min^{-1} to 180 ℃, 20 ℃.min^{-1} to 180 ℃, hold 1 min. Retention time: *trans*- β -nitrostyrene 6.5 min. Temperature program for **8**: injector and detector temperature at 320 ℃; split ratio 25:1; start at 100 ℃, hold 2 min, 10 ℃.min^{-1} to 180 ℃, 20 ℃.min^{-1} to 180 ℃, hold 1 min. Retention time: *trans*-β-methyl-β-nitrostyrene 6.5 min. Temperature program for **9**:

injector and detector temperature at 220 ℃; split ratio 25:1; starting at 100 ℃, hold 1 min, 20 ℃.min^{-1} to 220 ℃, hold 1 min. Retention time: 1-nitro-1-cyclohexene 8.2 min, nitrocyclohexane 16.3 min. Temperature program for **10**: injector and detector temperature at 300 ℃; split ratio 25:1; starting at 80 ℃, hold 2 min, 15 ℃.min^{-1} to 290 ℃, hold 4 min. Retention time: 2,4-dinitrotoluene 8.1 min. Temperature program for **11**: injector and detector temperature at 300 ℃; split ratio 25:1; starting at 80 ℃, hold 5 min, 10 ℃.min^{-1} to 290 ℃, hold 5 min. Retention time: nitrobenzene 5.6 min, aniline 3.2 min, nitrosobenzene 2.2 min, azobenzene 14.1 min, phenylhydroxylamine 8.0 min. Temperature program for **12**: injector temperature at 150 ℃ and detector temperature at 220 ℃; split ratio 25:1; starting at 50 ℃, hold 3 min, 30 ℃.min^{-1} to 200 ℃, hold 2 min. Retention time: 2-nitrofuran 4.6 min. Temperature program for **13**: injector temperature at 150 ℃ and detector temperature at 220 ℃; split ratio 25:1; starting at 50 ℃, hold 3 min, 30 ℃.min^{-1} to 200 ℃, hold 2 min. Retention time: 2-methyl-5-nitrofuran 6.1 min. Temperature program for **14**: injector temperature at 150 ℃ and detector temperature at 220 ℃; split ratio 25:1; starting at 50 ℃, hold 3 min, 30 ℃.min^{-1} to 200 ℃, hold 2 min. Retention time: 2-(2nitrovinyl)-furan 6.4 min.

Compounds 2-methyl-2-cyclopentenone (**2**), 3-methyl-2-cyclohexenone (**3**), ketoisophorone (**4**), and citral (**5**) were analyzed using Rt-BDEXcst chiral column (30 m, 0.32 mm, 0.25 µm) (Restek, Bellefonte, PA). Temperature program for **2**: injector and detector temperature at 200 ℃; split ratio 25:1; start at 70 ℃, hold 8 min, 10 ℃.min^{-1} to 80 ℃, hold 2 min, 30 ℃.min^{-1} to 180 ℃, hold 5 min. Retention time: 2-methyl-2-cyclopentenone 16.3 min, (*R*)-2-methylcyclopentanone 15.5 min, (*S*)-2-methylcyclopentanone 15.4 min. The absolute configurations of the enantiomers were determined via CD method as described in literature.[25] Temperature program for **3**: injector and detector temperature at 200 ℃; split ratio 20:1; start at 90 ℃, 1 ℃.min^{-1} to 130 ℃, 5 ℃.min^{-1} to 180 ℃, hold 10 min. Retention time: 3-methyl-2-cyclohexenone 50.7 min, (*R*)-2-methylcyclohexanone 37.4 min, (*S*)-3-methylcyclohexanone 37.6 min.

Temperature program for **4**: injector and detector temperature at 210 ℃; split ratio 25:1; start at 100 ℃, 3 ℃.min^{-1} to 130 ℃, 20 ℃.min^{-1} to 200 ℃, hold 3 min. Retention time: ketoisophorone 15.4 min, (*R*)-levodione 15.9 min, (*S*)-levodione 15.7 min. Temperature program for **5**: injector and detector temperature at 210 ℃; split ratio 6.4:1; start at 80 ℃, 2.5 ℃.min^{-1} to 130 ℃, hold 10 min, 5 ℃.min^{-1} to 180 ℃, hold 5 min. Retention time: citral 31.2 min, (*R*)-citronellal 22.1 min, (*S*)-citronellal 21.9 min.

1-Nitro-2-phenylpropene (**6**) was analyzed using Cyclosil-B chiral column (30 m, 0.32 mm, 0.25 μm) (Agilent J&W Scientific, Santa Clara, CA). Temperature program for **6**: injector and detector temperature at 210 ℃; split ratio 25:1; start at 100 ℃, hold 10 min, 5 ℃.min^{-1} to 130 ℃, hold 15 min, 5 ℃.min^{-1} to 220 ℃, hold 2 min. Retention time: 1-nitro-2-phenylpropene 28.7 min and 35.3 min (isomers), (*R*)-1-nitro-2-phenylpropane 25.0 min, (*S*)-1-nitro-2-phenylpropane 24.7 min. The substrate synthesis and product identification were accomplished with the reported method.[1]

4.5 Publication Information

The work presented in Chapter 4 of this dissertation was published in the *Chemical Communications*, volume. 46 pages 8809-8811, 2010; with Hua-Hsiang Yu, Mélanie Hall, and my thesis advisor Andreas S. Bommarius as co-authors.

4.6 References

[1] M. Hall, *et al.*, "Asymmetric bioreduction of C=C bonds using enoate reductases OPR1, OPR3 and YqjM: Enzyme-based stereocontrol," *Advanced Synthesis & Catalysis*, vol. 350, pp. 411-418, Feb 2008.

[2] M. Hall, *et al.*, "'Old Yellow Enzyme' family and Enoate Reductases: Asymmetric Reduction of C=C Bonds and Aromatic Nitro Compounds " in *Encyclopedia on Industrial Biotechnology*, Wiley, Ed., ed Hoboken, NJ: Wiley, 2010, pp. 2234-2247.

[3] R. Stuermer, *et al.*, "Asymmetric bioreduction of activated C=C bonds using enoate reductases from the old yellow enzyme family," *Current Opinion in Chemical Biology*, vol. 11, pp. 203-213, Apr 2007.

[4] B. Kosjek, *et al.*, "Asymmetric bioreduction of alpha,beta-unsaturated nitriles and ketones," *Tetrahedron-Asymmetry*, vol. 19, pp. 1403-1406, Jun 30 2008.

[5] J. W. Pak, *et al.*, "Transformation of 2,4,6-trinitrotoluene by purified xenobiotic reductase B from Pseudomonas fluorescens I-C," *Applied and Environmental Microbiology*, vol. 66, pp. 4742-4750, Nov 2000.

[6] R. E. Williams, *et al.*, "Biotransformation of explosives by the old yellow enzyme family of flavoproteins," *Applied and Environmental Microbiology*, vol. 70, pp. 3566-3574, Jun 2004.

[7] D. S. Blehert, *et al.*, "Cloning and sequence analysis of two Pseudomonas flavoprotein xenobiotic reductases," *Journal of Bacteriology*, vol. 181, pp. 6254-6263, Oct 1999.

[8] M. E. Fuller, *et al.*, "Transformation of RDX and other energetic compounds by xenobiotic reductases XenA and XenB," *Applied Microbiology and Biotechnology*, vol. 84, pp. 535-544, Sep 2009.

[9] J. F. Chaparro-Riggers, *et al.*, "Comparison of three enoate reductases and their potential use for biotransformations," *Advanced Synthesis & Catalysis*, vol. 349, pp. 1521-1531, Jun 2007.

[10] J. J. Griese, *et al.*, "Xenobiotic reductase A in the degradation of quinoline by Pseudomonas putida 86: Physiological function, structure and mechanism of 8-hydroxycoumarin reduction," *Journal of Molecular Biology*, vol. 361, pp. 140-152, Aug 4 2006.

[11] O. Spiegelhauer, *et al.*, "Cysteine as a Modulator Residue in the Active Site of Xenobiotic Reductase A: A Structural, Thermodynamic and Kinetic Study," *Journal of Molecular Biology*, vol. 398, pp. 66-82, Apr 23 2010.

[12] D. J. Bougioukou, *et al.*, "Directed Evolution of an Enantioselective Enoate-Reductase: Testing the Utility of Iterative Saturation Mutagenesis," *Advanced Synthesis & Catalysis,* vol. 351, pp. 3287-3305, Dec 2009.

[13] D. J. Bougioukou and J. D. Stewart, "Opposite stereochemical courses for enzyme-mediated alkene reductions of an enantiomeric substrate pair," *Journal of the American Chemical Society,* vol. 130, pp. 7655-7658, Jun 18 2008.

[14] B. V. Adalbjornsson, *et al.*, "Biocatalysis with Thermostable Enzymes: Structure and Properties of a Thermophilic 'ene'-Reductase related to Old Yellow Enzyme," *Chembiochem,* vol. 11, pp. 197-207, Jan 25 2010.

[15] D. J. Opperman, *et al.*, "A novel chromate reductase from Thermus scotoductus SA-01 related to old yellow enzyme," *Journal of Bacteriology,* vol. 190, pp. 3076-3082, Apr 2008.

[16] D. J. Opperman, *et al.*, "Crystal structure of a thermostable Old Yellow Enzyme from Thermus scotoductus SA-01," *Biochemical and Biophysical Research Communications,* vol. 393, pp. 426-431, Mar 12 2010.

[17] R. R. Jiang, *et al.*, "Comparison of alkyl hydroperoxide reductase (AhpR) and water-forming NADH oxidase from Lactococcus lactis ATCC 19435," *Advanced Synthesis & Catalysis,* vol. 347, pp. 1139-1146, Jun 2005.

[18] P. Odman, *et al.*, "An enzymatic process to alpha-ketoglutarate from L-glutamate: the coupled system L-glutamate dehydrogenase/NADH oxidase," *Tetrahedron-Asymmetry,* vol. 15, pp. 2933-2937, Sep 20 2004.

[19] T. A. Rogers and A. S. Bommarius, "Utilizing simple biochemical measurements to predict lifetime output of biocatalysts in continuous isothermal processes," *Chemical Engineering Science,* vol. 65, pp. 2118-2124, Mar 15 2010.

[20] M. Mueller, *et al.*, "The role of Cys108 in Trigonopsis variabilis D-amino acid oxidase examined through chemical oxidation studies and point mutations C108S and C108D," *Biochimica Et Biophysica Acta-Proteins and Proteomics,* vol. 1804, pp. 1483-1491, Jul 2010.

[21] A. Fryszkowska, *et al.*, "Asymmetric Reduction of Activated Alkenes by Pentaerythritol Tetranitrate Reductase: Specificity and Control of Stereochemical Outcome by Reaction Optimisation," *Advanced Synthesis & Catalysis,* vol. 351, pp. 2976-2990, Nov 2009.

[22] Y. Yanto, *et al.*, "Nitroreductase from Salmonella typhimurium: characterization and catalytic activity," *Organic & Biomolecular Chemistry,* vol. 8, pp. 1826-1832, 2010.

[23] A. Agrawal and P. G. Tratnyek, "Reduction of nitro aromatic compounds by zero-valent iron metal," *Environmental Science & Technology,* vol. 30, pp. 153-160, Jan 1996.

[24] K. Durchschein, *et al.*, "The flavoprotein-catalyzed reduction of aliphatic nitro-compounds represents a biocatalytic equivalent to the Nef-reaction," *Green Chemistry,* vol. 12, pp. 616-619, Apr 2010.

[25] Partridg.Jj, *et al.*, "Asymmetric Synthesis of Loganin - Stereospecific Formation of "(1r,2r)-2-Methyl-3-Cyclopenten-1-Ol and "(1s,2s)-2-Methyl-3-Cyclopenten-1-Ol and (2r)-2-Methylcyclopentanone and (2s)-2-Methylcyclopentanone," *Journal of the American Chemical Society,* vol. 95, pp. 532-540, 1973.

CHAPTER 5

ASYMMETRIC BIOREDUCTION OF ALKENES USING YERS-ER AND KYE1, AND EFFECTS OF ORGANIC SOLVENTS

Asymmetric *trans*-bioreduction of activated alkenes by KYE1 from *Kluyveromyces lactis* and YersER from *Yersinia bercovieri*, two ene-reductases from the Old Yellow Enzyme Family, showed broad substrate spectrum with a moderate to excellent degree of stereoselectivity. Both substrate- and enzyme-based stereocontrol were observed to furnish opposite stereoisomeric products. The effects of organic solvents on enzyme activity and stereoselectivity were outlined in this study, where two-phase systems hexane and toluene are shown to sustain bioreduction efficiency even at high organic solvent content.

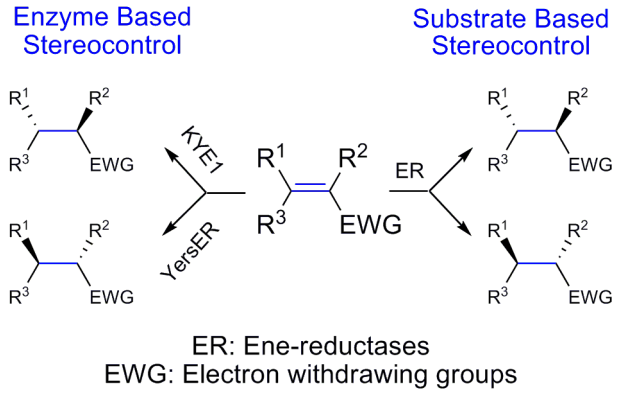

Figure 5.1. Enzyme and substrate based stereocontrol asymmetric *trans*-bioreduction of activated alkenes by KYE1 and Yers-ER.

5.1 Introduction

The application of biocatalyst has become an increasingly attractive route in the production of enantiomerically pure compounds in industry due to exquisite regio- and stereoselectivity.[1, 2] One of the emerging platforms is the asymmetric reduction of activated C=C bonds due to the potential to create up to two new stereogenic centers in the process.[3-7] Ene-reductase from the Old Yellow Enzyme (OYE) family have been reported to catalyze the reduction of a variety of different substrates such as α,β-unsaturated compounds (activated by electron-withdrawing groups such as aldehydes, ketones, imides, nitro groups, nitriles, carboxylic acids, esters) and nitro derivatives such as nitro esters and nitro aromatics.[8-11] The reduction reaction catalyzed by the OYE family of flavoproteins proceeds in a strict *trans* fashion, with hydride attack derived from the nicotinamide cofactor.[12, 13] Utilizing the coupled-enzyme approach, an efficient cofactor recycling system with enzymes such as glucose dehydrogenase (GDH) is commonly applied to decrease the high costs of redox cofactor for larger scale synthesis.[4, 14, 15] Furthermore, a light-driven cofactor regeneration system[16] and a nicotinamide-independent reduction system[17] were recently reported to yield high substrate conversion and product enantiopurity; again highlighting the potential of OYEs in industrial biotechnological applications.

In a previous work, we have begun to characterize three ene-reductases: KYE1 from *Kluyveromyces lactis*, YersER from *Yersinia bercovieri*, and XenA from *Pseudomonas putida*. We have shown that these three ene-reductases feature broad but different substrate specificity on various α,β-unsaturated carbonyl compounds. XenA was further demonstrated to possess moderate to excellent stereoselectivity and catalyze the reduction of various nitro compounds.[18, 19] In this study, we further explore the catalytic efficiency and stereoselectivity of YersER and KYE1 with a new set of substrates including α,β-alkyl substituted cyclic enones, enolethers, carboxylic esters,

nitrostyrenes, and maleimide-type compounds, and test both enzymes in aqueous-organic media.

5.2 Results & Discussion

5.2.1 Asymmetric bioreduction of alkenes

The substrate study for both KYE1 and YersER were performed over 12 hours with the GDH cofactor recycling system (Table 5.1). Both enzymes showed excellent stereoselectivity toward the reduction of α,β-alkyl substituted cyclic enones (**1** - **4**), and predominantly furnished the corresponding (*S*)-products. Substrate-based stereocontrol was observed for the reduction of α,β-substituted enolethers[20]. The reduction of five-membered cyclic-enolethers (**5-6**) furnished the corresponding (*S*)-products, but increasing the ring-size to cyclohexenone-enolether (**8**), the stereopreference switched to (*R*) for both enzymes; furthermore, by changing the side chain substitution from a methyl group (**8**) to a sterically more demanding *n*-propyl- (**10**) or phenylgroup (**9**), the substrate was flipped in the enzyme binding pockets to furnish the corresponding (*S*)-products. The results from substrates **1** – **13** showed that KYE1 and YersER strongly prefer α-substituted substrates, significantly lower activity was observed for β-substituted substrates (**2**, **4**, **7**, **11**, and **13**). The conversion of dicarboxylic esters, nitrostyrenes, maleimide, and citral (**14** – **21**) revealed moderate to high degree of enzymatic activity together with excellent product enantiopurity, except for **19**, where a racemic product was observed for both enzymes.[5] Enzyme based stereo-control was again seen in the reduction of **15** and **21**, where KYE1 and YersER formed the corresponding (*R*)- and (*S*)-products, respectively.[21]

Table 5.1. Asymmetric bioreduction study using ene-reductase KYE1 and YersER.

Enzyme		**KYE1**		**YersER**	
		Conv %	e.e %	Conv %	e.e %
α,β-alkyl substituted cyclic enones					
1. $R^1 = CH_3$, $R^2 = H$		65	(*S*) >99	45	(*S*) >99
2. $R^1 = H$, $R^2 = CH_3$	 **1-2**	6	(*S*) >99	3	(*S*) >99
3. $R^1 = CH_3$, $R^2 = H$		89	(*S*) >99	95	(*S*) >99
4. $R^1 = H$, $R^2 = CH_3$	**3-4**	27	(*S*) >99	5	(*S*) >99
α,β-substituted enolethers					
5. $R^1 = CH_3$	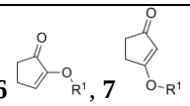 **5-6**, **7**	46	(*S*) 90	51	(*S*) 47
6. $R^1 = CH_2Ph$		0.4	(*S*) >99	26	(*S*) 99
7. $R^1 = CH_3$		nc[a]	-	nc	-
8. $R^1 = CH_3$	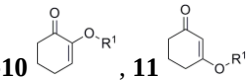	54	(*R*) 71	68	(*R*) 32
9. $R^1 = CH_2Ph$	**8-10**, **11**	29	(*S*) 90	100	(*S*) 92
10. $R^1 = CH_2CH_2CH_3$		1	(*S*) >99	68	(*S*) 94
11. $R^1 = CH_3$		0.5	-	nc	-
Monoesters					
12. $R^1 = H$	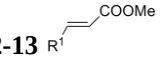	39	-	42	-
13. $R^1 = CH_3$	**12-13**	nc	-	nc	-
Dicarboxylic esters					
14	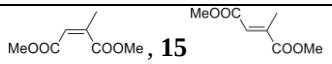	74	(*R*) 97	87	(*R*) >99
15	**14**, **15**	89	(*S*) 94	79	(*R*) 77
16	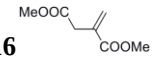 **16**	3	(*R*) >99	29	(*R*) >99
Nitrostyrene					
17. $R^1 = H$, $R^2 = H$		100	-	100	-
18. $R^1 = CH_3$, $R^2 = H$	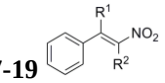	98	(*R*) 95	98	(*R*) 99
19. $R^1 = H$, $R^2 = CH_3$	**17-19**	99	racemic	99	racemic
Maleimide type					
20	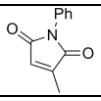	80	(*R*) 89	100	(*R*) 95
Citral					
21	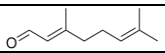	68	(*R*) 86	96	(*S*) >99

5.2.2 Effects of organic solvents on catalytic efficiency and stereoselectivity

To enhance the technological utility of ene-reductase for gram-scale synthesis, especially for less water-soluble substrates, we investigated the effects of organic solvents on catalytic efficiency and stereoselectivity. To date, there are only few data published addressing solvent effects on OYEs,[22, 23] and this work represents the first detailed study of organic solvent effects on ene-reductase. Water/organic binary co-

solvent systems often enhance the catalytic properties of enzymes and potentially offer significant advantages for increasing biocatalyst performance in synthetic chemistry.[24, 25] Twelve different organic solvents (both water miscible and immiscible), arranged according to denaturation capacity scale,[26] were tested with KYE1 and YersER for the bioreduction of 2-cyclohexen-1-one in 20% organic solvent / buffer system (Table 5.2).

Table 5.2. Catalytic activity for bioreduction of 2-cyclohexen-1-one in 20% organic solvent system.

Solvent	**DC**[a]	**logP**[b]	**YersER Conv %**	**KYE1 Conv %**
Ethylene glycol	18.7	-1.43	100	98.9
Methanol	30.5	-0.74	61.8	23.7
1,2-Propanediol	38.8	-0.74	3.1	3.2
Ethanol	54.4	-1.35	6.9	6.6
Dimethyl sulfoxide	60.3	-0.32	100	98.5
Dimethylformamide	63.3	-1.35	5.1	4.1
Acetonitrile	64.3	-0.32	0.6	0.2
Acetone	78.2	3.5	9.8	5.3
1,4-Dioxane	92.1	-0.27	10.7	9.1
Tetrahydrofuran	100	0.46	1.0	0.7
Toluene	137.9	2.46	98.1	97.8
Hexane	144.4	3.5	94.8	95.3

Screening results showed that both KYE1 and YersER retained highest enzyme activity in ethylene glycol, dimethyl sulfoxide (DMSO), and in the hexane- and toluene-buffer systems. Given the low level of amino acid identity and similarity between KYE1 and YersER (36% and 53%, respectively), the result also suggests that, in this case, the effect of organic solvents on enzyme stability is independent of both the denaturing capacity scale and the protein amino acid sequences. The experimentally determined threshold concentration (C_{50}), at which half inactivation of the enzyme is observed, for both KYE1 and YersER was 43.3% for ethylene glycol/buffer and 27.5% for dimethyl sulfoxide/buffer. For the two-phase hexane and toluene systems, the catalytic reaction

does not seem to be impaired even at 70% organic solvent level, corresponding to a phase ratio of organic to aqueous solvent of 2.33 (0.7:0.3). Since both hexane and toluene are immiscible with water, the enzymes are expected to be in the aqueous phase with minimum contact of organic solvents, and thus retained full enzyme activity. However, there is only one phase for ethylene glycol and DMSO systems, therefore the enzymes were much more exposed to the organic solvent, which resulted in decreased activity. A similar trend was observed for the bioreduction of citral with KYE1 and YersER, where the conversion and product enantiopurity were monitored in the presence of 0 – 50% organic solvent (Figure 5.2). Surprisingly, the product enantiopurity decreased tracking the diminishing enzyme activity (lower conversion) for ethylene glycol (Fig 5.2a) and DMSO (Fig 5.2b). The hexane- and toluene-buffer systems again showed constant enzymatic activity and product enantiopurity in the investigated range of phase ratio (Fig 5.2c-d).

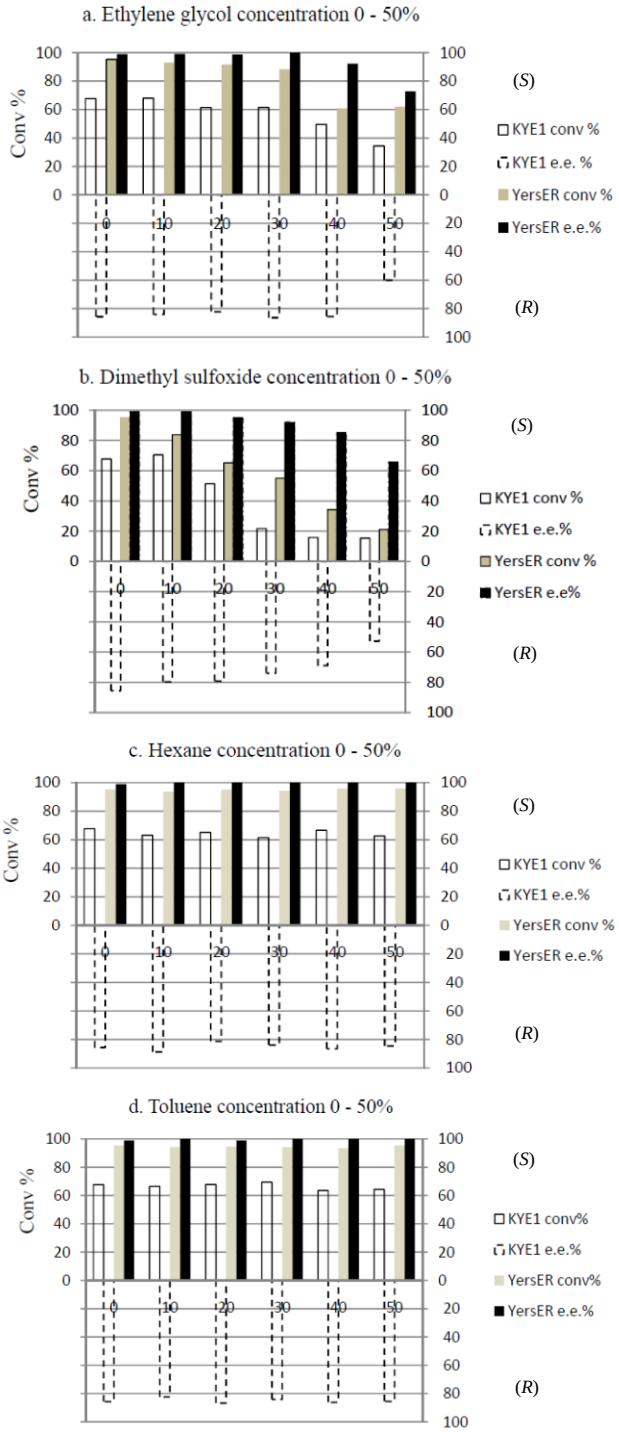

Figure 5.2**.** Dependence of organic solvent concentration on the catalytic activity and stereoselectivity of KYE1 and YersER in the asymmetric bioreduction of citral (**21**).

5.2.3 YersER and KYE1 denaturation studies

The denaturation process of KYE1 and YersER by a series of organic solvents of different nature was investigated in this study based on the bioconversion results were analyzed by gas chromatography. Ethylene glycol and dimethyl sulfoxide systems showed that the denaturation proceeded in an S-curve-type trend, with a rapid change in enzyme catalytic activity observed after a certain threshold concentration of organic solvent had been reached (Fig 5.3a-b). The experimentally determined threshold concentration (C_{50}) for both KYE1 and YersER was 43.3% for the ethylene glycol system and 27.5% for the dimethyl sulfoxide system. The C_{50} of enoate reductases appeared to be higher for systems with lower denaturing capacity (DC) factor such as ethylene glycol (DC 18.7), compared to dimethyl sulfoxide (DC 60.3). For hexane and toluene systems, the catalytic activities of both enzymes were not impaired. The bioconversion both enzymes remained constant even at 70% organic solvent level (Fig 5.3c-d).

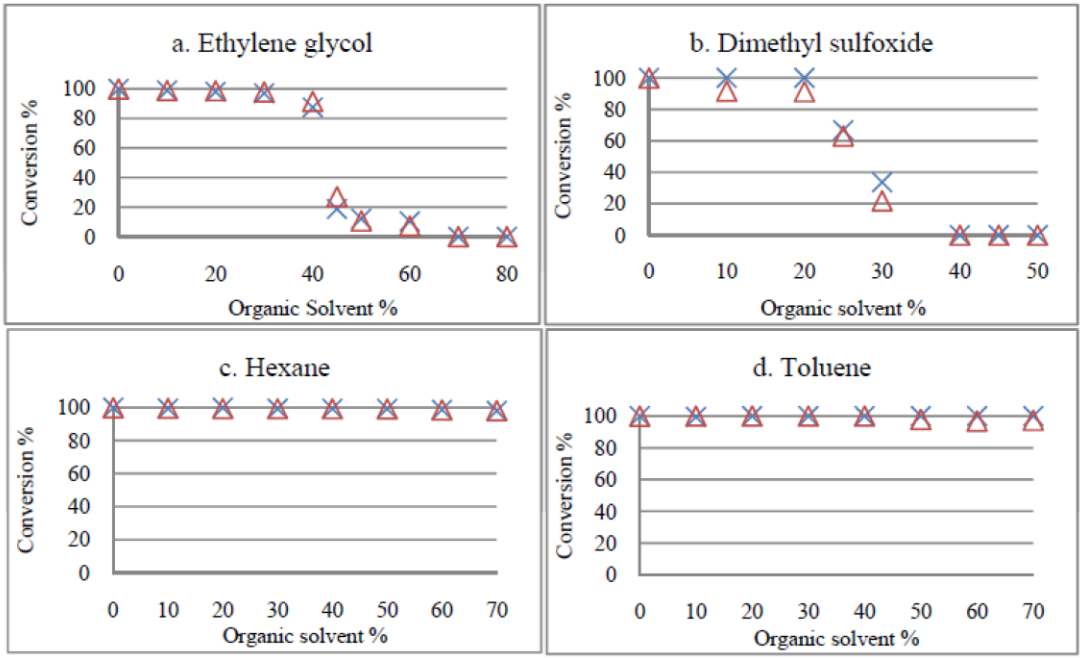

Figure 5.3. Dependence of catalytic activity of KYE1 (Δ) and YersER (X) on the concentration of organic solvents for bioreduction of 2-cyclohexen-1-one.

5.3 Conclusion

In conclusion, KYE1 and YersER showed broad substrate spectrum with a moderate to excellent degree of stereoselectivity. The results displayed both substrate-based (enolethers, diesters) and enzyme-based (citral, lactones) stereocontrol. Biphasic organic solvent / buffer system revealed no effect of the phase ratio (in the range of 0 – 2.3) on catalytic efficiency or stereoselectivity. In monophasic DMSO- and ethylene glycol-buffer systems, the activity declined markedly beyond 20% and 35% solvent, respectively, and stereoselectivity of citral bioconversion declined as well with rising solvent content. To further enhance the applicability of ene-reductases, future research efforts should focus on predictability and effective enhancement of product enantiopurity.

Acknowledgment: The experimental assistance of Clemens Stueckler and Hua-Hsiang Yu is gratefully acknowledged.

5.4 Materials & Methods

5.4.1 Enzyme expression and purification

KYE1 and YersER genes were isolated from the genomic DNA of *Kluyveromyces lactis* ATCC 8585 and *Yersinia bercovieri* ATCC 43970 respectively. The gene products were cloned into pET28a (+) vector (Novagen, San Diego, CA) at the following restriction sites: NdeI and XhoI for KYE1, and NdeI and HindIII for YersER. These constructs enabled the expression of mature ER with an N-terminal polyhistidine tag for convenient purification. The sequences of KYE1 and YersER are accessible from the NCBI databank with accession numbers P40952 and ZP_00823209, respectively.[18]

The KYE1 and YersER genes were transformed into *E. coli* BL21 for protein expression. The starter culture consisted of 5 ml LB_{Kan}, inoculated from frozen stock, and grown overnight at 37 °C. The starter culture was then used for inoculation of

300 mL culture (0.1% v/v), which was gently aerated until OD_{600} reached 0.5 for addition of 0.1 mM IPTG and then left overnight for protein expression. Harvested cell pellets were kept for -80 ℃ for protein purification. The polyhistidine tagged enzymes were purified according to the standard Ni2+-NTA bead protocol from Qiagen (Valencia, CA). The protein concentration was determined by the Bradford method with Coomassie Plus Protein assay reagent and BSA assay (Pierce Chemical, Chicago, IL) as the calibration curve.

5.4.2 Bioconversion assay

The bioconversions for substrates **1** – **4**, **17** – **19**, and **21** were performed with 200 mM phosphate buffer pH 7.5, 10 mM substrate, 20 $\mu g.mL^{-1}$ (0.5 µM) enzyme, 0.2 mM $NADP^+$, 20 mM glucose, 10 $U.mL^{-1}$ GDH, at room temperature incubated over 12 hours. The bioconversions for substrates **5** – **16**, and **20** were performed with 50 mM Tris/HCl buffer pH 7.5, 10 mM substrate, 15 mM NADPH incubated at 30℃ over 12 hours. Then an equal volume of ethyl acetate was added for extraction before analysis with GC. Substrates **12** and **13** were extracted using toluene. The phosphate buffer system was applied in the organic solvent study, where different ratios of organic solvents were mixed into the above assay while maintaining the same cofactor recycling system during the bioconversion. Substrates and products of **1** – **4**, **17** – **19**, and **21** were purchased from Sigma Aldrich or VWR with highest purity available. The enantiopurity of products of 1 and 3 were determined with published circular dichroism method.[27, 28] Products of **18** and **19** were synthesized according to previous published protocols.[29, 30] Substrates and products of **5** – **16**, and **20** were prepared as reported previously, together with absolute configuration determination.[4, 8, 20, 21]

5.4.3 Analytical procedures

Reaction assays were analyzed with a Shimadzu GC-2010 HPLC instrument using RT-BDEXcsf chiral column (30 m, 0.32 mm, 0.25 µm film, Restek) for entry **1** – **4**, **21**; Hydrodex-beta-TBDAc (25 m, 0.25 mm, 0.25 µm film, Macherey-Nagel) for entry **5** – **6**, **8**, and **14** – **16**; Chiraldex B-TA (40 m, 0.25 mm, 0.12 µm film, Supelco) for entry **9** – **10**; HP5 19091J-413 (30 m 0.320 mm 0.25 µm JW Scientific) for entry **7**, **11**, **12** – **13**, **20**; and Cyclosil-B chiral column (30 m 0.32 mm 0.25 µm, J&W Scientific) for entry **17** – **19**. The carrier gas for GC was He at 14.5 psi for entry **1** – **4**, **17** – **19**, and **21**; and H_2 at 14.5 psi for entry **5** – **16** and **20**.

Temperature program for **1**: injector and detector temperature at 200 ℃; split ratio 25:1; starting at 70 ℃, hold 8 min, 10 ℃.min^{-1} to 80 ℃, hold 2 min, 30 ℃.min^{-1} to 180 ℃, hold 5 min. Retention time: substrate 13.4 min, (*S*)-product 12.3 min, (*R*)-product 12.4 min.

Temperature program for **2**: injector and detector temperature at 220 ℃; split ratio 25:1; starting at 80 ℃, hold 5 min, 1 ℃.min^{-1} to 110 ℃, 20 ℃.min^{-1} to 200 ℃, hold 10 min. Retention time: substrate 14.9 min, (*S*)-product 12.9 min, (*R*)-product 13.0 min.

Temperature program for **3**: injector and detector temperature at 220 ℃; split ratio 20:1; starting at 100 ℃, hold 5 min, 1 ℃.min^{-1} to 140 ℃, 20℃.min^{-1} to 200 ℃, hold 10 min. Retention time: substrate 30.8 min, (*R*)-product 20.1 min, (*S*)-product 20.3 min.

Temperature program for **4**: injector and detector temperature at 200 ℃; split ratio 20:1; starting at 90 ℃, hold 8 min, 1 ℃.min^{-1} to 130 ℃, 50 ℃.min^{-1} to 180 ℃, hold 10 min. Retention time: substrate 35.8 min, (*R*)-product 15.4 min, (*S*)-product 15.6 min.

Temperature program for **5**: injector and detector temperature at 200 ℃; split ratio 20:1; starting at 50 ℃, hold 5 min, 10 ℃.min^{-1} to 100 ℃, hold 10 min, 20

℃.min^{-1} to 180 ℃, hold 10 min. Retention time: substrate 24.5 min, (*S*)-product 20.7 min, (*R*)-product 21.3 min.

Temperature program for **6**: injector and detector temperature at 200℃; split ratio 25:1; starting at 100 ℃, hold 20 min, 10 ℃.min^{-1} to 130 ℃, hold 30 min, 15 ℃.min^{-1} to 170 ℃, hold 20 min. Retention time: substrate 67.0 min, (*R*)-product 57.6 min, (*S*)-product 58.1 min.

Temperature program for **7**, **11**, **12** – **13**: injector and detector temperature at 200 ℃; split ratio 20:1; starting at 40 ℃, hold 2 min, 20 ℃.min^{-1} to 180 ℃, hold 5 min, Retention time: entry **7** substrate 5.9 min, product 4.8 min; entry **11** substrate 8.0 min, product 5.8 min; entry **12** substrate 2.5 min, product 2.6 min; entry **13** substrate 3.8 min, product 3.5 min.

Temperature program for **8**: injector and detector temperature at 200 ℃; split ratio 25:1; starting at 80 ℃, hold 1 min, 2.5 ℃.min^{-1} to 100 ℃, 15℃.min^{-1} to 180℃, hold 5 min. Retention time: substrate 14.6 min, (*R*)-product 13.5 min, (*S*)-product 13.7 min.

Temperature program for **9**: injector and detector temperature at 200 ℃; split ratio 25:1; starting at 130 ℃, hold 40 min, 2 ℃.min^{-1} to 180 ℃, hold 10 min. Retention time: substrate 72.7 min, (*R*)-product 57.4 min, (*S*)-product 57.8 min.

Temperature program for **10**: injector and detector temperature at 200 ℃; split ratio 25:1; starting at 40 ℃, hold 2 min, 4 ℃.min^{-1} to 120 ℃, hold 1 min, 150 ℃.min^{-1} to 180 ℃, hold 5 min. Retention time: substrate 27.9 min, (*R*)-product 23.2 min, (*S*)-product 23.5 min.

Temperature program for **14 - 16**: injector and detector temperature at 180 ℃ and 200 ℃ respectively; split ratio 20:1; starting at 90 ℃, hold 4 min, 0.5 ℃.min^{-1} to 95 ℃, 15 ℃.min^{-1} to 130 ℃, hold 3 min. Retention time: entry **14** substrate 15.1 min; entry **15** substrate 15.5 min, entry **16** substrate 15.1 min, (*R*)-product 11.8 min, (*S*)-product 12.3 min (substrates **14, 15** and **16** yield the same product).

Temperature program for **17 - 19**: injector and detector temperature at 210 ℃; split ratio 25:1; start at 100 ℃, hold 10 min, 5 ℃.min^{-1} to 130 ℃, hold 15 min, 5 ℃.min^{-1} to 220 ℃, hold 2 min. Retention time: entry **17** substrate 25.3 min, product 19.0 min; entry **18** substrate 20.3 min, (*S*)-product 15.6 min, (*R*)-product 15.9 min; entry **19** substrate 28.7min, (*S*)-product 24.7 min, (*R*)-product 25.0 min.

Temperature program for **20**: injector and detector temperature at 200 ℃; split ratio 25:1; starting at 40 ℃, hold 2 min, 20 ℃.min^{-1} to 180 ℃, hold 5 min. Retention time: substrate 10.4 min, product 11.1 min. Enantioselectivity of **24** was determined with HPLC equipped with Chiralcel OD-H column (25 cm, 0.46 cm, Daicel Chemical), with 60 min running buffer of *n*-heptane / isopropanol 95:5 (isocratic) set at 1 mL/min 18℃. Retention time: substrate 15.0 min, (*R*)-product 31.5 min, (*S*)-product 34.30 min.

Temperature program for **21**: injector and detector temperature at 210℃; split ratio 6.4:1; starting at 80℃, 2.5℃.min^{-1} to 130℃, hold 10 min, 20℃.min^{-1} to 180℃, hold 2 min. Retention time: substrate 17.4 min and 19.8 min, (*R*)-product 12.2 min, (*S*)-product 12.4 min.

5.5 Publication Information

This work presented in Chapter 5 of this dissertation has been submitted as a manuscript to *Organic Letters* with my Christoph K. Winkler, Stephanie Lohr, Mélanie Hall, Kurt Faber, and thesis advisor Andreas S. Bommarius, as co-authors.

5.6 References

[1] M. Muller, "Chemical diversity through biotransformations," *Current Opinion in Biotechnology*, vol. 15, pp. 591-598, Dec 2004.

[2] A. Zaks, "Industrial biocatalysis," *Current Opinion in Chemical Biology*, vol. 5, pp. 130-6, Apr 2001.

[3] M. Hall, *et al.*, "'Old Yellow Enzyme' family and Enoate Reductases: Asymmetric Reduction of C=C Bonds and Aromatic Nitro Compounds " in *Encyclopedia on Industrial Biotechnology*, Wiley, Ed., ed Hoboken, NJ: Wiley, 2010, pp. 2234-2247.

[4] M. Hall, *et al.*, "Asymmetric bioreduction of activated alkenes using cloned 12-oxophytodienoate reductase isoenzymes OPR-1 and OPR-3 from Lycopersicon esculentum (Tomato): A striking change of stereoselectivity," *Angewandte Chemie-International Edition*, vol. 46, pp. 3934-3937, 2007.

[5] R. Stuermer, *et al.*, "Asymmetric bioreduction of activated C=C bonds using enoate reductases from the old yellow enzyme family," *Current Opinion in Chemical Biology*, vol. 11, pp. 203-213, Apr 2007.

[6] H. S. Toogood, *et al.*, "Structure-Based Insight into the Asymmetric Bioreduction of the C=C Double Bond of alpha,beta-Unsaturated Nitroalkenes by Pentaerythritol Tetranitrate Reductase," *Advanced Synthesis & Catalysis*, vol. 350, pp. 2789-2803, Nov 2008.

[7] H. S. Toogood, *et al.*, "Biocatalytic Reductions and Chemical Versatility of the Old Yellow Enzyme Family of Flavoprotein Oxidoreductases," *Chemcatchem*, vol. 2, pp. 892-914, Aug 2010.

[8] M. Hall, *et al.*, "Asymmetric bioreduction of C=C bonds using enoate reductases OPR1, OPR3 and YqjM: Enzyme-based stereocontrol," *Advanced Synthesis & Catalysis*, vol. 350, pp. 411-418, Feb 2008.

[9] B. Kosjek, *et al.*, "Asymmetric bioreduction of alpha,beta-unsaturated nitriles and ketones," *Tetrahedron-Asymmetry*, vol. 19, pp. 1403-1406, Jun 30 2008.

[10] R. E. Williams, *et al.*, "Biotransformation of explosives by the old yellow enzyme family of flavoproteins," *Applied and Environmental Microbiology*, vol. 70, pp. 3566-3574, Jun 2004.

[11] Y. Yanto, *et al.*, "Nitroreductase from Salmonella typhimurium: characterization and catalytic activity," *Organic & Biomolecular Chemistry*, vol. 8, pp. 1826-1832, 2010.

[12] K. Stott, *et al.*, "Old Yellow Enzyme - the Discovery of Multiple Isozymes and a Family of Related Proteins," *Journal of Biological Chemistry,* vol. 268, pp. 6097-6106, Mar 25 1993.

[13] A. D. N. Vaz, *et al.*, "Old Yellow Enzyme - Aromatization of Cyclic Enones and the Mechanism of a Novel Dismutation Reaction," *Biochemistry,* vol. 34, pp. 4246-4256, Apr 4 1995.

[14] A. Muller, *et al.*, "Asymmetric alkene reduction by yeast old yellow enzymes and by a novel Zymomonas mobilis reductase," *Biotechnology and Bioengineering,* vol. 98, pp. 22-29, Sep 1 2007.

[15] M. A. Swiderska and J. D. Stewart, "Stereoselective enone reductions by Saccharomyces carlsbergensis old yellow enzyme," *Journal of Molecular Catalysis B-Enzymatic,* vol. 42, pp. 52-54, Oct 2 2006.

[16] A. Taglieber, *et al.*, "Light-driven biocatalytic oxidation and reduction reactions: Scope and limitations," *Chembiochem,* vol. 9, pp. 565-572, Mar 3 2008.

[17] C. Stueckler, *et al.*, "Nicotinamide-independent asymmetric bioreduction of C=C-bonds via disproportionation of enones catalyzed by enoate reductases," *Tetrahedron,* vol. 66, pp. 663-667, Jan 16 2010.

[18] J. F. Chaparro-Riggers, *et al.*, "Comparison of three enoate reductases and their potential use for biotransformations," *Advanced Synthesis & Catalysis,* vol. 349, pp. 1521-1531, Jun 2007.

[19] Y. Yanto, *et al.*, "Characterization of xenobiotic reductase A (XenA): study of active site residues, substrate spectrum and stability," *Chemical Communications,* vol. 46, pp. 8809-8811, 2010.

[20] C. K. Winkler, *et al.*, "Asymmetric Synthesis of O-P

[21] C. Stueckler, *et al.*, "Stereocomplementary bioreduction of alpha,beta-unsaturated dicarboxylic acids and dimethyl esters using enoate reductases: Enzyme- and substrate-based stereocontrol," *Organic Letters,* vol. 9, pp. 5409-5411, Dec 20 2007.

[22] D. J. Bougioukou, *et al.*, "Towards preparative-scale, biocatalytic alkene reductions," *Chemical Communications,* vol. 46, pp. 8558-8560, 2010.

[23] C. Stueckler, *et al.*, "Bioreduction of alpha-methylcinnamaldehyde derivatives: chemo-enzymatic asymmetric synthesis of Lilial (TM) and Helional (TM)," *Dalton Transactions,* vol. 39, pp. 8472-8476, 2010.

[24] P. A. Fitzpatrick and A. M. Klibanov, "How Can the Solvent Affect Enzyme Enantioselectivity," *Journal of the American Chemical Society,* vol. 113, pp. 3166-3171, Apr 10 1991.

[25] A. M. Klibanov, "Improving enzymes by using them in organic solvents," *Nature,* vol. 409, pp. 241-246, Jan 11 2001.

[26] Y. L. Khmelnitsky, *et al.*, "Denaturation Capacity - a New Quantitative Criterion for Selection of Organic-Solvents as Reaction Media in Biocatalysis," *European Journal of Biochemistry,* vol. 198, pp. 31-41, May 23 1991.

[27] M. Duraisamy and H. M. Walborsky, "Syntheses of Chiral Cyclohexylidenepropenes and Cyclohexylideneacetaldehydes," *Journal of the American Chemical Society,* vol. 105, pp. 3252-3264, 1983.

[28] Partridg.Jj, *et al.*, "Asymmetric Synthesis of Loganin - Stereospecific Formation of "(1r,2r)-2-Methyl-3-Cyclopenten-1-Ol and "(1s,2s)-2-Methyl-3-Cyclopenten-1-Ol and (2r)-2-Methylcyclopentanone and (2s)-2-Methylcyclopentanone," *Journal of the American Chemical Society,* vol. 95, pp. 532-540, 1973.

[29] A. Fryszkowska, *et al.*, "Highly enantioselective reduction of beta,beta-disubstituted aromatic nitroalkenes catalyzed by Clostridium sporogenes," *Journal of Organic Chemistry,* vol. 73, pp. 4295-4298, Jun 6 2008.

[30] H. Ohta, *et al.*, "Asymmetric Reduction of Nitro Olefins by Fermenting Bakers-Yeast," *Journal of Organic Chemistry,* vol. 54, pp. 1802-1804, Apr 14 1989.

CHAPTER 6

COMPUTATIONAL PROTEIN ENGINEERING OF YERSER WITH PRINCIPAL COMPONENT ANALYSIS

6.1. Introduction

Enzymes are highly versatile and proficient catalysts. The ideal biocatalyst can greatly accelerate chemical reactions, combined with high substrate specificity, as well as exquisite enantioselectivity and stereoselectivity. Recent advances in the development of both experimental and computational protein engineering tools have enabled improvements in biocatalyst for better large-scale industrial applications.[1] Over the past two decades, directed evolution has transformed the field of protein engineering with an iterative two-step protocol, first creating molecular diversity by random mutagenesis and *in vitro* recombination, then followed by identifying library members of improved enzyme functions with established high-throughput screening method.[2] Alternative rational library design combines structural, mechanistic, and sequence-based knowledge to further enable new routes for smaller and more efficient library design. Another promising area employed computational engineering strategies as tools to evaluate protein sequence data and analyze the possible conformational variation within proteins allowing for novel enzyme function design.[3] These tools have enabled numerous improved biocatalysts, especially for the application in the field of pharmaceutical industry. Examples are (*R*)-transaminase for the synthesis of active pharmaceutical ingredients of sitagliptin (Januvia®), and ketoreductases, glucose dehydrogenase, and haloalkane dehalogenases for the synthesis of intermediate toward atorvastatin (Lipitor®) and montelukast (Singulair®).

6.1.1. Sequence-based enzyme engineering

Evolutionary information from protein sequences was studied in order to effectively navigate and identify the functionalities in protein sequence space. Tools such as multiple sequence alignments and phylogenetic analysis have become standard analysis for the exploration of amino acid relationships among groups of homologous protein sequence and structures. The exploited data were valued for functional identification such as enzyme hot spots, local amino acid variability, and as guide for possible back-to-consensus designs.[4, 5]

Examples of sequence-based data analysis tools include The HotSpot Wizard and 3DM database. The HotSpot Wizard combines protein functionality data from sequence library and structure database to create a mutability map for target protein.[6] Similarly, 3DM database integrates protein sequence and structure data from GeneBank and the PDB to produce protein superfamily alignments.[7] These tools collect protein functionality data effectively through a series of built-in filters to identify evolutionary features such as correlated mutations and amino acid conservation, and in return provided information on the functional role of individual amino acid residues including possible mutability for enzyme improvement.

6.1.2. Structure-based enzyme engineering

Structure-based methods probe protein function linked to three dimensional structures by making mutations of one or more amino acids in the macromolecules sequence to cause a change in structural topology. The method is rendered possible by the rapidly growing number of protein structures in the PDB along with developments in homology modeling, rendering structure-based analogy a valuable additional tool for protein engineers to pinpoint key residues more effectively in active sites and design more efficient libraries. One of the examples using structural based method is structural-guided consensus, which combines sequence-based and structural data and employs a set

of phylogenetically diverse but functionally proven proteins.[8, 9] Smaller library size can be further achieved via structural criteria such as distance to active site, addition of helix stabilizer, and salt-bridge formation. The conditions resulted in highly constrained mutational space and improve the percentage of positive hits within a library.

6.1.3. Computationally-based enzyme engineering

The third wave of protein engineering is data-driven protein engineering [10]. By using available data in the form of structures and sequences to limit the library size, at the same time improving the chances of a 'hit' through computational algorithm design. Advances in computational protein design algorithms have made modeling a highly promising strategy for redesign of biocatalysts. Together with the aid of evolutionary information as a guide for sequence alterations and combinatorial library preparation, computational strategies calculate amino acid variations on the overall protein structure, and greatly reduce the library size to a handful of rational designs. A more recent data-driven approach is that involving advanced statistical methods (or machine learning) [11]. Machine learning and multivariate statistical methods can help identify hidden patterns in sequence-activity relationships and accelerate enzyme improvement. The requirements for the number of variants to be screened is also potentially low [12]. Thus, in situations where a high-throughput screening assay condition may not be a good choice for selecting improved variants, then due to time and resource constraints we can test only a selected set of mutants for activities in the actual process conditions (Fig 6.1)

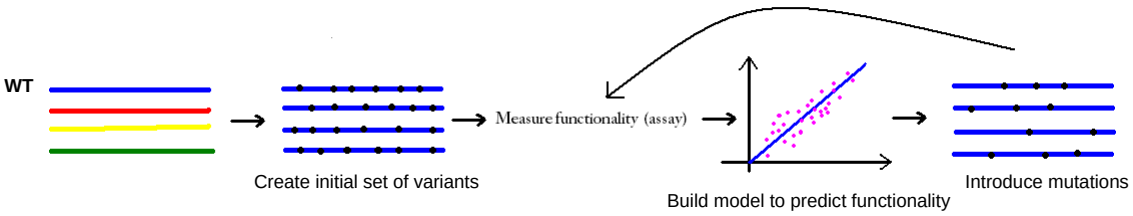

Figure 6.1. Overview of computational based protein engineering.

Some recent works that have shown how statistical methods can be incorporated into protein engineering to improve upon enzyme functionality include: ProSAR (Protein Structure Activity Relationship) using partial least squares regression [13], probabilistic model developed specifically for protein systems [14-16], 'Mt. Fuji' type landscape model [17, 18], and usage of multiple regression methods [19]. One of the major bottlenecks for almost all protein engineering methods is the selection and generation of the initial set of mutants. Even some of the above-mentioned statistical methods, for which this step serves to provide the initial data set for model building, use directed evolution to create the first set of mutants. Under conditions of low throughput assays however, this may not be desirable. In spite of all the protein engineering efforts so far, systematic methods for identifying target mutations a priori to any experimental work remain elusive. Examples of published techniques that have shown promise include SCHEMA [20], Rosetta [21], and CASTing [22].

6.2 Principal Component Analysis

In this work, a data-driven method to identify target positions and residues for mutations is presented. The idea is to identify patterns in a protein family's sequences, and locate possible changes (mutations) in the targeted protein of interest such that the new variant is closer to the underlying low dimensional manifold of the sequences. This low dimensional topology is identified by subjecting the protein family sequences to principal component analysis (PCA). Figure 6.2 below, shows the overall approach for identifying the mutations.

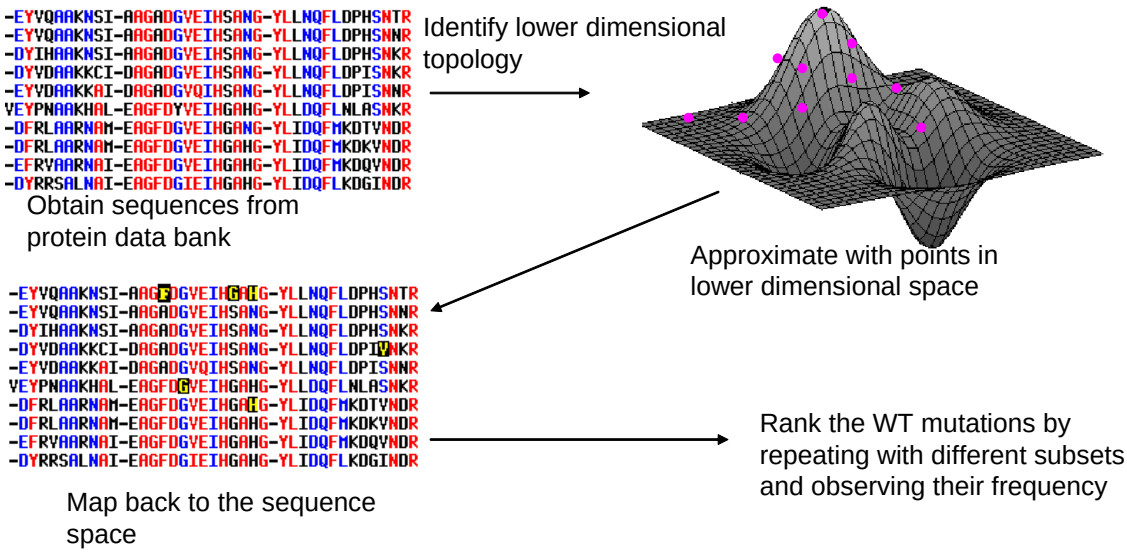

Figure 6.2. Computational protein engineering with principal component analysis.

Principal component analysis general approach includes: (Step 1) Collect protein sequences from PDB, and align them with an alignment tool available such as ClustalW. To represent the sequences mathematically, we assign 20 dimensions to each position (corresponding to each amino acid), which are all zero expect for the amino acid residue present at that position (which will be assigned a value of unity). (Step 2) Subject the sequence data set to PCA, and reconstruct the protein sequence of interest with a limited number of principal components. For the i^{th} position, in the original data matrix we had a 20 dimensional array – [0 0 0 0 …. 1 0 0 0] where there is a 1 for the residue present at that position and 0 otherwise. In the reconstructed matrix, this may not be the case: [0 0 0 0 …. 0.3 0.45 0.25 0]. The value highest in magnitude (closest to 1) is then rounded off to 1 and others to 0 to approximate the residue present in the reconstructed array. This number is the weighting; in the above example the weighting is 0.45. Positions that upon reconstruction have a residue different than the one present originally are the positions of interest for mutating, and the suggested residues from the PCA is the target residue. (Step 3) Repeat the PCA and sequence mapping (reconstruction) with different data sets of the

collected sequences, and rank the mutations based on the weight of the suggested residue and its frequency of occurrence. Gaps are excluded when considering mutations.

There are two parameters that the user has to define: (1) Window sizes: As stated above, different sub-sets of the sequences are used to identify mutations. The reason for this is to avoid biasing of the suggested residue by the closest homologues. Therefore, our protein of interest (say, protein number 1), is selected with (say) *n* other proteins from the sequences. This sub set then cascades down by one in the table, and so on. The number *n* is the window size. This procedure can be repeated with multiple window sizes, the range of which is up to the user. To test for variance in the mutations, any two sequences can be swapped to repeat the PCA. (2) Percentage cut-off for excluding positions having gaps: Upon alignment, there will be some positions having gaps in many of the sequences. These positions are considered as having no residue, or in mathematical terms, having lack of information for the data set. To avoid biasing the results from these positions with lack of information, only those positions with a certain percentage of information are included in the PCA. The cut-off is to be set by the user. The number of principal components can also be set as a parameter, but we suggest that these be varied from 1 to the maximum number (in this work, it will be the number of data points/sequences). The parameters used in the current analysis were set as: window size – varied from 16 to 24 in steps of 2, cut-off – 70%.

The PCA method was applied to the Old Yellow Enzyme family for validation. YersER from *Yersinia bercovieri* was used as model enzyme to mutation changes. In previous works, YersER showed broad ER specificity and broad temperature and pH optima but different specificity patterns; with strong cofactor preference for NADPH as over NADH and are stable up to 40 ^{o}C.[23] YersER also asymmetrically reduced a series of alkenes with moderate to excellent degree of stereoselectivity, where both substrate- and enzyme-based stereocontrol were observed to furnish opposite

stereoisomeric products (Chapter 5). All the above traits render YersER a potentially interesting enzyme for improvement with PCA analysis.

The protein sequence data, expressed as given below, was subject to principal component analysis. More details of PCA can be found in [24].

$$X^T = \begin{pmatrix} x_{11} & x_{12} & \ldots\ldots\ldots x_{1p} \\ \cdot & & \\ \cdot & & \\ x_{n1} & x_{n2} & \ldots\ldots\ldots x_{np} \end{pmatrix}_{n\times p}$$

where n is the number of sequences = 28 for the OYE family, p is the number of dimensions = (....)20*number of positions in alignment.

To find the principal components (vectors in the n dimensional space along which the data might be concentrated), singular value decomposition (SVD) of the Z matrix (given below) has to be done. The Z matrix is obtained by mean centering the columns and making them of unit variance:

$$Z^T = \begin{pmatrix} \frac{x_{11}-\bar{x}_1}{s_1} & \frac{x_{12}-\bar{x}_2}{s_2} & \ldots\ldots\ldots \frac{x_{1p}-\bar{x}_p}{s_n} \\ \cdot & & \\ \cdot & & \\ \frac{x_{n1}-\bar{x}_1}{s_1} & \frac{x_{n2}-\bar{x}_2}{s_2} & \ldots\ldots\ldots \frac{x_{np}-\bar{x}_p}{s_p} \end{pmatrix}_{n\times p}$$

$\bar{x}_1$ and s_1 are the mean and standard deviation of the first column in X^T and so on.

SVD of the Z matrix will give the principal components through:

$$Z=U_{p\times p}S_{p\times n}V^T_{n\times n}$$

U and V are matrices consisting of orthonormal vectors.

$$S = \begin{pmatrix} \sigma_1\ 0\ 0\ 0..... & 0 \\ 0\ \sigma_2 0\ 0 & 0 \\ . \quad . & \\ . \quad\quad . & \\ 0 & \sigma_n \\ 0 & 0 \\ M & M \\ M & M \\ 0 & 0 \end{pmatrix}_{p \times n}$$

$\sigma's$ are the singular values.

The relatively larger values of $\sigma's$ will tell what the principal components are (the corresponding column vectors in U). The transformation of Z in the direction of the principal components is given by:

$$Z_{tf} = U^T_L Z = S_L V^T_L$$

where L denotes that we have taken only the first L principal $\sigma's$.

As there were many columns with zeros, the columns were not normalized with the standard deviation. Also, one of the reasons for standard deviation normalization is to make the variables dimensionless. However, since the protein sequences expressed mathematically are of the same dimension, standard deviation normalization is not required.

6.3 Results & Discussion

6.3.1. Suggested YersER mutation from PCA

As the PCA aligned the sequences of known Old Yellow Enzyme sequences, the analysis suggested total of 133 mutants for YersER (Table 6.1). The mutants were ranked according to the averaged importance compared to the phylogenetic tree. In order to further reduce the library size, structural analysis were used to identify the possible "hot-spots" among the 133 suggested mutations. Crystal structure of PETN reductase (PDB

2ABA), who shared 76% and 85% amino acid identity and similarity with YersER were used.[25] The OYE family catalyzes reduction of activated alkenes through a two-step process: oxidation of cofactor by hydride transfer to the FMN cofactor (reductive half reaction), followed by the reduction of activated alkenes by hydride transfer from the reduced flavin (oxidative half reaction).[26, 27] The importance of FMN in catalytic pocket of OYEs greatly affects the enzyme efficiency in the reduction process, which becomes the center focus of targeted mutations. The crystal structure PDB 2ABA was analyzed centralized at the FMN ligand in the crystal structure and by setting the first- and second-shell residues within 4 Å and 8 Å, the modeling result reduced the library size down to twelve suggested mutations, with two mutants located within first shelf related to FMN.

Table 6.1. Suggested mutations of YersER from PCA analysis.

Average rank	WT Residue	Position#	Suggested residue
1.6	S	329	A
1.8	I	179	V
3.4	M	193	L
4.2	L	81	I
6	S	227	G
6.4	H	265	G
8.2	T	212	A
10.2	E	93	A
13.2	Q	117	G
14	E	248	P
14.6	T	222	V
14.8	I	161	V
16.2	P	240	T
17	T	168	A
17	A	196	S
18	Y	178	G
18.4	D	259	E
22.4	F	64	A
22.8	L	75	I
24.4	E	229	D
25.2	G	348	P
25.6	Q	89	A
26	A	72	T
28.4	Q	225	E

Table 6.1. Suggested mutations of YersER from PCA analysis continued.

30.8	F	317	L
31	I	231	V
31	D	249	N
31.6	N	246	D
32.4	A	83	G
33.4	I	235	L
33.6	A	253	D
34.8	I	126	L
34.8	Q	250	E
35.2	H	185	N
35.8	T	133	S
37.4	H	190	D
37.4	T	215	L
37.8	W	226	I
37.8	I	318	A
38.4	I	271	M
38.4	Y	178	L
39.8	T	215	V
40	L	214	F
44	A	90	G
45.4	L	181	I
47.2	L	238	I
47.6	A	99	F
47.6	I	235	V
48	A	224	E
49.2	N	242	Q
50.6	E	345	P
50.8	I	37	V
50.8	V	134	L
52.8	T	154	L
53.6	A	289	K
55	H	97	K
58.2	T	77	S
58.4	I	208	V
59.8	T	350	S
60	G	243	N
60.2	I	258	A
60.4	P	346	Q
60.6	D	347	R
62	T	57	S
64	K	295	H
64.8	T	132	V
65.4	Q	250	P
65.4	E	155	D
65.8	E	153	T
67	A	183	S
67.8	V	334	P
69.2	D	245	G

Table 6.1. Suggested mutations of YersER from PCA analysis continued.

72	V	105	T
74	H	76	Y
75.2	L	189	I
76.8	D	288	E
78.4	E	314	G
81	D	288	Q
82.4	I	108	V
83	I	266	L
83	A	303	R
83.6	L	244	T
83.6	E	311	D
86.6	T	168	V
87.2	D	129	N
89	F	64	P
89.8	N	262	G
92	Q	203	E
92.8	E	79	A
97.2	E	156	D
97.2	G	71	D
98.4	S	194	R
99.4	L	312	A
99.8	A	253	T
100	A	253	L
101.2	G	279	D
102.6	I	233	V
104.2	R	131	K
104.4	T	133	F
106.2	A	127	K
107	H	76	W
107	P	195	S
110.2	E	260	Q
111.6	S	111	P
111.8	E	310	N
112.2	R	172	M
112.2	Q	89	E
114.6	G	348	A
116	F	317	K
117	A	128	I
118.2	R	172	I
118.2	E	94	A
118.8	G	239	A
122	E	155	A
122.4	Q	89	D
122.6	L	337	F
122.8	F	164	Y
125	L	244	M
127.8	R	293	V
127.8	E	94	K

Table 6.1. Suggested mutations of YersER from PCA analysis continued.

128	I	313	L
128.8	E	248	S
129.2	A	70	P
131.8	S	283	P
133.8	A	277	I
138.2	A	183	G
139.6	D	249	E
140.2	T	305	D
141	A	320	L
142.2	R	135	V
144.4	P	346	Y
157.4	E	229	G
161	T	212	C

6.3.2. YersER mutants activity and stereoselectivity study

Total of 12 mutants were analyzed and compared with regard to wild type YersER activity for substrates of 2-cyclohexen-1-one and ketoisophorone (Table 6.2). The specific activity study showed 5 improved activity for mutants of I235L, T350S, T57S, A183S, and T350D; with improvement as high as 159.8% for reduction of 2-cyclohexen-1-one with A183S variant. 4 mutants (G348P, I271M, A3030R, and P346Y) showed comparable specific activity with the wild-type YersER, with activity difference of < 10%. Only 3 mutants showed decreased in specific activity: A72T, H185N, and L181I; especially variant H185N appeared to lose all the activity.

The mutants were also studied for possible change in stereoselectivity and nitro reductase activity with substrates of ketoisophorone, 1-nitro-2-phenylpropene, citral, and nitrobenzene (Table 6.3). However, no significant stereoselectivity difference was observed, and all mutants showed to be non-active with aromatic nitro substrate. This is possibly because the residue selections were focused on the FMN as localized center, which differences in catalytic hydride transfer between FMN and substrate were

expected, but no substrate flipping being forced in the binding pocket as the result of these mutations.

Table 6.2. Specific activity study of YersER mutants.

Avg Rank	Mutant	Specific Activity [U/mg]			
		2-cyclohexen1-one		Ketoisophorone	
	WT	2.76	-	5.95	-
25.2	G348P	2.53	91.7%	5.87	98.6%
26	A72T	0.49	17.8%	1.28	21.5%
33.4	I235L	3.70	134.1%	7.14	120.0%
35.2	H185N	0.05	1.8%	0.18	3.0%
38.4	I271M	2.72	98.6%	4.80	80.7%
45.4	L181I	1.98	71.7%	4.41	74.1%
59.8	T350S	4.04	146.4%	7.70	129.4%
62	T57S	5.03	182.3%	8.42	141.5%
67	A183S	4.41	159.8%	8.42	141.5%
83	A303R	2.82	102.2%	6.73	113.1%
140.2	T305D	3.87	140.2%	9.11	153.1%
144.4	P346Y	2.61	94.6%	5.38	90.4%

Table 6.3. Conversion and stereoselectivity study of YersER mutants.

Avg Rank	Mutant	Ketoisophorone		1-nitro-2-phenylpropene		Citral		Nitrobenzene
		Conv	e.e. %	Conv	e.e. %	Conv	e.e. %	Conv
	WT	96.3	(*S*) 5.8	39.6	(*R*) 98	96.0	(*S*) 99	-
25.2	G348P	97.1	(S) 2.1	34.7	(*R*) 99	55.4	(*S*) 99	-
26	A72T	92.7	(*R*) 7.3	21.1	(*R*) 99	36.0	(*S*) 99	-
33.4	I235L	97.7	(*S*) 2.1	39.9	(*R*) 99	98.6	(*S*) 99	-
35.2	H185N	15.4	(*R*) 15.3	24.7	(*R*) 99	41.6	(*S*) 99	-
38.4	I271M	99.1	racemic	27.7	(*R*) 99	62.1	(*S*) 99	-
45.4	L181I	42.3	(*S*) 6.9	27.7	(*R*) 99	89.2	(*S*) 99	-
59.8	T350S	97.7	racemic	25.9	(*R*) 99	23.7	(*S*) 99	-
62	T57S	97.8	racemic	22.1	(*R*) 99	65.6	(*S*) 99	-
67	A183S	48.8	(*S*) 2.4	36.3	(*R*) 99	87.7	(*S*) 99	-
83	A303R	98.8	(*S*) 1.5	43.3	(*R*) 99	78.7	(*S*) 99	-
140.2	T305D	58.7	(*S*) 5.5	49.7	(*R*) 99	18.8	(*S*) 99	-
144.4	P346Y	88.5	(*S*) 2.0	53.6	(*R*) 99	94.9	(*S*) 99	-

6.3.3. Chemical TTN study

The total turnover number (TTN) is an indicator of lifetime biocatalyst productivity and is defined as the maximum number of molecules of substrate that an enzyme active site can convert over its life cycle. The chemical TTN (TTN) [28, 29] was experimentally determined by measuring the maximum amount of substrate 2-cyclohexenone and citral that can be reduced with a set amount of purified enzyme before the enzyme is chemically deactivated (Table 6.4). In this study, we found the inhibition effect of substrate 2-cyclohexenone with enzyme YersER, which the enzyme showed improvement TTN with substrate citral. Temperature doesn't seem to influence the chemical TTN much in this case as we did not observe significant improvement by lowering reaction temperatures to 25 ^{o}C. All twelve mutants were analyzed with citral as substrate for chemical TTN. Interestingly, the improvement in TTN only observed for mutants T350S, T57S, A303R, and T305D; which most of these mutants showed higher specific activity compared to the wild-type YersER (Table 6.5). However, the TTN of both YersER and KYE1 were both lower to be interesting for industrial application, which usually required biocatalyst to have TTN in the order of 10^4. Future improvement in enzyme specific activity and TTN will be necessary to apply these enzymes in large scale reaction system.

Table 6.4. YersER and KYE1 TTN comparison.

Enzyme	**Substrate**	**Temp [^{o}C]**	**TTN**	**Halflife [min]**
YersER	2-cyclohexen-1-one	37	2808	1488
	Citral	37	8230	1488
	Citral	30	10083	13124
	Citral	25	11201	-
KYE1	2-cyclohexen-1-one	37	2827	210
	Citral	37	1880	210
	Citral	30	3670	1146

Table 6.5. YersER WT and mutant TTN study.

Avg Rank	YersER	TTN
-	WT	8283
25.2	G348P	7275
26	A72T	802
33.4	I235L	2927
35.2	H185N	160
38.4	I271M	4705
45.4	L181I	3957
59.8	T350S	11032
62	T57S	14130
67	A183S	5599
83	A303R	10233
140.2	T305D	9614
144.4	P346Y	3199

6.4 Conclusion

In summary, computational protein design has fundamentally changed the way protein engineers can alter protein functions, however, the most efficient result only can be achieved with the complementary angle of both directed revolution and computational modeling. The PCA method incorporated both sequence alignments and structural analogy knowledge to produce suggested mutations at specific positions. The work in this chapter focused on the mutations suggested by PCA with localized center focus on the FMN, the catalytic center of YersER. Total twelve mutants were studied for improvement in specific activity, conversion efficiency, and stereoselectivity. The mutants showed positive improvement in specific activity with 5 out of 12 mutants demonstrated higher specific activity compared to wild type enzyme. However, no significant changes were observed for stereopreference. The future work will focus on altering enzyme stereoselectivity with localized PCA on residues that affect the orientation of substrate within enzyme binding pocket.

6.5 Materials & Methods

6.5.1 YersER QuikChange® mutagenesis protocol

The mutations on YersER were accomplished with the QuikChange® mutagenesis protocol with the following PCR primers design. The *YersER* gene from *Yersinia bercovieri* in pET27 vector was used as the template for mutations. Failsafe buffer J (EPICENTER® Biotechnology, Madison, WI) was used in the standard PCR protocol with Pfu polymerase from New England Biolabs (Marlborough, MA). PCR assay: 25 µL of Failsafe buffer J, 125 ng *YersER* DNA plasmid template, 0.25 µM each of both forward and reverse primers, and sterile water to 50 µL in total volume. The mixed sample was first denatured at 98 ℃ for 5 minutes, supplemented with 1 µL of Pfu buffer, followed by denaturation at 98 ℃ for another 30 seconds. The annealing temperature was set at 55 ℃ for 1 minute, extension at 72 ℃ for 16 minutes, and repeated for total of 18 cycles. The final extension was set at 72 ℃ for 25 minutes, and finished with temperature hold at 4 ℃. All mutants were sequenced with Eurofins MWG Operon (Birmingham, AL) service and transformed into *E. coli* BL21 strain for protein expression and purification.

Table 6.6. YersER mutants design.

Mutants	Forward 5' to 3'
G348P	CCCCACTGAATGAGCCTGATCCGGAAACATTCTACGGCGGCGG
A72T	AGGCAAAAGGCTACGCGGGAACCCCGGGGTTACACACTCAGGA
I235L	GTGCTGAACGTATTGGTATCCGTCTGTCCCCATTAGGGCCGTTCAAT
H185N	TATATCGAACTCCATGCCGCCAATGGTTATTTGCTGCATCAATTTATGTCTC
I271M	GCATATCGCCTACCTGCACATGTCCGAGCCAGATTGGGCC
L181I	CGAAGCGGGTTTTGACTATATCGAAATTCATGCCGCCCATGGTTATTTG
T350S	CTGAATGAGCCTGATGGCGAAAGCTTCTACGGCGGCGGTGCT
T57S	GCCAGTGCCGGTTTGATTATCAGCGAAGCAACCCAGATCTCTTTC
A183S	GGGTTTTGACTATATCGAACTCCATAGCGCCCATGGTTATTTGCTGCAT
A303R	GGGTTATTATCGGTGCGGGTCGTTATACCGCCGAGAAGGCCG
T305D	TTATTATCGGTGCGGGTGCCTATGATGCCGAGAAGGCCGAAGAGT
P346Y	CAGCATGCCCCACTGAATGAGTATGATGGCGAAACATTCTACGGC

6.5.2 Enzyme purification and bioconversion assay

YersER genes starter culture consisted of 5 ml LB_{Kan}, inoculated from frozen stock, and grown overnight at 37 ℃. The starter culture was then used for inoculation of 300 mL culture (0.1% v/v), which was gently aerated until OD_{600} reached 0.5 for addition of 0.1 mM IPTG and then left overnight for protein expression. Harvested cell pellets were kept for -80 ℃ for protein purification. The polyhistidine tagged enzymes were purified according to the standard Ni^{2+}-NTA bead protocol from Qiagen (Valencia, CA). The protein concentration was determined by the Bradford method with Coomassie Plus Protein assay reagent and BSA assay (Pierce Chemical, Chicago, IL) as the calibration curve.

The specific activity assays were performed with 200 mM phosphate buffer pH 7.5, 10 mM substrate, 0.2 mM cofactor NADPH, and 10 $\mu g.mL^{-1}$ enzyme. The conversion assay were performed with 200 mM phosphate buffer pH 7.5, 10 mM substrate, 20 $\mu g.mL^{-1}$ (0.5 μM) enzyme, 0.2 mM $NADP^{+}$, 20 mM glucose, 10 $U.mL^{-1}$ GDH, at room temperature incubated over 12 hours. Then an equal volume of ethyl acetate was added for extraction before analysis with GC.

6.6 References

[1] A. S. Bommarius, "PROTEIN ENGINEERING Check nature first, then evolve," *Nature Chemical Biology*, vol. 6, pp. 793-794, Nov 2010.

[2] E. G. Hibbert, *et al.*, "Directed evolution of biocatalytic processes," *Biomolecular Engineering*, vol. 22, pp. 11-19, Jun 2005.

[3] S. Lutz, "Beyond directed evolution-semi-rational protein engineering and design," *Current Opinion in Biotechnology*, vol. 21, pp. 734-743, Dec 2010.

[4] J. M. Pei, "Multiple protein sequence alignment," *Current Opinion in Structural Biology*, vol. 18, pp. 382-386, Jun 2008.

[5] T. S. Wong, *et al.*, "The diversity challenge in directed protein evolution," *Combinatorial Chemistry & High Throughput Screening*, vol. 9, pp. 271-288, May 2006.

[6] A. Pavelka, *et al.*, "HotSpot Wizard: a web server for identification of hot spots in protein engineering," *Nucleic Acids Research*, vol. 37, pp. W376-W383, Jul 2009.

[7] R. K. Kuipers, *et al.*, "3DM: Systematic analysis of heterogeneous superfamily data to discover protein functionalities," *Proteins-Structure Function and Bioinformatics*, vol. 78, pp. 2101-2113, Jul 2010.

[8] J. Minshull, *et al.*, "Engineered protein function by selective amino acid diversification," *Methods*, vol. 32, pp. 416-427, Apr 2004.

[9] C. R. Otey, *et al.*, "Structure-guided recombination creates an artificial family of cytochromes P450," *Plos Biology*, vol. 4, pp. 789-798, May 2006.

[10] J. F. Chaparro-Riggers, *et al.*, "Better library design: data-driven protein engineering," *Biotechnology Journal*, vol. 2, pp. 180-191, 2007.

[11] R. J. Fox and G. W. Huisman, "Enzyme optimization: moving from blind evolution to statistical exploration of sequence-function space," *Trends in Biotechnology*, vol. 26, pp. 132-138, Mar 2008.

[12] J. Minshull, *et al.*, "Predicting enzyme function from protein sequence," *Current Opinion in Chemical Biology*, vol. 9, pp. 202-209, Apr 2005.

[13] R. J. Fox, *et al.*, "Improving catalytic function by ProSAR-driven enzyme evolution," *Nature Biotechnology*, vol. 25, pp. 338-344, Mar 2007.

[14] M. Brouk, *et al.*, "Improving Biocatalyst Performance by Integrating Statistical Methods into Protein Engineering," *Applied and Environmental Microbiology*, vol. 76, pp. 6397-6403, Oct 2010.

[15] Y. Barak, *et al.*, "Enzyme improvement in the absence of structural knowledge: a novel statistical approach," *Isme Journal*, vol. 2, pp. 171-179, Feb 2008.

[16] Y. Nov and L. M. Wein, "Modeling and analysis of protein design under resource constraints," *Journal of Computational Biology*, vol. 12, pp. 247-282, 2005.

[17] T. Aita, *et al.*, "A cross-section of the fitness landscape of dihydrofolate reductase," *Protein Engineering*, vol. 14, pp. 633-638, Sep 2001.

[18] T. Aita, *et al.*, "Analysis of a local fitness landscape with a model of the rough Mt. Fuji-type landscape: Application to prolyl endopeptidase and thermolysin," *Biopolymers*, vol. 54, pp. 64-79, 2000.

[19] J. Liao, *et al.*, "Engineering proteinase K using machine learning and synthetic genes," *Bmc Biotechnology*, vol. 7, p. 19, Mar 2007.

[20] M. M. Meyer, *et al.*, "Library analysis of SCHEMA-guided protein recombination," *Protein Science,* vol. 12, pp. 1686-1693, Aug 2003.

[21] J. B. Siegel, *et al.*, "Computational Design of an Enzyme Catalyst for a Stereoselective Bimolecular Diels-Alder Reaction," *Science,* vol. 329, pp. 309-313, Jul 2010.

[22] M. T. Reetz and J. D. Carballeira, "Iterative saturation mutagenesis (ISM) for rapid directed evolution of functional enzymes," *Nature Protocols,* vol. 2, pp. 891-903, 2007.

[23] J. F. Chaparro-Riggers, *et al.*, "Comparison of three enoate reductases and their potential use for biotransformations," *Advanced Synthesis & Catalysis,* vol. 349, pp. 1521-1531, Jun 2007.

[24] I. T. Jolliffe, *Principal Component Analysis,* 2nd ed.: Springer-Verlag New York, Inc. , 2002.

[25] T. M. Barna, *et al.*, "Crystal structure of pentaerythritol tetranitrate reductase: "Flipped" binding geometries for steroid substrates in different redox states of the enzyme," *Journal of Molecular Biology,* vol. 310, pp. 433-447, Jul 6 2001.

[26] R. M. Kohli and V. Massey, "The oxidative half-reaction of old yellow enzyme - The role of tyrosine 196," *Journal of Biological Chemistry,* vol. 273, pp. 32763-32770, Dec 4 1998.

[27] C. Breithaupt, *et al.*, "X-ray structure of 12-oxophytodienoate reductase 1 provides structural insight into substrate binding and specificity within the family of OYE," *Structure,* vol. 9, pp. 419-429, May 9 2001.

[28] R. R. Jiang, *et al.*, "Comparison of alkyl hydroperoxide reductase (AhpR) and water-forming NADH oxidase from Lactococcus lactis ATCC 19435," *Advanced Synthesis & Catalysis,* vol. 347, pp. 1139-1146, Jun 2005.

[29] P. Odman, *et al.*, "An enzymatic process to alpha-ketoglutarate from L-glutamate: the coupled system L-glutamate dehydrogenase/NADH oxidase," *Tetrahedron-Asymmetry,* vol. 15, pp. 2933-2937, Sep 20 2004.

CHAPTER 7

CONCLUSION & FUTURE PERSPECTIVES

Asymmetric synthesis with biocatalysts has become an increasingly interesting and cost-effective manufacturing option in fine chemicals, pharmaceuticals, and agrochemical intermediates. Ene reductases from the Old Yellow Enzyme family offer high substrate efficiency, regio-, stereo-, and enantiomeric selectivity in the catalyzed biotransformations. Asymmetric reduction of activated C=C bond is one of the most widely applied synthetic tools for the potential to generate up to two stereogenic centers in a one-step reaction. Current existing synthetic methods of asymmetric hydrogenation involve the use of precious metals in conjunction with chiral phosphines as well as organocatalytic hydrogenation of cyclic enones to allow a wider choice of substrates and products. However, the addition of biocatalytic hydrogenation of activated alkenes has proven to be highly effective to produce enantiomerically pure compounds and has become an additional precious tool for both the established synthetic pathways and novel methods.

The thesis contributed to the enzymes development and characterization of the Old Yellow Enzyme family with regards to addition of new chemistry such as exploitation of nitroreductase activity with NRSal from *Salmonella typhimurium*, where we investigated the reduction of α,β-unsaturated carbonyl compounds, nitroalkenes, and nitroaromatics substrates. We also reported the first single-isolated enzyme-catalyzed reduction of nitrobenzene to aniline through the formation of nitrosobenzene and phenylhydroxylamine as intermediates. The development and characterization of novel enzymes YersER from *Yersinia bercovieri* and KYE1 from *Kluyveromyces lactis* demonstrated that both enzymes have broad ene reductase specificity and are able to operate under broad temperature and pH optima but with different specificity patterns.

Both substrate- and enzyme-based stereocontrol were observed for both YersER and KYE1 to furnish opposite stereoisomeric products. Further improvement and characterization on XenA from *Pseudomonas putida* showed broad catalytic activity to reduce various α,β-unsaturated and nitro compounds with moderate to excellent stereoselectivity. Mutations C25G and C25V of XenA are able to reduce nitrobenzene, a non-active substrate for the wild type, to produce aniline. The combination of computational protein engineering in form of the method of Principal Component Analysis together with structure-guided consensus enabled the improvement of YersER, where significant improvements of specific activity were detected. Lastly, the work also contributed towards larger-scale system preparation by investigating enzyme stability and organic solvent behavior. We studied the total turnover number (TTN) as an indicator of lifetime biocatalyst productivity for YersER, KYE1, and XenA. The TTN of XenA proved to be dominated by chemical rather than thermal instability. The effects of organic solvents on enzyme activity and stereoselectivity were tested with YersER and KYE1 to show the sustainable bioreduction efficiency even at high organic solvent content. Future work will concentrate on enabling of a sustainable and stable scale-up system to demonstrate the possible applications of these enzymes.

The field of Old Yellow Enzyme has evolved in the past few decades. Starting with the discovery of new enzymes and initial characterization for enzyme activity in the 1980s – 1990s, in the 2000s, more groups have focused efforts on enzyme selectivity studies together with the biochemistry of the discovered ene reductases. Numerous enzymes such as OYE from *Saccharomyces carlsbergensis*, OYE2-3 from *Saccharomyces cerevisiae*, KYE1 from *Kluyveromyces lactis*, OYE from *Candida macedoniensis*, YqjM from *Bacillus subtilis*, YersER from *Yersinia bercovieri*, PETN reductase from *Enterobacter cloacae*, OPR1 and OPR3 from *Arabidopsis thaliana*, have been thoroughly studied and characterized in term of its chemo-, regio-, and stereoselectivity. A few groups have also contributed to the search of key residues within

OYE family. Given the vast developments in all these fields, the immediate future perspectives focus on the possible enzyme engineering of OYE family members for altered substrate specificity and better stereocontrol of final product, together with reaction scale-up research for actual industrial applications in the near future.

The thesis contributions highlighted above have added valuable insights into all the recent development efforts within ene reductases. The enzymes characterization results shown in Chapter 2 – 5, together with published works on other OYE candidates, have mapped out the sequence substrate relationship within the OYE family. Based on these findings, the community will able to categorize enzymes into strong ene reductases, bi functional enzymes of ene and nitro reductases, and strong nitroreductases, all of which showed a favorable set of substrate range and stereochemistry in the biotransformation. The work on PCA analysis on YersER (Chapter 6) showed the first initiation of computational protein engineering efforts within the OYE family. Current PCA analysis showed promising results with significant improvements observed for suggested mutants; however, further effort is currently in progress to enable the wide application of the PCA method on the protein engineering front. The PCA will focus on finding the key residues within the OYE family that controls the chemistry and stereoselectivity of these enzymes. By comparison of binding pocket residues across the whole OYE family, PCA will analyze the distinct differences among the amino acid residues and suggest possible mutations at each specific location. This effort will further the understanding of OYE's biochemistry and improve upon better protein engineering in the future. Enzyme stability with ene reductase is also a current issue for further scale up development. As we have discussed in both Chapter 4 and 5, ene reductase showed poor enzyme stability with low chemical TTN measured for all the tested enzymes (XenA, YersER, and KYE1). We foresee additional effort to improve upon the stability through possible enzyme engineering procedures before the actual large scale application of these OYE enzymes. A possible method will be to increase the enzyme activity through

mutations around enzyme FMN, as current initial result have suggested variants with improved specific activity have shown to yield higher chemical TTN compared with the wild type enzymes. These entire contributions center around the final goal to derive the sequence functionality relationship among these OYE enzymes, with better understanding about the key residues, achieve product stereocontrol, and develop stable enzyme variant. We are at the forefront of OYE engineering for better future applications of ene and nitro reductases.

7.1 Future Perspectives

7.1.1 Effects of organic solvents on catalytic efficiency and stereoselectivity

Processes with enzymatic conversions are advancing in the fields of food industry, fine chemical synthesis, pharmaceuticals, and even for environmental purposes. Traditional batch reactors with temperature control often required an enzyme deactivation step at the end of run before recovering final products. Although such a reactor system is relatively simple with control of only pH and temperature, it comes with several disadvantages such as low productivity, high operating cost, enzyme deactivation, and inconsistent product quality.[1] To overcome the limitations of the batch reactor, the development of immobilized enzyme became popular in the 1970s. Various immobilized enzyme systems were proposed to localize the biological catalyst in a definite surface, which allowed for the preservation of enzymatic activity and reusability. However, immobilization of enzyme on carrier beads resulted in the loss of enzymatic activity as the active site of the enzyme was distorted during the immobilization process, and interfacial limitation at the surface prevent the diffusion of substrate towards the immobilized enzyme.[2] The introduction of membrane technology leads to a revolution in the immobilized enzyme technology.

The enzyme membrane reactor (EMR) is a continuous stirred tank system in which enzymes are separated with the final products with the help of a selective membrane. Unlike the immobilized system, EMR allows either the enzyme molecules to circulate freely on the retentate side or immobilize onto the membrane surface by maintaining full activity inside the reactor. Dependent on the selectivity requirement for specific reaction, ultrafiltration membranes with molecular weight cut-off between 3 kDa and 100 kDa are available .[3] In the reported studies, enzyme membrane reactors successfully enhanced the productivity and practicality of bioconversions by increased the substrate / enzyme contact ratio, provided a simple and reversible platform for enzyme localization, and effectively removed both reaction products and possible inhibitory compounds.

In the industrial application of enzyme membrane system also increase due to the advancement in the multiphase reaction systems. The majority of the enzyme-catalyzed reactions took place in aqueous solutions, but many substrates of industrial interest exhibit very low water solubility. Although substrate solubility can be increased with addition of organic solvents in multiphase systems, there are mass-transfer limitations for the diffusion of low-water-soluble substrates and the separation and recovery of product is difficult. [4]

The use of whole-cell system with ene reductases was generally limited with carbonyl compounds by the presence of endogenous ketoreductases in the host cells, which also employ nicotinamide cofactors to reduce the carbonyl function. Although the reported stereoselectivity is often adequate, the chemoselectivity of whole-cell reduction with respect to C=C and C=O bonds is poor. Since the amount of cofactor is limited in the whole cell, there is a need to introduce cofactor regeneration into the system. The system designed to couple ene reductase with cofactor recycling system will consist of glucose dehydrogenase (GDH). Cofactor regeneration system is a key to the development of large-scale process because the high price of nicotinamide cofactors (e.g. $3250/mol

NAD^+, $10853/mol NADH, $13973/mol $NADP^+$, and $205418/mol NADPH [5]), which prohibits their stoichiometric use and thus required a robust regeneration system.[6] Enzyme cofactor regeneration is performed by isolated enzymes in enzyme-coupled system. Two coupled enzymes, ene reductase and glucose dehydrogenase, will carry out two parallel redox reactions: substrate target biotransformation by ERs and cofactor recycling with auxiliary substrate. In the proposed scheme, GDH catalyzes the oxidation of glucose to gluconic acid with the concomitant reduction of $NAD(P)^+$ to NAD(P)H.[7]

The future research may focus to set up a *stable cofactor regeneration system* without using an EMR or a whole-cell system. Isolated ene reductase candidates will be coupled with the GDH regeneration system. The ideal cofactor regeneration should show fast conversion of substrate with the minimum loading of GDH into the system without any side reactions. A thermostable GDH has been provided by Vazquez-Figueroa [8] with great stability showing half-life of 3.5 days at 65^oC. Data comparison with different amount of GDH, ER, substrate of interest, and auxiliary substrate will suggest the most efficient system to generate chiral nitroalkanes with the highest possible enantiomeric excess, the highest biocatalyst productivity (both in terms of g product / g catalyst and of total turnover number), and volumetric productivity (space-time-yield). Possible inhibition effects of either enzyme will also be eliminated at this point for better reaction conversion. The established cofactor recycling method will then be transferred into the EMR system.

The *EMR with continuous stirred tank system* will be tested for enantiomer product synthesis. The EMR manufactured by Forschungszentrum Jülich consisted of a 2 – 10 mL stainless steel, thermostatted vessel with one flat-sheet of membrane placed in the middle of the reactor stabilized by a supporting disk. The selected membrane will have a molecular weight cutoff of 3-10 kDa since most of the ene reductases have molecular weights ranging from 30 kDa to 60 kDa. The aqueous stream consisting of reactants, cofactor, and enzyme will be fed into the bottom part of the reactor, where a

magnetic stir bar is present to ensure the homogeneity of the system for efficient reactant to product conversion. The product formed then passes the UF membrane and is collected for further analysis. The membrane reactors will be optimized with respect to the following input variables: (1) enzyme loading, (2) pH, (3) temperature, (4) reaction volume, and (6) feed substrate concentration. The optimization process will be performed with one variable at a time, and then used the optimum value for next parameter optimization. The final product will be analyzed with regard to the enantiopurity, membrane reactor productivity, operational stability of the enzymes, and product yield. A successful system should provide ≥ 50% substrate conversion with product enantiopurity of ≥ 70%. Also, parameters such as enzyme total turnover number and space-time yield will be calculated to ensure satisfactory catalytic function of the enzyme.

The cofactor recycling system will also be *coupled into the whole cell* for *in vitro* application of ene reductase. The whole cell system will analyze the difference of conversion efficacy in: (1) one plasmid vs. two plasmid cloning, (2) resting vs. dead vs. growing cell system, (3) natural cell metabolism vs. with cloned GDH. Comparison between the EMR and whole cell systems will be calculated base on the system conversion efficiency for the reaction of interest, the enantiopurity of the final product, and the ease of recovering product at the end of the reaction cycle.

7.2 References

[1] G. M. Rios, *et al.*, "Progress in enzymatic membrane reactors - a review," *Journal of Membrane Science,* vol. 242, pp. 189-196, Oct 15 2004.

[2] I. Chibata, "Industrial Application of Immobilized Enzyme-Systems," *Pure and Applied Chemistry,* vol. 50, pp. 667-675, 1978.

[3] D. Paolucci-Jeanjean, *et al.*, "A comprehensive study of the loss of enzyme activity in a continuous membrane reactor - application to starch hydrolysis," *Journal of Chemical Technology and Biotechnology,* vol. 76, pp. 273-278, Mar 2001.

[4] J. L. Lopez and S. L. Matson, "A multiphase/extractive enzyme membrane reactor for production of diltiazem chiral intermediate," *Journal of Membrane Science,* vol. 125, pp. 189-211, Mar 5 1997.

[5] R. Wichmann and D. Vasic-Racki, "Cofactor regeneration at the lab scale," *Technology Transfer in Biotechnology: From Lab to Industry to Production,* vol. 92, pp. 225-260, 2005.

[6] S. M. A. De Wildeman, *et al.*, "Biocatalytic reductions: From lab curiosity to "first choice"," *Accounts of Chemical Research,* vol. 40, pp. 1260-1266, Dec 2007.

[7] A. Weckbecker and W. Hummel, "Cloning, expression, and characterization of an (R)-specific alcohol dehydrogenase from Lactobacillus kefir," *Biocatalysis and Biotransformation,* vol. 24, pp. 380-389, Sep-Oct 2006.

[8] E. Vazquez-Figueroa, *et al.*, "Development of a thermostable glucose dehydrogenase by a structure-guided consensus concept," *Chembiochem,* vol. 8, pp. 2295-2301, Dec 17 2007.

VITA

YANTO YANTO

Yanto was born in Jakarta, Indonesia in 1984. He moved to Singapore for high school, graduated from Loyang Secondary School in 2001, and earned a B.S in Chemical Engineering from University of California at Davis in 2006 with honor degree graduation. He interned as fermentation research engineer at AgraQuest Inc at Davis, CA, before continued to Georgia Tech for his PhD study in August 2006. At Georgia Tech, Yanto joined Dr. Andreas S. Bommarius research group focusing on development of novel biocatalyst for asymmetric bioreduction of C=C bonds. He is a coauthor on three journal publication, one book chapter, and one patent application. Yanto also chaired the 2007 Chemical & Biomolecular Engineering Annual Symposium in 2007 and received Leadership of Excellence Award. In his personal time, Yanto enjoy reading, movies, working out, and many outdoor activities such as snowboarding, hiking, and scuba diving.